ALMA MATER STUDIORUM
UNIVERSITÀ DI BOLOGNA

DOTTORATO DI RICERCA
IN SCIENZE DELLA TERRA

XXVIII CICLO

Settore Concorsuale di afferenza: 04/A4 - GEOFISICA

Settore Scientifico disciplinare: GEO/11 – GEOFISICA APPLICATA

Geomorphic features revealed by the acquisition, processing and interpretation of high-resolution seismic reflection profiles across a large debris-flow fan (Vinschgau/Val Venosta, Italian Alps).

Presentata da: Dr. Stefano Maraio

Coordinatore dottorato

Prof. Jo De Waele

Relatore

Prof. Vincenzo Picotti

Correlatore

Prof. Pier Paolo Bruno

Esame finale anno 2016

INDEX

1 **Introduction** p.3

1.1 Aims of the research p.5

1.2 Methods p.6

1.3 Thesis outline p.9

1.4 References p.10

2 **High-resolution seismic imaging of large debris flow fans by comparison of CRS stack, CMP stack and refraction tomography: the example of Gadria Fan in Venosta Valley, Italian Alps.** p.12

2.1 Abstract p.13

2.2 Introduction p.14

2.3 The CRS Method p.17

2.4 Local setting p.19

2.5 Data acquisition and analysis p.21

2.6 Results p.32

2.7 Discussion p.40

2.8 Conclusions p.41

2.9 References p.43

3 **Linking geomorphology and alluvial fan seismic stratigraphy for defining geomorphic process domains in Vinschgau/Val Venosta (Eastern Alps, Italy).** P.46

3.1 Abtract p.47

3.2 Introduction p.48

3.3 Local setting p.51

3.4 Methods p.52

3.5 Results p.56

3.6 Discussion p.62

3.7 Conclusions p.65

3.8 References p.66

3.9 Data repository p.70

4 **Seismic stratigraphy of the post LGM alluvial/colluvial sedimentary dynamics of an Alpine valley (Vinschgau/Venosta, Eastern Alps, Italy**). p.80

4.1 Abstract p.81

4.2 Introduction p.82

4.3 Last deglaciation of the Alps background p.84

4.4 Local setting p.85

4.5 Methods and acquisition p.87

4.6 Seismic Unit interpretation p.89

4.7 Depositional Systems p.96

4.8 Evolution of the valley p.97

4.9 Conclusion p.102

4.10 References p.103

4.11 Data repository p.107

5 **Conclusion** p.111

1 Introduction

Researches concerning the Quaternary sedimentary dynamics in the European Alps have become of increasing interest in the late decades, producing a large volume of literature (Darnault et al., 2012). Many of these studies have been focused on Late Pleistocene and Holocene interval, since this time span was marked by a very peculiar climate signal, that strongly influenced the landscape evolution. Alpine environment was repeatedly affected by glaciations since the Pleistocene; recent filling sediments within the valleys were deposited during and after the Last Glacial Maximum, recording the climatic and the environmental conditions that characterize the area during the whole Late Glacial to Holocene time span. At the same time, fingerprints of glacial activity, still preserved in the landscape, represent an archive for the reconstruction of the glacial and paraglacial sedimentary dynamics (e.g. Church and Ryder, 1972). In this context, source to sink studies represent a powerful approach to understand and detail these climate oscillations.

This thesis uses high-resolution seismic reflection data and seismic stratigraphic methods to examine the formation and evolution of a major alluvial/glacial fan in the eastern Italian Alps. The work uses stratigraphic, geophysical and morphologic data to characterize the fan and valley deposits and their evolution throughout post-glacial times. Using this information, we model the evolution of the valley fill in the framework of post-glacial climate fluctuations. The results provide an understanding of the landscape geomorphic evolution in response to the main climatic changes and also can represent a tool in policy decision regarding natural hazards, given that construction of residential buildings and transport infrastructures on alluvial fans has increased the vulnerability to catastrophic events (i.e. mass-flow, debris-flow), thus augmenting the overall risk (Comiti et al., 2014).

The Vinschgau/Val Venosta is a glacial trough that runs west to east within the Austroalpine nappe of the Eastern Alps, between the Engandine and Periadriatic lineaments and its geological and tectonic evolution

has been discussed by Ratschbacher (1986]; Thöni & Hoinkes (1987); Ratschbacher et al. al., (1989); Thöni (1999); Sölva et al. al., (2005). The valley, drained by the Etsch/AdigeRiver, originates near the Resia pass and extend for about 74 km down to the city of Meran, where it changes direction, flowing to the south (Fig. 1). The valley is imposed along the Vinschgau shear-zone, a brittle/ductile lineament that separate the Oetzal Unit, outcropping to the northern side, from the Campo Unit on the southern slopes of the valley. The spatial transition between the two units is covered by the presence of thick Quaternary deposits that fill the valley; the valley floor hosts a series of impressive large fan developed at the junctions between some tributary catchments and the trunk valley. Quaternary deposits in Vinschgau/Val Venosta and particularly the Gadria fan have been object of many research in the last years. The pioneer work of Fischer (1965; 1990) on the Gadria fan of the Vinschgau/Val Venosta put the basis for a first assessment of the evolutionary dynamics of the fans through debris-flow processes. This author discovered and dated rests of subfossil trees, providing the first constraints for the stratigraphy of the fan in the frame of the controlling factors, such as the climate changes. Jarman et al. (2011) provided a genetic interpretation of the fan cluster of the Vinschgau/Val Venosta, addresing their research on the morphometric analysis of the so-called megafans or outsize fan that characterize the valley. These authors, based on the analysis of the morphology of the tributary catchments, hypothesized the formation of all fans through catastrophic landslides, occurred soon after the deglaciation and later covered with debris-flow to alluvial deposits. On the other hand, Brardinoni et al. (2012), analyzing the correlation between contemporary debris-flow and the fans areas, hypothesized the formation of the fan in Vinschgau/Val Venosta by means of a progradation of paraglacial and glacio-fluvial sediments transferred from the source basins mainly via debris-flow processes. Cavalli et al., (2013) by means of a morphometric analysis, studied the connectivity of hillslopes to the channel network to help understanding the different transport processes within the Gadria and Strimm catchments that supply the large Gadria fan. These two catchments were also the objects of the Comiti et al. (2014) research; in this work the authors examined the preliminary results of an experimental monitoring site equipped at the outlet of the Gadria catchment. Savi et al. (2014) based their research on seismic and borehole datasets collected across the

Zielbach fan, some tens of km downstream toward Meran, and they provided a reconstruction of the evolution of the Zielbach catchment throughout the Holocene.

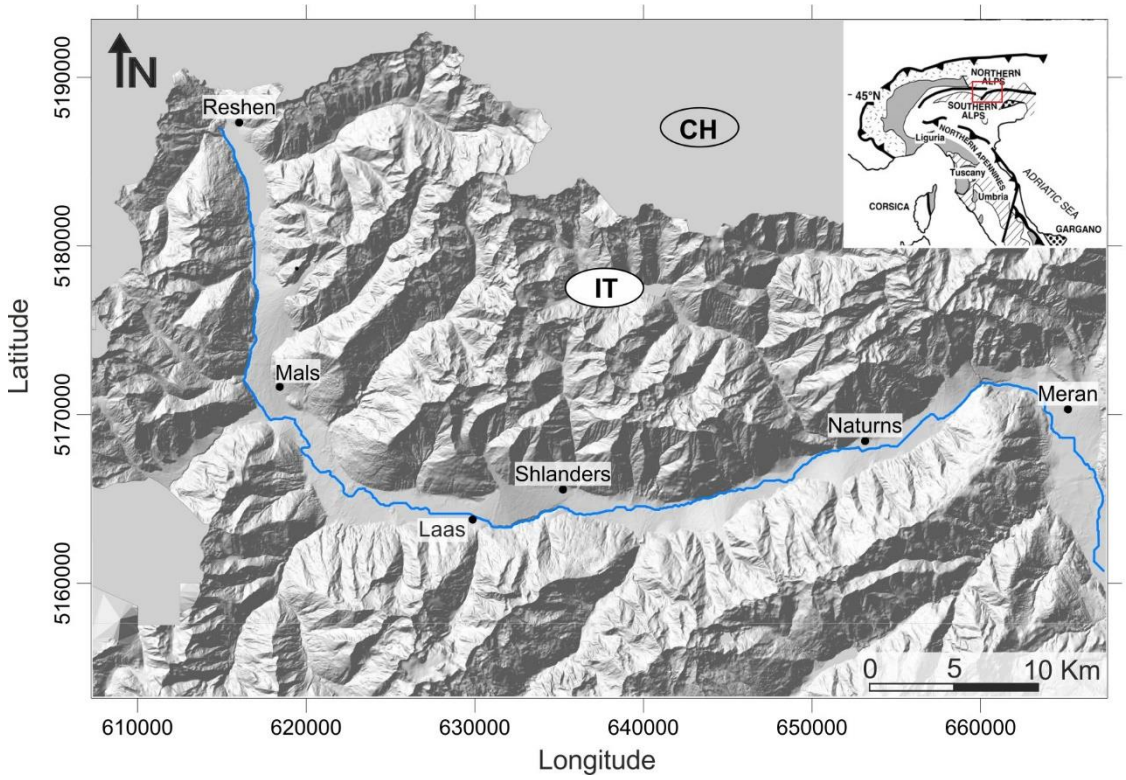

Figure 1: Digital Elevation Model of the Vinschgau/Val Venosta

1.1 Aims of the research

To obtain a general picture of the geomorphic evolution of the Vinschgau/Val Venosta in relation to the climate changes occurred the Last Glacial Maximum in the Eastern Alps. The specific of this thesis are:

- to obtain information about the general morphology of the valley basement, and the internal stratigraphy of Quaternary deposits that fill it, identifying the main sedimentary processes and source of sediments;
- to understand the genesis of this big fan belonging to a cluster of one of the largest colluvial/alluvial fan within the Italian Alps;

- to provide spatial and temporal constraints for the post-glacial evolution of the Vinschgau/Val Venosta, using stratigraphical, geophysical and morphological data;
- to distinguish the geomorphic processes involved in the evolution of the valley and to model this evolution in the frame of the climate fluctuations the last post-glacial.

1.2 Methods

This thesis integrates data sets obtained from different geological disciplines, but principally high resolution reflection and refraction seismic data were acquired in order to recognize the various depositional patterns and to provide the subsurface geometry of the stratigraphical units. The use of high resolution seismic instrumentation in the data acquisition, together with non-standard processing of the seismic data, allowed us to reconstruct the geometry of the valley subsurface and the internal architecture of the reflector packages, with a metric resolution. We acquired four seismic profiles, with a total profile length of ~4 km (Figure 2). P-wave seismic reflection data were collected using a single 6382kg IVI-Minivib® truck and data were recorded by Dense-wide-aperture (DWA) arrays (Bruno et al., 2010, 2013). DWA geometry allowed a meaningful interaction between refraction and reflection data processing and overcome most of the factors limiting the data quality in those complex environments. We applied the CRS (Common Reflection Surface) method as an alternative to the conventional CMP stack processing. The CRS was originally developed as a data-driven and velocity-independent stacking method for producing zero-offset sections with high signal-to-noise ratios, improved resolution, more continuous reflectors, and enhanced images of dipping reflectors (see Mann et al., 1999 and references therein). Conventional CMP stacking is based on assumption of planar interfaces in a homogeneous layer and depend on the RMS velocity model. The CRS stack method has an a more generic approach, that considers the location, orientation and curvature of interfaces through three parameters, called CRS attributes (Mann et al. 1999; Jager et al. 2001). With the optimum three CRS attributes, the pre-processed data (pre-stack) were stacked, to yield the final CRS stacked section, and compared with the CMP section.

The high resolution of seismic data also permitted to link the internal architecture of the fan deposits to the main geomorphic processes active in the catchments. In order to reconstruct these processes, using high resolution Digital Elevation Model of the valley, the analysis of the topographic signatures within some selected tributary catchments was carried out. Here we seek to demonstrate a source to sink connection between catchment geomorphic processes, the creation, storage, and transport of sediment to an alluvial fan, and the resulting fan allostratigraphy as revealed by high-resolution reflection seismology. In the process, we are able to better identify the main sediment transport processes in Val Venosta (Eastern Alps, Italy) and test an intriguing idea that a cluster of anomalously large alluvial fans are the result of immediate post-glacial mega-landslides (Jarman, 2011). The results of this analysis, combined with the detailed interpretation of the seismic facies within the fan deposits, depicted, with a good approximation, a picture about the formation and the development of the Gadria fan. Based on the preliminary analysis of the seismic data results, the target and the location of few boreholes has been established, with the purpose of provide a detailed lithologic calibration of the seismic line. The final integration between the stratigraphic data from the boreholes and the seismostratigraphic investigation of seismic units from the acquired and processed seismic profiles, allowed us to reconstruct the main depositional systems of the valley fill. Furthermore, a reconstruction of the landscape evolution of the valley, highlighting the interaction between different depositional systems is provided, pinpointed with the few dates in the area in the frame of the main climate fluctuations from the last deglaciation.

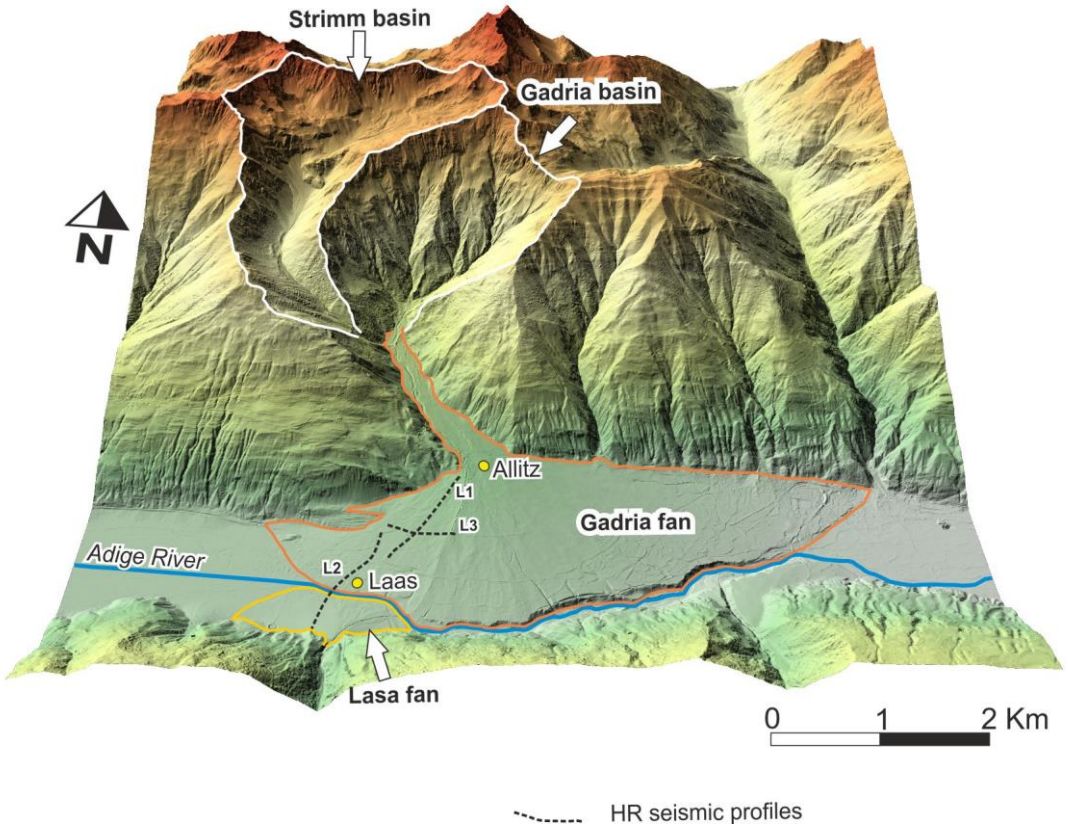

Figure 2: Digital Elevation Model of the seismic survey area by Provincia Autonoma di Bolzano, with the high resolution seismic profiles location across the Gadria and Lasa fans. Two profiles (Lasa1 and Lasa2) are transverse to the valley, while Lasa3 profile is parallel to the valley axes.

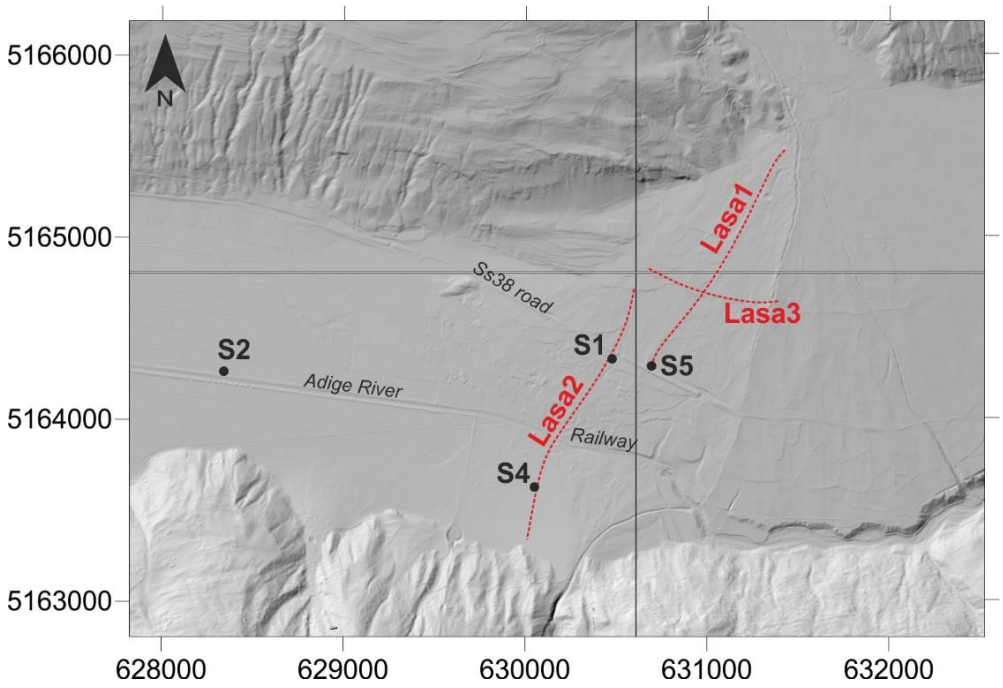

Figure 3: location of the high resolution seismic profiles (red dashed lines) and the boreholes (black dots).

1.3 Thesis outline

The outline of this thesis reflects the order and the rationale of the aims described above and consists of 5 chapters.

Chapter 1 provides the general introduction to the thesis topics, illustrating the aims of the work and the approach used in the research and containing a review of literature availability about the investigated area.

Chapter 2 discusses the acquisition, the processing and the preliminary interpretation of the seismic dataset across a transect of Vinschgau/Val Venosta and across one of largest fan in the valley (i.e. Gadria fan). This part illustrates all the problems and the difficulties in acquiring high resolution seismic reflection data in Alpine environment, describing the methodology used during the data acquisition and the data processing phases to overcome these limitations. This chapter also shows the application of a non-standard seismic reflection processing flow for obtain high-quality data results in complex environment, using the Common Reflection Surface technique. By combining the results of seismic reflection and refraction processing, a preliminary interpretation of the migrated seismic sections is made, pointing out the structure of the valley, the thickness of sediment of both fans present in the investigated transect and of Etsch/AdigeRiver deposits.

Chapter 3 is dedicated to the geomorphological analysis of the source basins, linking the sedimentology of the fan investigated by the seismic profiles to its catchment geomorphology. This part also exhibits the study of the topographic signature that characterize the channels within the tributary catchments on the basis of stream power law-based slope-area analysis, in order to define the sediment transport processes and to highlight the glacial signatures in the source basins. Finally, a discussion about the paraglacial processeses active in the area and a genetic hypothesis about the fan formation in the valley are provided.

Chapter 4 is dedicated to the detailed interpretation of the seismic facies from the seismic profiles, the definition of the different seismic units and the correlation between the seismic and the drilling data. This chapter describes the different depositional systems that fill the valley and the dynamics of both fluvial and fan systems during the Late Glacial to Holocene transition in the frame of the main climate oscillations

characterizing this period. Finally, a possible reconstruction of the main evolutionary stages of the valley is provided.

Chapter 5 provides a general conclusion of the thesis, combining the results and the discussions from all the previous chapters and highlighting the key finding of the research.

Chapters 2, 3 and 4 have been prepared for submission as a separate paper, consequently repetitions, especially in the geological and physical settings sections, are unavoidable; each chapter also contains the list of cited references.

My role in the work

During the work exposed in this thesis, I have been responsible in the planning and execution of the seismic experiment. I also managed the logistics for data acquisition and the preliminary scouting of the test sites. I processed the seismic data presented in chapter 2, in collaboration with professor P. P. Bruno and successively I collaborated on the establishment of the target and the location of the boreholes. During my experience at the Lehigh University I performed the geomorphic analysis showed in chapter 3 in collaboration with professor F. J. Pazzaglia. Finally, I worked with my tutor prof. V. Picotti and F. Brardinoni, M. Cucato, C. Morelli in order to provide a detailed interpretation of the seismic and borehole data and a reconstruction of the main depositional systems of the valley.

1.4 References

Brardinoni, F., Church, M., Simoni, A., & Macconi, P. (2012). Lithologic and glacially conditioned controls on regional debris-flow sediment dynamics. Geology, 40(5), 455-458.

Cavalli, M., Trevisani, S., Comiti, F., & Marchi, L. (2013). *Geomorphometric assessment of spatial sediment connectivity in small Alpine catchments*, Geomorphology, 188, 31-41.

Comiti, F., Marchi, L., Macconi, P., Arattano, M., Bertoldi, G., Borga, M. & Theule, J. (2014), *A new monitoring station for debris flows in the European Alps: first observations in the Gadria basin*. Natural Hazards, 73(3), 1175-1198.

Darnault, R., Rolland, Y., Braucher, R., Bourlès, D., Revel, M., Sanchez, G., & Bouissou, S. (2012). Timing of the last deglaciation revealed by receding glaciers at the Alpine-scale: impact on mountain geomorphology. Quaternary Science Reviews, 31, 127-142.

Fischer, K. 1965. Murkegel, Schwemmkegel und Kegelimse in den Alpentalern. Mitteilungen der Geographischer Gesellschaft in Munchen, 56, 127–159.

Fischer, K. (1990). *Entwicklungsgeschichte der Murkegel im Vinschgau*. Der Schlern, 64(2), 93-97.

Jarman, D., Agliardi, F., & Crosta, G. B. (2011). *Megafans and outsize fans from catastrophic slope failures in Alpine glacial troughs: the Malser Haide and the Venosta Valley cluster, Italy.* Geological Society, London, Special Publications, 351(1), 253-277.

Ratschbacher, L. (1986). *Kinematics of Austro-Alpine cover nappes: changing translation path due to transpression.* Tectonophysics, 125(4), 335-356.

Ratschbacher, L., Frisch, W., Neubauer, F., Schmid, S. M., & Neugebauer, J. (1989). *Extension in compressional orogenic belts: the eastern Alps.* Geology, 17(5), 404-407.

Savi, S., Norton, K. P., Picotti, V., Akçar, N., Delunel, R., Brardinoni, F & Schlunegger, F. (2014). Quantifying sediment supply at the end of the last glaciation: Dynamic reconstruction of an alpine debris-flow fan. Geological Society of America Bulletin, 126(5-6), 773-790.

Sölva, H., Grasemann, B., Thöni, M., Thiede, R., & Habler, G. (2005). *The Schneeberg normal fault zone: normal faulting associated with Cretaceous SE-directed extrusion in the Eastern Alps (Italy/Austria).* Tectonophysics, 401(3), 143-166.

Thoni, M. (1999). *A review of geochronological data from the Eastern Alps.* Schweizerische Mineralogische und Petrographische Mitteilungen, 79(1), 209-230.

Thöni, M., & Hoinkes, G. (1987). *The southern Ötztal basement: geochronological and petrological consequences of Eoalpine metamorphic overprinting*. Geodynamics of the Eastern Alps, 200-213.

Chapter 2

High-resolution seismic imaging of large debris flow fans by comparison of CRS stack, CMP stack and refraction tomography: the example of Gadria Fan in Venosta Valley, Italian Alps.

Stefano Maraio [(1)], Pier Paolo G. Bruno[(2,*)], Vincenzo Picotti [(3)] and Volkmar Mair [(4)]

[1] University of Bologna, Department of Biological, Geological and Environmental Sciences, Italy.

[2] The Petroleum Institute, Department of Petroleum Geosciences, Abu Dhabi, UAE.

[*] Formerly, Istituto Nazionale di Geofisica e Vulcanologia, Roma, Italy

[3] ETH Zürich, Department of Earth Sciences, Zürich, Switzerland.

[4] Province of Bolzano, Office for Geology and material testing, Italy.

2.1 Abstract

Alluvial fan environments, often pose significant challenges for high-resolution seismic exploration, due to high heterogeneity of deposits and rugged topography. Using both non-conventional field and processing techniques, we were able to obtain high-quality seismic reflection and refraction images across a representative transect of Venosta Valley. The CRS stack technique was used, together with conventional CMP, to process seismic reflection data. Wide-aperture seismic arrays permitted to develop reliable tomographic images across the Adige Valley in overlap with depth migrated CMP and CRS stacks. Redundant information from seismic reflection and seismic tomography provided a better constrained interpretation. All results are in excellent agreement with surface geology and allowed us to: 1) depict the internal architecture of Gadria Fan and of Adige River sediments; 2) study the growth of the Gadria Fan and its recent interaction with Laas Fan and Adige River development; 3) image the asymmetrical structure of the valley, which is clearly set over a blind trust fault; 3) evaluate thickness of sediment accumulation of both Gadria and Laas fans and of Adige River deposits. In particular, the internal reflective configuration of Gadria Fan suggests that, rather than catastrophic formation, a paraglacial progradation, mainly mediated by debris flows, is the most probable formation mechanism of the fan.

2.2 Introduction

Alluvial fans are common in alpine environments, especially where steep tributary valleys join wide formerly glaciated valleys [*Harvey*, 2003]. A cluster of exceptionally large debris-flow-dominated fans characterizes the Venosta Valley, a major relict trough drained by the Adige River in the east-central Alps, Italy. The study of alluvial fans is important because their stratigraphic archive records the hydrological processes that affected their development. In alpine environments, the closely linked depositional and erosional processes and the relationship between sediments of the tributary fan and main river may also reveal abrupt climatic/anthropic changes affecting precipitation style and trend, and/or the hillslope sediment production. In studying alluvial fan development, it is also important to differentiate among mass-flow, debris-flow and stream-flow processes. Moreover, estimates of the volume of materials involved in alluvial fans formation provide information that can be of importance for numerical modeling focused on natural hazards prevention. To fully understand all processes that control alluvial fan formation in terms of both spatial and temporal variability, information provided by surface data alone is often insufficient, because the limited size of the outcrop prevents continuous stratigraphic correlations [*Franke et al.,* 2015]. Additional and complementary information can be obtained by means of a high-resolution geophysical approach. In the last years alluvial fans have mainly been studied using ground-penetrating radar techniques aimed to characterize the very shallow portion of subsurface, i.e.~10-30 m [*Ékes & Hickin*, 2001; *Ékes & Friele*, 2003; *Hornung et al.,* 2010; *Franke et al.,* 2015]. If, on one hand, ground-penetrating radar can reveal the sedimentary structure from decimeter to meter scale, on the other hand the low penetration of this technique prevents to investigate the entire thickness of large alluvial fans with significant volumes of sediment accumulation.

In this paper, we discuss the results of one of the first attempts to characterize continental alluvial fans by high-resolution reflection seismology. We acquired and processed three high-resolution seismic reflection profiles across a representative transect of Venosta Valley, over the Gadria and Laas fans, and throughout the Adige Valley near the village of Laas/Lasa. Our goal was the seismic imaging of the shallow

portion (i.e. ~ first 500m deep) of the Gadria alluvial fan. We needed seismic data with a quality and resolution adequate to: 1) study the internal reflective configuration of the fan; 2) image both the pattern of the bedrock below the valley and thickness of the sediment accumulation above it; 3) evaluate the geometrical relationships between the Gadria Fan and the Adige River sediments. The main factors hindering seismic imaging of alluvial fans, especially in continental environments, are related to the extreme complexity of mountain environments, which, being characterized by strong heterogeneities and severe topographic variations as well as presence of contrasting dips of subsurface layers (e.g. the valley bedrock), pose significant challenges for high-resolution seismic exploration. Hence, non-conventional acquisition and processing approaches should be used when surveying those areas. A limited number of studies published on this topic [*Bruno et al.,* 2010; *Bruno et al.,* 2013; *Savi et al.,* 2014] witness the poor results obtained by conventional reflection seismology on alluvial fans. A field technique known as Dense-wide-aperture profiling was successfully used by *Bruno et al.,* [2010] to image a dry alluvial fan in the Southern Apennines. We used the dense, wide-aperture profiling to acquire our data. Dense, wide-aperture geometry differs from the typical common midpoint, narrow-aperture reflection surveying in that it records both multi-fold reflection data spanning a large range of offsets (from short-offset, near-vertical reflections to large-offset, large amplitude post-critical reflections) and deep penetrating refracted waves, which are suitable for first-arrival travel time tomography. To evaluate the optimal seismic imaging strategy to apply to our dense, wide-aperture data, we compared the Common-Reflection-Surface (CRS) stack technique, [e.g. *Muller*, 1998] with results from conventional common midpoint (CMP) reflection processing. The CRS was originally developed as a data-driven and velocity-independent stacking method for producing zero-offset sections with high signal-to-noise ratios, improved resolution, more continuous reflectors, and enhanced images of dipping reflectors [see *Mann et al.,* 1999 and references therein]. Consequently, this method has become a viable alternative to classic CMP stack for seismic imaging in environments where the CMP assumptions of flat reflectors and smooth velocity variations are strongly violated, or where it is difficult to estimate stacking velocities for NMO correction. Comparison between CRS and CMP stacks allowed us assessing possible artifacts generated by the CRS processing.

2.3 The CRS method

Conventional CMP stacking is based on assumption of planar interfaces and homogeneous layers and depends on the stacking velocity model. The stacking velocity is the only and critical parameter that needs to be known for the normal moveout (NMO) correction of the reflected phase before stacking. The CRS stack method has a more generic approach, that considers location, orientation and curvature of interfaces; in this way the CRS method can be applied to any reflector shapes, producing stack sections that matches more with true subsurface models [*Mann et al.,*1999]. More details about the CRS method and the CRS attributes can be found in the following literature: *Hubral* [1983], *Mann et al.,* [1999], *Jager et al.,* [2001], *Hoecht* [2002], *Menyoli* [2002], *Mann* [2002] and *Garabito et al.,* [2011].

In contrast to CMP stacking, the CRS method does not directly depend on the stacking velocity model, but it uses three parameters, called "CRS attributes". The three parameters describe the reflected wavefront associated with two so-called *eigenwaves* [*Hubral*, 1983]. These hypothetical waves, measured at the surface, are obtained by: 1) a point source at the reflector, that produce an upgoing "normal incidence point" (*NIP*) wave; and 2) an "exploding" reflector, that develops the second "upgoing normal wave" (*N*). Following this theory, the CRS attributes consist of an emergence angle of the zero-offset ray α, the radius of curvature R_{NIP} of *NIP* wave and the radius of curvature R_N of the normal wave [*Mann* et al., 1999; *Jager et al.,* 2001; *Menyoli,* 2002]. As exposed in *Mann et al.,* [1999] and in *Jager et al.,* [2001], the two-dimensional hyperbolic travel-time of the CRS operator for point (x_0, t_0) in the zero-offset section, is defined by the following approximation:

$$t^2(x_m, h) = \left[t_0 + \frac{2\sin\alpha}{v_0}(x_m - x_0)\right]^2 + \frac{2t_0 cos^2\alpha}{v_0} \cdot \left[\frac{(x_m - x_0)^2}{R_N} + \frac{h^2}{R_{NIP}}\right]; \qquad (1)$$

where h represents the half offset between the source and receiver position; x_m denotes the midpoint between source and receiver; t_0 is the two-way travel-time along the normal ray between the emergence point x_0 and the reflection point and v_0 is the near-surface velocity.

The search for the three CRS parameters is a 3D optimization problem, and different strategies with a different degree of complexity have been developed in the recent years [see *Jager et al.,* 2001; *Hoecht,* 2002; *Garabito et al.,* 2011 and references therein]. However, solving 3D optimization problems for all the points in the Z_O section is highly time-consuming. Therefore, a three-step search algorithm has been adopted for this purpose [see *Muller* 1998; *Mann et al.,* 1999 and *Jager et al.,* 2001]. It contains three 1D optimization steps and searches for the CRS parameters in the NMO stacked section, assuming that the conventional NMO stacked section approximates a Z_O section. Therefore, optimal CRS parameters are obtained only if the NMO stacked section is a good approximation of a Z_O section, as is the case for high-fold / high signal-to-noise data. In such case, to a good approximation, each parameter can be constrained independently, consequently fast (i.e. cost effective) and efficient implementations are possible. The CMP stack section (zero-offset) can also used to determine the wavefront attributes.

For a three-step search algorithm we start considered the intersection of the two-dimension CRS operator (1) with the plane $x_m=x_0$ of the common midpoint (CMP) gather. In this way, the operator reduces to CMP hyperbola expressed in terms of CRS attributes:

$$t^2(h) = t_0^2 + \frac{2t_0h^2cos^2\alpha}{v_0R_{NIP}} \qquad (2)$$

Comparing equation (2) to the well-known NMO formula:

$$t_{CMP}^2(h) = t_0^2 + \frac{4h^2}{v_{NMO}^2} \qquad (3)$$

we can see the NMO velocity can be expressed in terms of two CRS attributes:

$$v_{NMO}^2 = \frac{2v_0R_{NIP}}{t_0cos^2\alpha} \qquad (4)$$

The equation allows determining the optimum stacking velocity V_{NMO} in a one-parametric search in the pre-stack (i.e. CMP gather) domain. After we consider the intersection of the CRS operator (1) with the plane of the zero-offset section from CMP stack: for h=0, the two-dimension CRS operator reduces to the one-dimension operator:

$$t_{ZO}^2(x_m) = \left[t_0 + \frac{2\sin\alpha}{v_0}(x_m - x_0)\right]^2 + \frac{2t_0 cos^2\alpha}{v_0 R_N}(x_m - x_0) \qquad (5)$$

In a first order approximation, we can assume $R_N=\infty$, which implies plane normal wave emerging at the surface; we obtain:

$$t_{ZO}(x_m) = t_0 + \frac{2\sin\alpha}{v_0}(x_m - x_0) \qquad (6)$$

Equation (6) allows us to perform a second one-parameter search in order to determine the emergence angle α from equation (6). Then, knowing α, we can substitute it into equation (5) and perform a third one-parameter search for R_N. With the knowledge of α and V_{NMO}, we can determine R_{NIP} by means of equation (4). With the optimum three CRS attributes, the pre-processed data (pre-stack) can be stacked in each location (x_0, t_0), using the two dimensional CRS operator (1), to yield the final CRS stacked section.

2.4 Local setting

The survey area is located in Venosta Valley (Fig.1a) in the Eastern Italian Alps, a series of nappes, which belong to the Helvetic, Penninic and Austroalpine realm. The geological and tectonic evolution of the Eastern Alps is discussed in detail by *Ratschbacher* [1986]; *Thöni & Hoinkes* [1987]; *Ratschbacher et al.,* [1989]; *Thöni* [1999]; *Sölva et al.,* [2005]. The valley originates near the Resia Pass (~1500 m a.s.l.), where the Adige River originates, and extends for ~74 km down to the city of Meran (~500 m a.s.l.), where Venosta Valley connects into the north-trending Adige Valley (Fig. 1b). Venosta Valley runs above the Venosta Shear Zone, which separates the Oëtztal Unit (north) from the underlying Campo Nappe. The Oëtzal unit consists of paragneisses, with interlaced micashists, orthogneisses and metabasites, while Campo Nappe Unit consists of polymentamorphic rock, similar to those of the Oëtzal unit with granites and abundant pegmatites [*Solva et al.,* 2005]. Both Oëtztal and Campo Nappe fm. are characterized by fractures oriented along N, E, NE and SW directions, and these structural patterns control the spatial structure of the drainage network and influence rock strength [*Agliardi et al.,* 2009; *Jarman et al.,* 2011; *Comiti et al.,* 2014]. Quaternary alluvial and fluvio-lacustrine deposits that hide the transition between the two units [*Comiti et al.,* 2014] fill the valley.

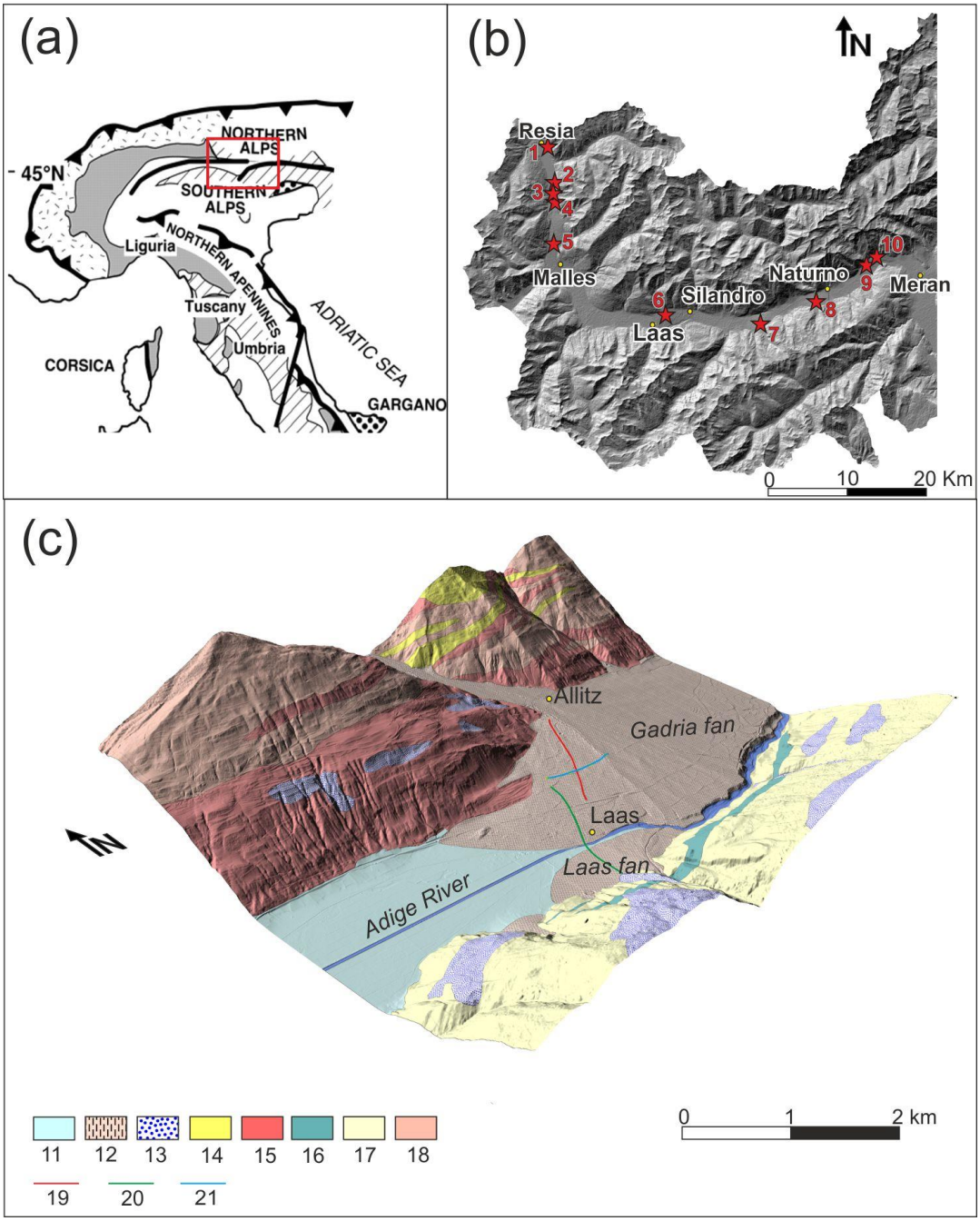

Figure 1: a): geologic and tectonic setting of north-central Italy (red box encloses the area in b) [modified from *Aiello and Hagstrum*, 2001]; b): map of Venosta Valley and most prominent megafans and outsize fans identified in the literature and from satellite imagery: 1, Reschen outsize fan; 2, St Valentin North outsize Fan; 3, St Valentin South outsize Fan; 4, Fischerhauser outsize fan; 5, MalserHaide megafans; 6, Gadria/Lasa megafan; 7, Tarres/Laces megafan; 8, Tablàmegafan; 9, Parcines West megafan; 10. Parcines East megafan. c): DEM (2m resolution) by Autonomous Province of Bolzano – Alto Adige – Informatical, Geographical and Statistical Office overlaid with digitalized Geological Map of Italy 1:100000: 11, quaternary alluvional deposits and peat soils; 12, alluvial fan deposits; 13, moraine deposits; 14, phyllonites of alps age; 15, granitic or granodioritic orthogneiss; 16, amphibolites, gneiss and amphibolitic schist; 17, micashists and paragneiss; 18, micashists and paragneiss of Adige north zone; Oëtzal Fm is made of units 14,15 and 18, while Units 16 and 17 constitute Campo Nappe Fm. 19, “Lasa1” profile location; 20, “Lasa2” profile location; 21, “Lasa3” profile location.

The valley bottom hosts a number of fans, unusually large within the Alps, which often obstruct and deviate the course of the Adige River. For instance, near village of Laas, the Adige River is deviated toward the southern slope of the valley by the very large Gadria alluvial fan (Fig 1c). This fan is one of the targets of our seismic survey. *Jarman et al.,* [2011] also describes the Gadria Fan as one of the largest symmetrical alluvial fans in the Alps. Its origin is still matter of debate: *Jarman et al.,* [2011] hypothesizes a catastrophic formation for the fan, modulated by large, rapid slope failures. *Brardinoni et al.,* [2012] hypothesize instead as source a mechanism of paraglacial progradation, mainly mediated by debris flows. In the figure 1 it is also evident a smaller fan (i.e. Laas fan), that was built by variable amounts of fluvial and debris flow inputs [*Jarman et al.,* 2011].

Debris-flows within the Gadria channel network are facilitated by the combination of steep topography, highly weathered and fractured metamorphic bedrock surface and thick glacio-fluvial deposits [*Comiti et al.,* 2014]. Gadria catchment morphology and evolution has been the target of several studies and has been actively monitored because of the relatively high frequency of debris flow events [*Comiti et al.,* 2014; *Cavalli et al.,* 2013; *Brardinoni et al.,* 2012]. An important Gadria tributary basin (i.e. Strimm basin) joins the Gadria channel close to a retention basin located near the apex of Gadria fan. The Gadria and Strimm basins are characterized by contrasting morphology and different types and intensities of sediment transfer processes: Gadria stream shows frequent debris flows, whereas Strimm is essentially a “bedload” stream [*Cavalli et al.,* 2013].

2.5 Data acquisition and analysis

We acquired three high-resolution individual seismic profiles, partly overlapping and partly intersecting each other above Gadria and Laas fans, for a total surveyed length of ~4 km (Figs. 1-2). The profiles cover almost entirely the entire valley transect. Two profiles (Lasa1 and Lasa2) are transversal to the valley, and one profile (Lasa3) cuts the alluvial fan as a longitudinal section, intersecting profile Lasa1 at CMP

360 (Fig.2). The acquisition was very challenging for profile Lasa2, as we had to accommodate logistic obstacles in the residential area of Laas (i.e. “Lasa” in Italian, Fig. 2). Furthermore, it was necessary to accommodate and minimize acquisition gaps in seismic coverage where profile Lasa2 intersects the Adige River and a railway line (see Figs. 2 and 4). All profiles are characterized by a crooked geometry, therefore “processing” lines, which smooth the acquisition lines, were chosen to project the CMPs falling outside the acquisition line.

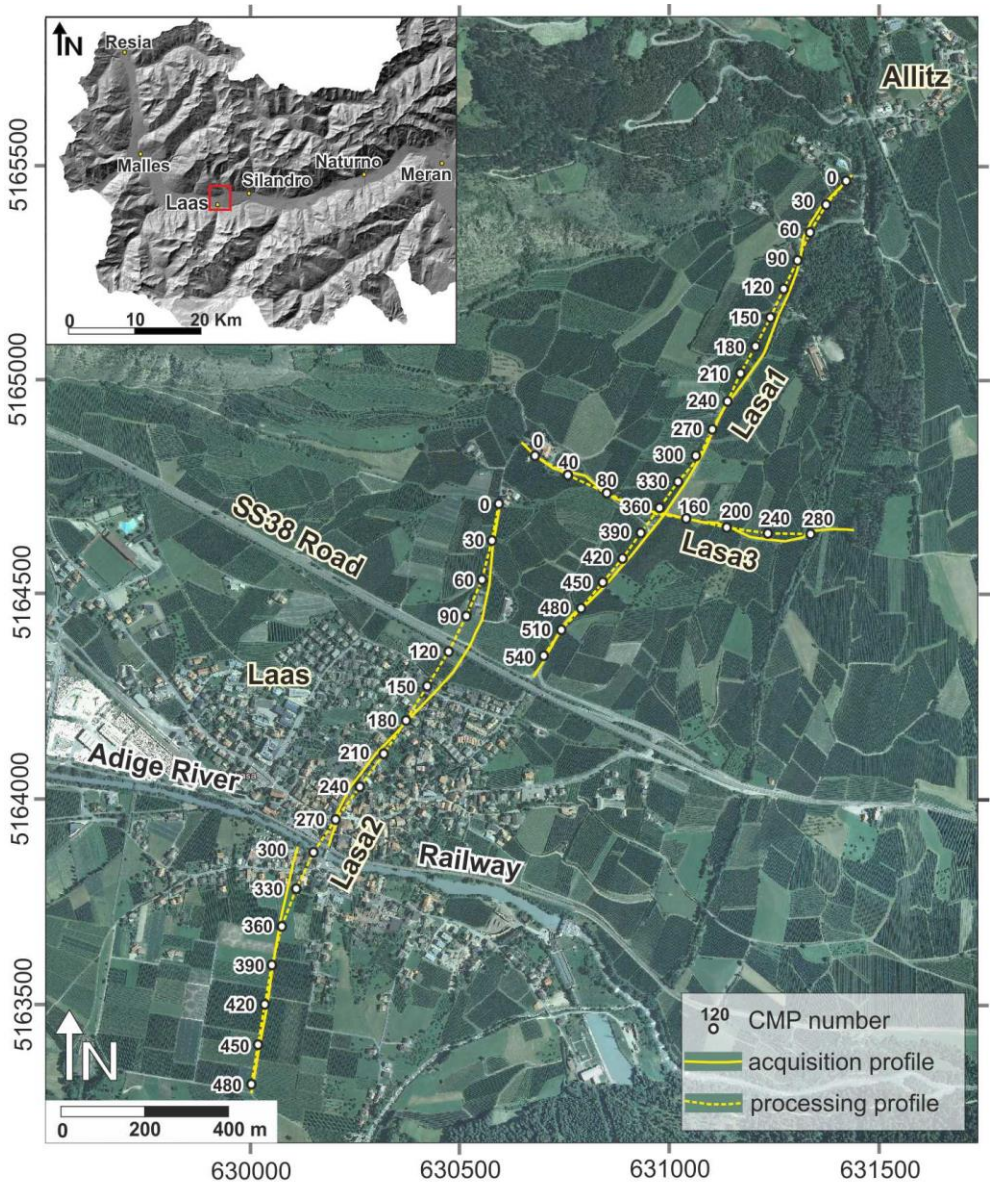

Figure 2: location of seismic profiles plotted on the aerial photograph provided by the Province of Bolzano. A red rectangle in the inset shows the location of the survey area with respect to the map of the Venosta Valley. Profiles “Lasa1” and “Lasa2” overlap for ~ 300m, with a horizontal separation that varies from 180 to 360 m. Profile “Lasa2” consists of two separate segments, acquired to the north and to the south of the Adige River.

Even though these segments were acquired with a horizontal separation of ~ 70 m, they were processed as a single, crooked line. There is no acquisition gap along profile "Lasa2", but just a fold decrement along the Adige River (see Fig. 4b) because of the additional shooting pattern we did to the north and to the south of the segments ending at the river.

Our priority goals in the field work were to obtain:1) a high data redundancy along the profiles (i.e. maximum folds between 100-200 in Figs 3-5) and 2) a dense spatial sampling of the seismic wavefield 3) a broad power spectrum in recorded signal. P-wave seismic reflection data were collected using a single 6,382kg IVI-MiniVIB® high-frequency vibrating source. At each vibration point we stacked two, 15 s long, 10–200 Hz upsweeps. Listening time was set to 16 s, with 1ms sample interval. These parameters allowed us to record data for a total time of 1s after correlation. Source move-up was 5 m on profiles Lasa1 and Lasa3, and for logistic reasons was 10 m on profile L2. Differential GPS technology was used to record source and geophone positions with an error of less than 2mm on x,y coordinates and less than 1 cm on z coordinate. Data were recorded by dense, wide-aperture arrays [*Bruno et al.*, 2013 and *Bruno et al.*, 2010] made by 192 vertical geophones with a 10 Hz eigenfrequency. Sensors were spaced each 5 m allowing an array aperture of 955 m; about 3 to 10 times larger than the depth of the basement across the valley. Differently from typical common-midpoint apertures, dense, wide-aperture arrays allow capturing both hypocritical and hypercritical reflected phases as well as deep penetrating head waves, which permit first-arrival travel-time tomography to reach almost the same investigation depth of reflected phases. Good signal-to-noise ratio characterizes the acquired data: indeed, clear reflected phases from fluvial and alluvial fan deposits layers are visible in raw common-shot gathers (Fig.3-5). A high-energy, often asymmetrical reflection from the top of the valley bedrock (Fig. 4b) is also evident. High-amplitude Rayleigh waves (event G in Figs. 3-5) obscure reflected phases, in the central part of the raw common-shot records and were reduced during processing. Our data processing flow is shown in the chart of Fig. 6. After vibroseis correlation and minimum phase conversion, we proceeded to first arrival picking that provided data for travel traveltime tomography. High-redundant global-offset first arrivals were checked for consistency using the reciprocity rules of *Ackermann et al.,* [1986]. Theoretical uncertainty on first arrivals readings, in noise free data, is ~1/8 of the dominant period (i.e. ≈ 1.5 ms). Indetermination was higher in some parts of profile Lasa2, because of presence both cultural and

ambient (wind) noise. Theoretical traveltimes were obtained via a ray-tracing method, based on Huygens principle [*Hayashi and Takahashi,* 2001] using a preliminary p-wave velocity provided by classical refraction methods of interpretation. Residuals between observed and theoretical traveltimes were minimized upgrading the preliminary velocity model with an iterative tomographic approach based on the SIRT image reconstruction technique [*Gilbert,* 1972]. Inversion results are shown in Figs. 7-9. The residual times root-mean-square error of profile Lasa1 is 2.7 ms, close enough to the theoretical picking error (~1.5 ms), while Lasa2 and Lasa3 models show slightly higher errors (i.e.3.4 ms and 3.7 ms respectively) that are associated to higher anthropic and/or ambient noise recorded on those lines. Resolution of tomographic images was assessed by "a posteriori" checkerboard tests [*Hearn and Ni,* 1994], using input perturbation values of ± 10% of cell p-wave velocity on cell patterns of dimension 100x50m (Figs 7-9). Analysis of checkerboard test shows an achieved depth penetration of about 100-150 m, which is sufficient to reach the top of the metamorphic bedrock. Tomography provides p-wave velocity information about the subsurface that overlaps almost entirely with the reflectivity images for seismic interpretation.

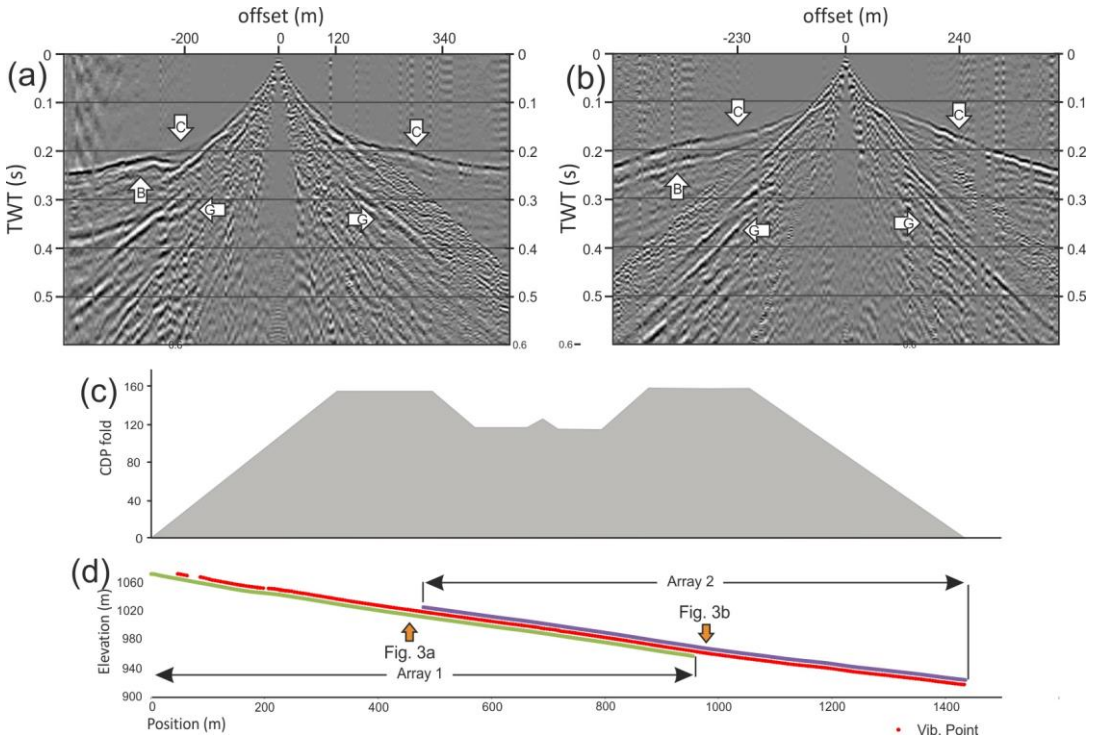

Figure 3. a) and b): two common shot gathers acquired on the profile "Lasa1" with the source located as pointed by the two orange arrows in (d) (i.e. 460m and 985m). Some basic processing, i.e. automatic gain control and trace kill, is applied to the data. The white arrows on the shot gathers outline: bedrock reflection

(B); high-angle refractions (C); surface waves (G). c): pattern of fold coverage along the profile; d): acquisition layout showing with a different color the two wide-aperture geophones arrays (green and purple) and the vibration points (red dots).

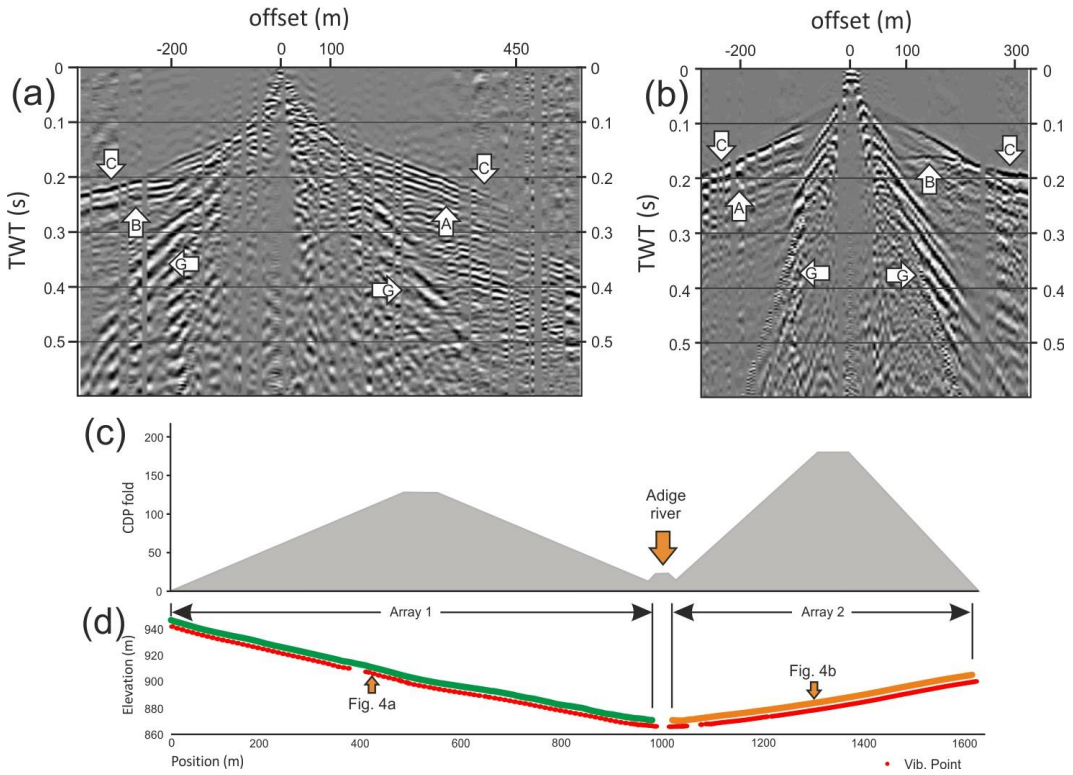

Figure 4: a) and b): two common shot gathers acquired on the profile “Lasa2” with the source located as pointed by the two red arrows in (d) (i.e. 415 m and 1315 m). Some basic processing, i.e. automatic gain control and trace kill, is applied to the data. The white arrows on the shot gathers outline: fluvial and alluvial fan deposits reflections (A); bedrock reflection (B); high-angle refractions (C); surface waves (G). c): pattern of fold coverage along the profile; d): acquisition layout showing with a different color the two wide-aperture geophones arrays (green and orange) and the vibration points (red dots).

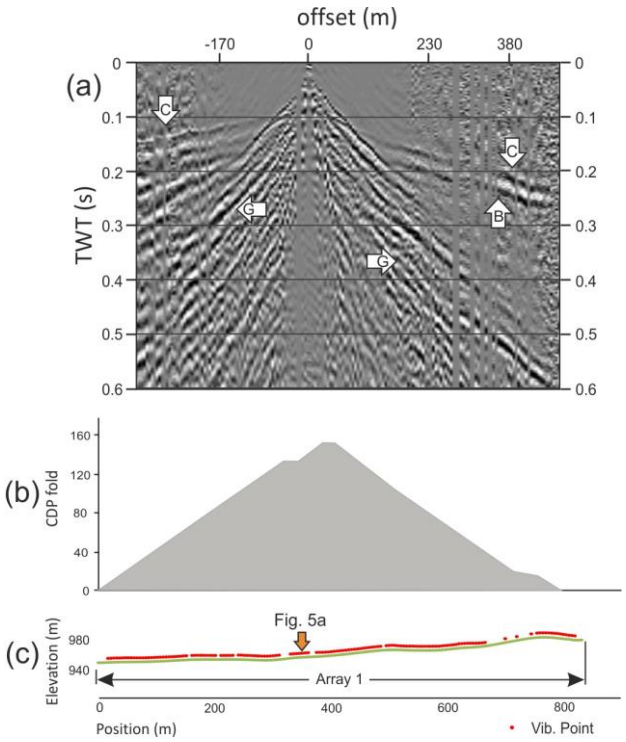

Figure 5: a) common shot gather acquired on the profile "Lasa3" with the source located as pointed by the orange arrow in (d) (i.e. 350m). Some basic processing, i.e. automatic gain control and trace kill, is applied to the data. The white arrows on the shot gathers outline: bedrock reflection (B); high-angle refractions (C); surface waves (G). b): pattern of fold coverage along the profile; c): acquisition layout showing the wide-aperture geophones arrays (green) and the vibration points (red dots).

The first part of reflection data processing (in green in the flow chart of Fig. 6), was mainly aimed at improving signal temporal and spatial resolution and signal-to-noise ratio, in particular some efforts were made in trying to attenuate the high-amplitude of Rayleigh waves. This phase was followed by refraction static correction [*Taner et al.,* 1998] that was performed using the first-arrival traveltimes previously picked; all data then were referenced to a datum at 1050 m a.s.l.. We estimated stacking velocities, which are needed for the normal moveout correction, by picking the maxima of the semblance [*Neidel & Taner*, 1971] functions on selected CMP super-gathers. The velocity models and the CMP stacks were refined by two cycles of residual static corrections [*Ronen & Clerabout*, 1985] followed by a further velocity analysis. This phase is colored in pink on the flow chart of Fig. 6.

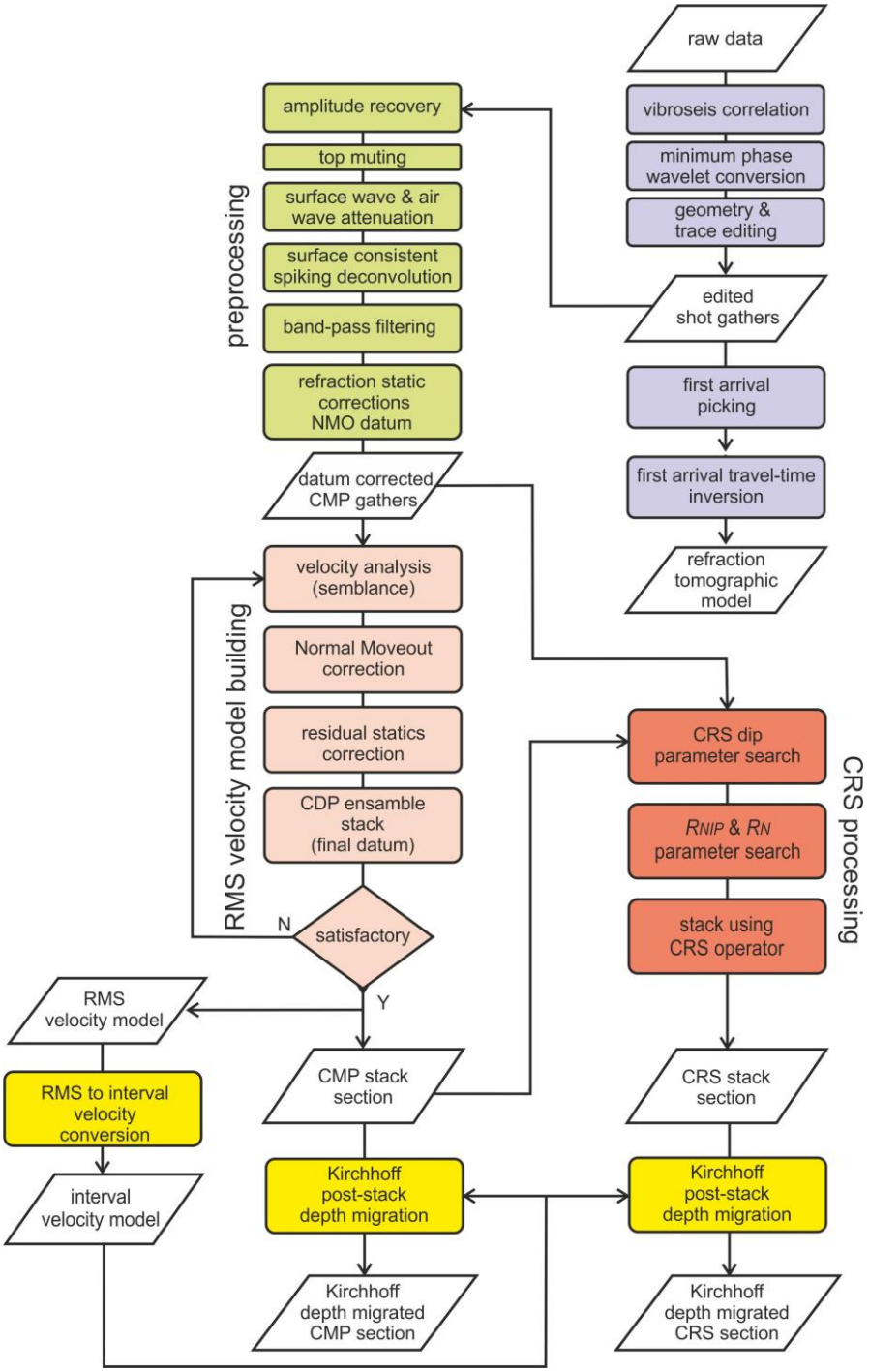

Figure 6: Data-processing flow. The upper right side of the diagram (violet) illustrates the correlation of the field data, and the refraction processing, with first arrivals picking and refraction tomographic model. Pre-processing (green) was applied to all data and included some processes to attenuate random noise and improve signal. Pre-processing included also refraction statics correction [*Taner et al.,* 1998], to compensate thin heterogeneous weathering layers and topographical variations along the profiles. Starting from preprocessed data, the left side of the diagram (pink) represents a CMP processing scheme that includes: (1) velocity analysis with semblance method; (2) normal moveout (NMO) correction; (3) residual statics to correct small inaccuracies in the near-surface model used for statics corrections; (4) stack. The bottom right part of diagram (red) represents the CRS processing with the CRS parameters search and the CRS stack. Both CMP and CRS stacks have been migrated using a post-stack Kirchhoff algorithm with the final velocity models build during CMP processing. See text for further explanation.

Both CMP stacks and pre-stack CMP gathers, with refraction and residual static applied, were used as inputs for the CRS processing (in red in the chart of Fig. 6). The CRS stack operator (eq. 1), as discussed above, does not depend a velocity macro-model, but stacking velocity information from previous CMP processing was also used as a guide function for the initial V_{NMO} velocity search in the three "one-parametric" CRS search strategies [*Mann*, 2002].

We started the search for dips (α) of emerging zero-offset wavefronts in the zero-offset domain, simulated by the CMP stacks obtained during NMO processing. Subsequently, dip attributes, V_{NMO} information and near surface velocity (V_0) were used for searching for the other CRS attributes (i.e., R_{NIP} and R_N: Fig. 10), needed by the CRS operator in order to perform the CRS stack. In high resolution data, aperture of the CRS operator is the most important parameter to test. It defines a CMP-domain radius within which the data will be stacked and determines how much signal-to-noise is enhanced at the cost of lateral resolution along the reflection. A careful preliminary analysis of shot gathers was very helpful to choose CRS operator apertures for the best trade-off between seismic resolution and signal-to-noise ratio [*Deidda et al.,* 2012]. After the test analysis we chose an optimum t_{min} and t_{tmax} apertures of 50 and 100 m respectively on the profiles Lasa1 and Lasa3. On profile Lasa2 we obtained the best results using t_{min} and t_{tmax} CRS apertures of 25 m and 100 m.

To perform a Kirchhoff post-stack depth migration on both CMP and CRS stacks, the final stacking velocity macromodels from the CMP processing were converted in interval velocity vs. depth using the *Dix* [1955] formula and applying smoothing functions to the conversion. As shown by *Trappe et al.,* [2001] and *Bergler et al.,* [2002], post-stack depth migration of CRS stacked section may be considered as an alternative to pre-stack depth migration (PSDM) in complex environments, and can lead to better results than PSDM.

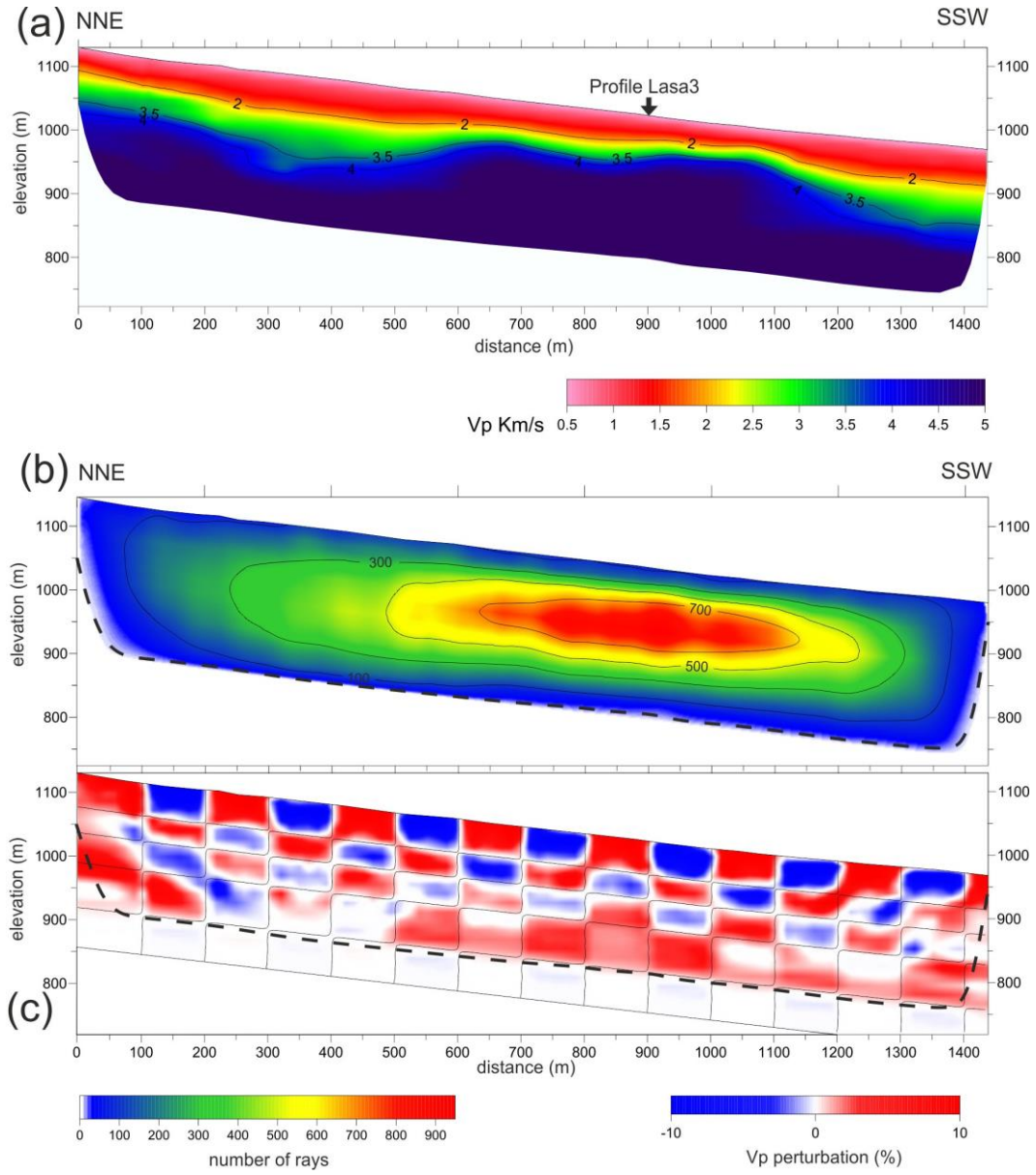

Figure 7: a): Results of Vp refraction tomography along the "Lasa1" profile; b): number of rays per cell; c): perturbation pattern retrieved after the a posteriori checkerboard resolution tests. The RMS traveltime error for the final model is 2.7 ms. The input perturbation pattern has values of ± 10 m/s in the cell with horizontal size 100 m and vertical size 50 m. Resolution depth is evaluated according to the retrieved pattern and the value of velocity perturbations, along with the ray coverage. Vertical and horizontal scales are equal.

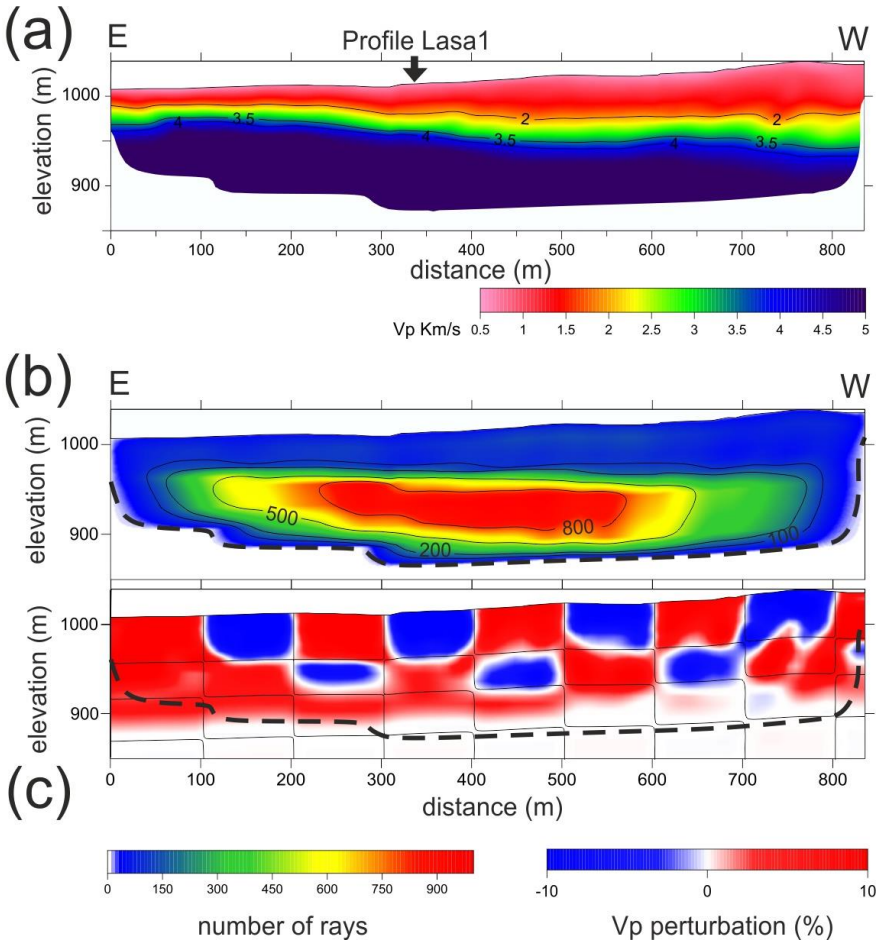

Figure 8: a): Results of Vp refraction tomography along the "Lasa3" profile; b): number of rays per cell; c): perturbation pattern retrieved after the a posteriori checkerboard resolution tests. The RMS traveltime error for the final model is 3.7 ms. The input perturbation pattern has values of ± 10 m/s in the cell with horizontal size 100 m and vertical size 50 m. Resolution depth is evaluated according to the retrieved pattern and the value of velocity perturbations, along with the ray coverage. Vertical and horizontal scales are equal. Along this tomographic model, ray penetration is lower (on average between 50 and 100 m) because the basement is shallower than on the other profiles.

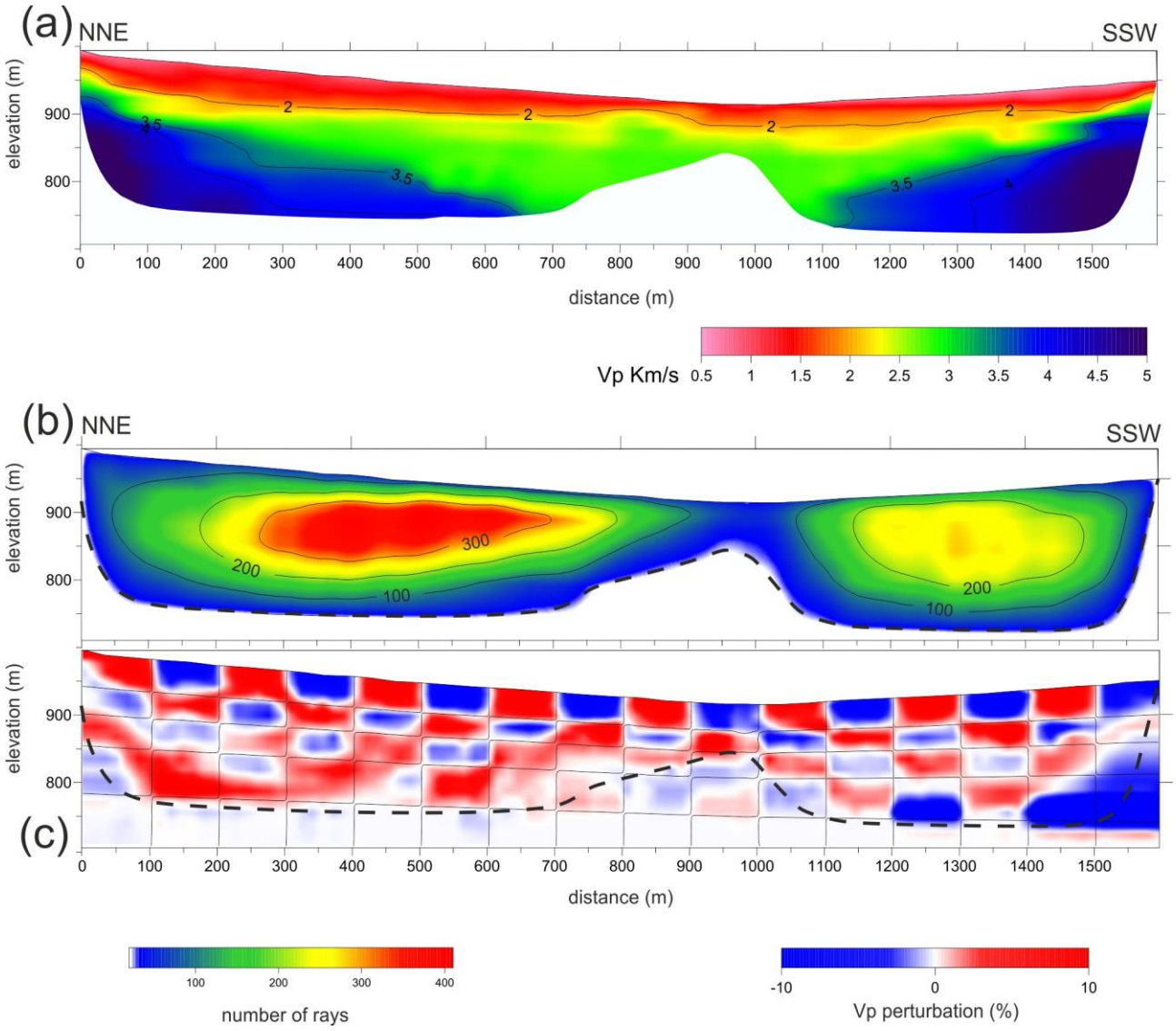

Figure 9: a): Results of Vp refraction tomography along the "Lasa2" profile; b): number of rays per cell; c): perturbation pattern retrieved after a posteriori checkerboard resolution tests. The RMS traveltime error for the final model is 3.4 ms. The input perturbation pattern has values of ± 10 m/s in the cell with horizontal size 100 m and vertical size 50 m. Resolution depth (thick dashed white line in (a)) is evaluated according to the retrieved pattern and the value of velocity perturbations, along with the ray coverage. Vertical and horizontal scales are equal. The tomographic model of Lasa2 clearly images the structure of the valley and the trend of the top of the metamorphic bedrock below.

2.6 Results

Seismic tomography

Tomographic images, with their associated ray density models and checkerboard tests are shown in Figs.7, 8 and 9. Ray density and checkerboard tests allow evaluating the resolved areas of the tomographic models, which extend on average ~200 m deep for Lasa1 and Lasa2 and ~120 m deep for profile Lasa3. In all tomographic images, p-wave velocity ranges from ~0.5 km/s to ~4.5 km/s. We associate low p-wave velocities (i.e. less than 1.5 km/s) to dry loose alluvial-fan sediments; velocity between 1.5 and 2.2 km/s to water saturated alluvial and fluvio-lacustrine deposits and finally velocity between 2.2 and 3.5 km/high cemented quaternary sediments. P-wave velocities greater than 3.5 km/s are associated to basement rocks (i.e. Oëtztal and Campo Nappe fm.).

The tomogram of profile Lasa1 (Fig. 7) shows a rather laterally heterogeneous P-wave velocity distribution and a strong vertical gradient of velocity. The shape of bedrock top, outlined by the 3.5 km/s contour line, is quite complex; its minimum depth from surface is found at a distance of 650-1050 m from the left of the profile. Profile Lasa3 (Fig. 8) intersects profile Lasa1 at metric location 900 m, above bedrock high; therefore, Lasa3 is characterized by a very low penetration and by a high vertical gradient of velocity.

Tomographic inversion for profile Lasa2 (Fig. 9) shows instead a very interesting picture across the deepest part of Adige Valley, although a limited penetration depth is achieved in the central part of the profile, due to the above-mentioned gap in seismic coverage. Despite this limitation, P-wave velocity depicts very well the valley structure showing a v-shaped, central low velocity area, due to thickening of alluvial ad river sediments. This low-velocity area is bounded to the bottom by two high velocities zones (i.e. from 3.5 to 4 km/s) that outline the trend of the buried bedrock below the valley on the north and south margin of the profile.

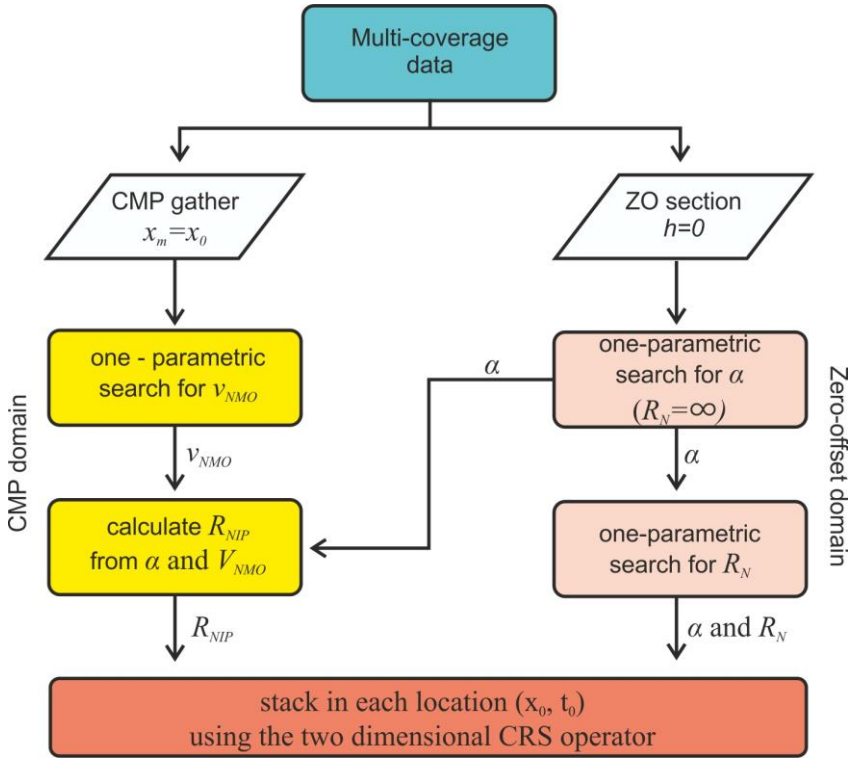

Figure 10: Simplified flowchart of the three one-parametric search for the determination of the CRS attribute according to *Mann et al.,* [1999] and *Jager et al.,* [2001]. The approach is described in detail in the text.

Seismic reflection

Both CMP and CRS depth-migrated images shown in Figs 11, 12 and 13 are characterized by an overall good signal-to-noise ratio. In general, CRS stacks provide a slightly higher signal-to-noise ratio and reflectors that are more continuous. However, it is well known that CRS may enhance continuity of truly discontinuous reflectors and random/coherent noise (Bruno, 2015). *Bruno*, [2015] also suggests that CRS and CMP stacks should be used together to avoid pitfalls during interpretation of CRS images; in this paper we follow this recommendation. All seismic profiles show an upper low-reflectivity package, on average 100 m thick, which we associate to alluvial fans. Below it, and only on profile Lasa2, we find a high-frequency, high-reflectivity package relative to the Adige River sediments. This package is visible between CMPs 75-450 in Figs 11 and 13.

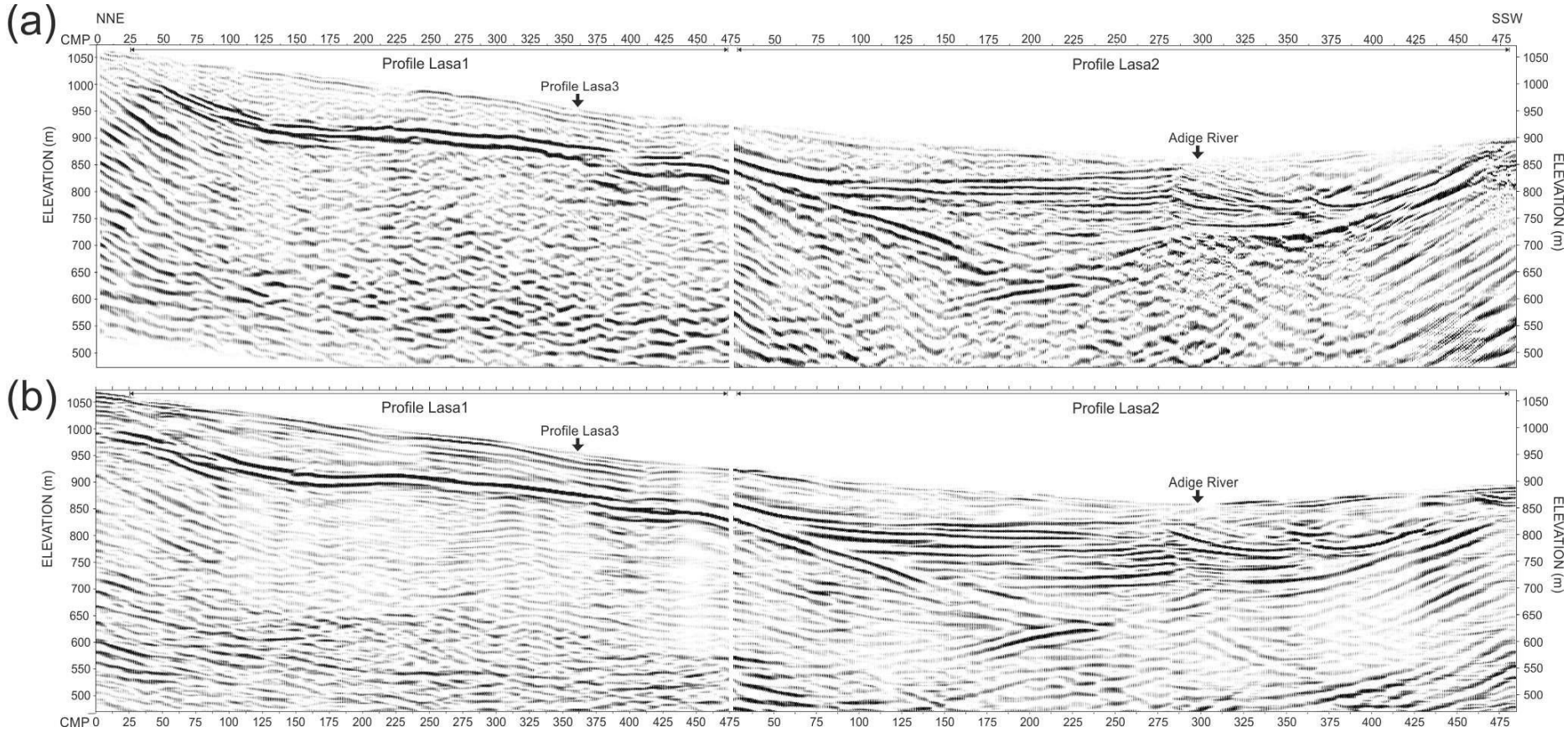

Figure 11: migrated stack of profile Lasa1 (on the left side) and Lasa2 (on the right side): a): post-stack depth-migrated sections after conventional CMP stacking; b): post-stack depth-migrated sections after CRS stacking. The image shows the improvement in terms of S/N ratio and reflectors continuity on the CRS migrated stack. Vertical and horizontal scales are equal.

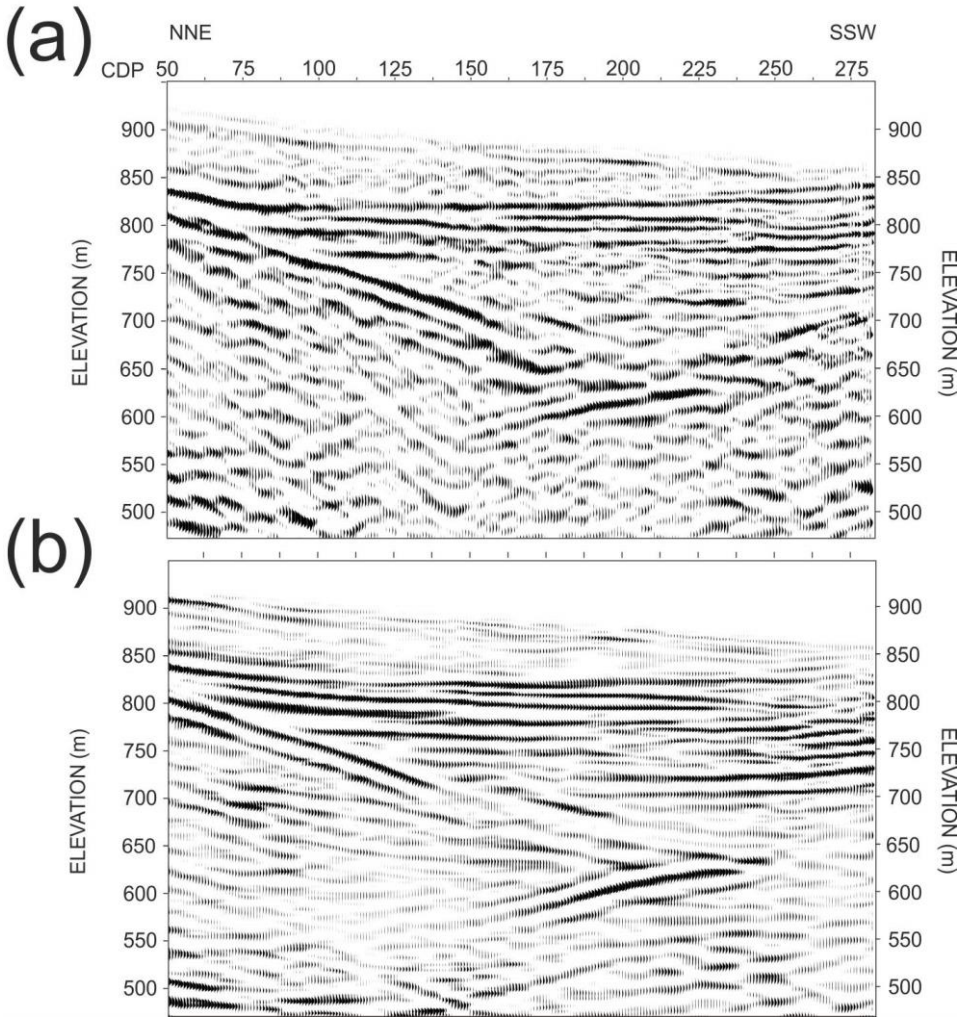

Figure 12: A representative part of the seismic profile “Lasa2” shows the difference between the conventional CMP stacking (a) and CRS stack method (b) results. The image clearly shows an improvement in the S/N ratio and in the continuity of the reflectors on the CRS migrated stack.

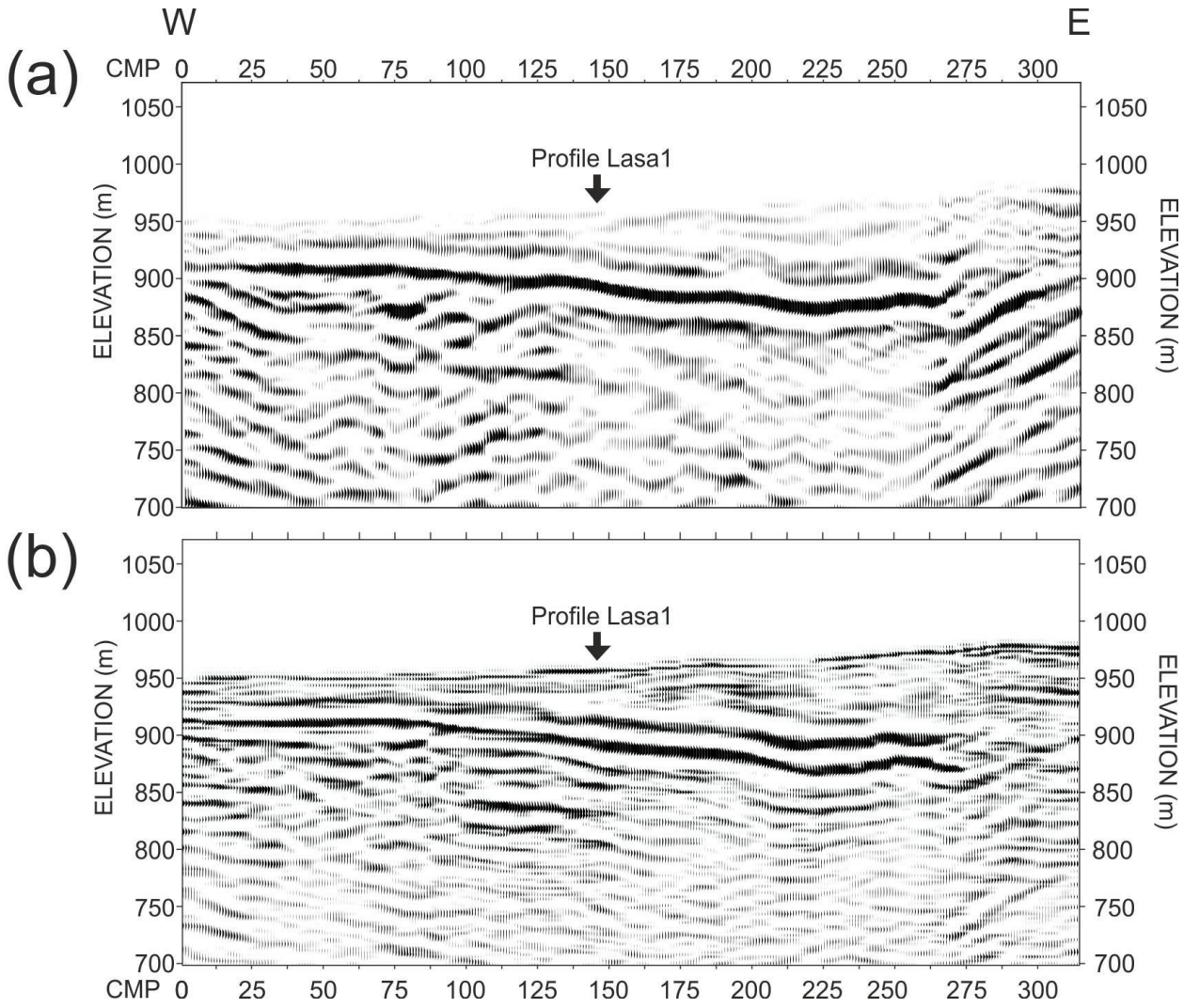

Figure 13: Lasa3 seismic profile: a): post-stack depth-migrated sections after conventional CMP stacking; b): post-stack depth-migrated sections after CRS stacking. As profiles shown in figure 11, on the CRS migrated profile the continuity of the events and the S/N ratio are enhanced. Vertical and horizontal scales are equal.

The top of bedrock corresponds to a low-frequency, high-amplitude reflective duplet of events, found unconformably below the Adige sediments or directly at contact with the alluvial fan reflective package (lines Lasa1 and Lasa3). Below the bedrock, reflectivity is again low. Inspection of the of both CMP and CRS migrated stacks in Fig. 13 reveals that maximum depth of the valley (~250 m) occurs along line Lasa2, below CMP 215, that is about 700 m to the north of Adige River (Fig. 11).

Fig.11 compares the depth-migrated CMP and CRS stacks of contiguous profiles Lasa1 (left side) and Lasa2 (right). Although these profiles partially overlap, they are separated of about 180-360 m along the

crossline direction (see Fig. 2), therefore reflectors dipping in the 3D space, such as the top of the bedrock, do not perfectly coincide at the two edges. Both CMP and CRS seismic images show the bedrock unconformity, which dips from north and south side of valley towards the Adige River and reaches a maximum depth of more than 200 m at CMP 215. This bedrock reflection is a bit more continuous on the CRS images below the Adige River. Even thought, as discussed previously, this continuity can be artificially enhanced, the CRS section allow to better following the morphologic pattern of the valley bedrock to the south of Adige. Vice-versa, the north of the Adige the CMP stack better shows the relative amplitude relationships among the reflective series. To the left (i.e. north) of the Adige river, both CMP and CRS stacks also well depict (CMPs 50-275) the fluvial sediments of the Adige River. This sequence is characterized by sub-horizontal and continuous high-frequency reflectors passing to less reflective packages to the bottom. This Adige River sequence clearly onlaps above a bedrock diving to the south (see also a zoomed image of this area in Fig. 13). To the south of Adige (i.e. from CMP 285 until the end of profile Lasa2), this fluvial series is disrupted by two shallow synform reflections, which are better focused on the migrated CRS stack but are also visible on the CMP stack. These features are highly reflective and are located at ~800m elevation, i.e. in the depth range of the more reflective fluvial package found to the north of the Adige. CRS stack also shows that Laas fan is prograding directly above these two synform features. In the next section we discuss of these synforms as erosional features caused by lateral migration to the south of the Adige River, possibly forced by the coeval evolution of the Gadria Fan from the north and Laas fan from the south. The reflective package of the Adige River sediments is not visible on profiles Lasa1 and Lasa3. These lines being located at a higher elevation on the northern side of the valley, only display the Gadria Fan sediments emplaced directly above the metamorphic bedrock. The sediment accumulation along these two profiles ranges from a minimum of less than 40m at the west end of profile Lasa3 (Fig. 13) up to a maximum of ~150m below CMP 137 on profile Lasa1 (Fig. 11).

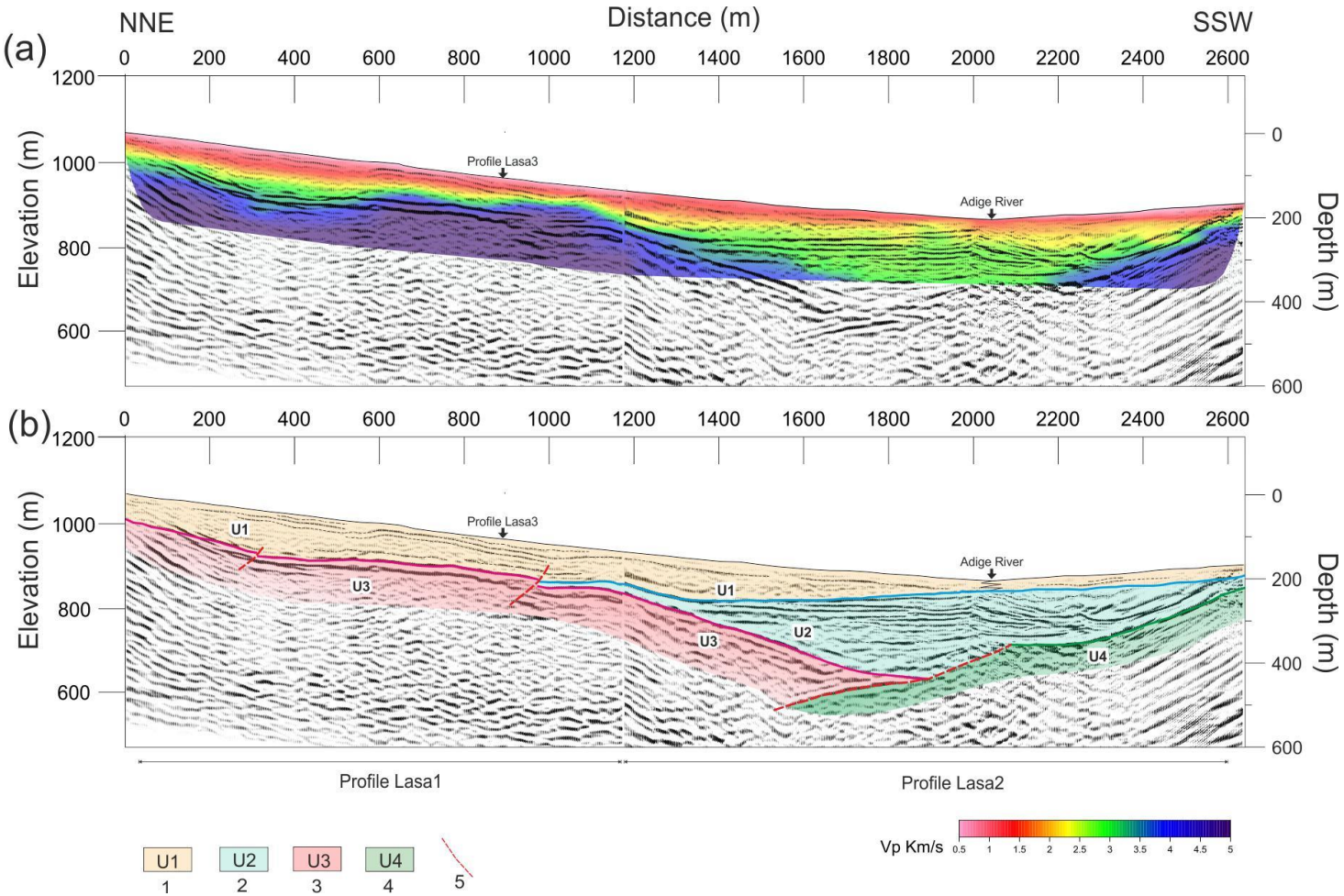

Figure 14: a): Post-stack depth migrated section from CMP stacking along Lasa1 and Lasa2 profiles, overlaid with the results of refraction tomography b): Seismic and structural interpretation superimposed on CMP migrated image: alluvial – debris-flow fan deposits (1); fluvio-lacustrine deposits (2); metamorphic bedrock (Oëtzal Unit) (3); metamorphic bedrock (Campo Nappe Unit) (4); presumed faults (5). See text for further explanation. Vertical and horizontal scales are equal.

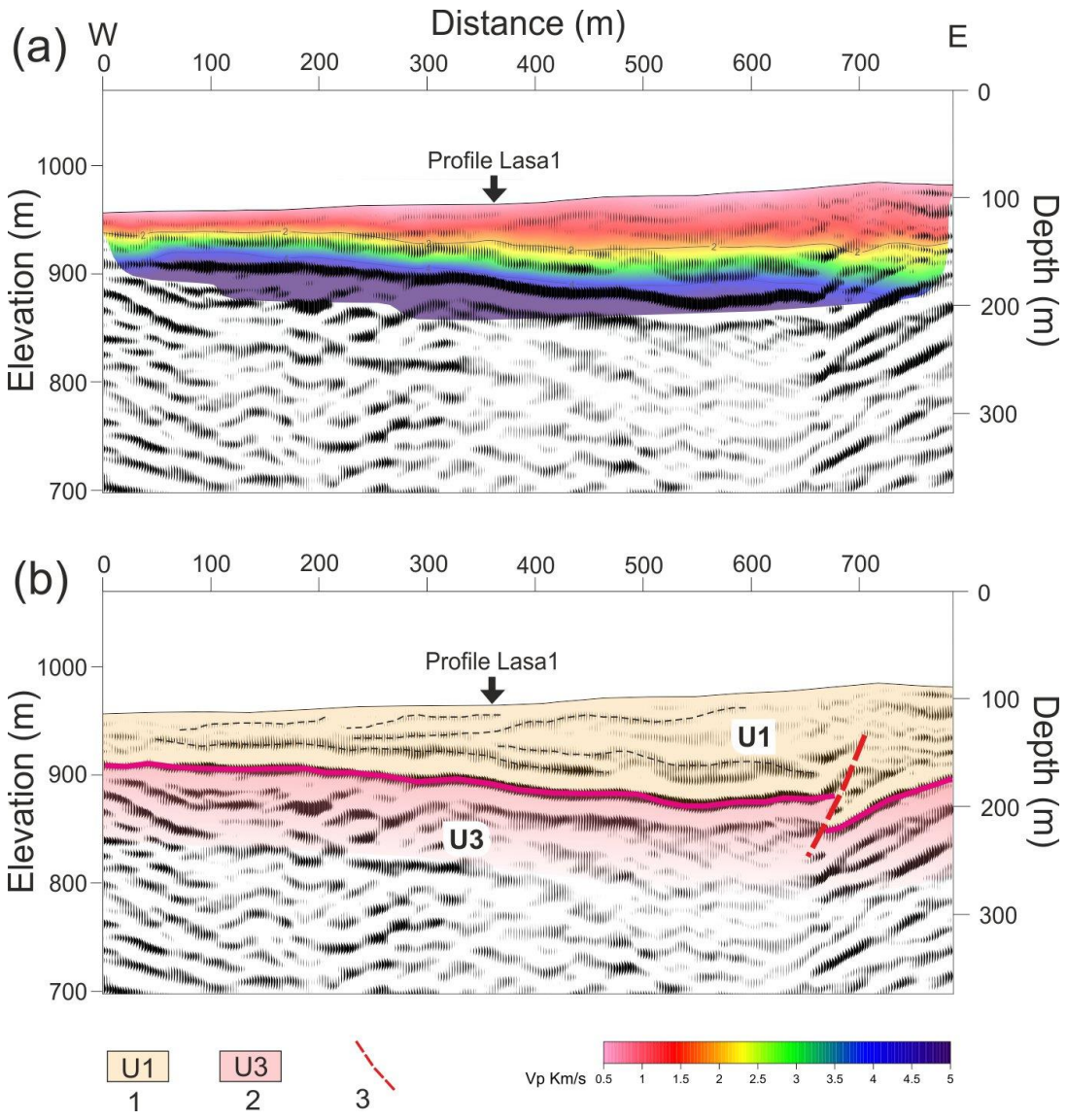

Figure 15: a): Post-stack depth migrated section from CMP stacking along Lasa3 profile, overlaid with the results of refraction tomography; b): Seismic and structural interpretation superimposed on CMP migrated image: alluvial – debris-flow fan deposits (1); metamorphic bedrock (Oëtzal Unit) (2); presumed inverse fault (3). See text for further explanation. Vertical and horizontal scales are equal.

Results of seismic tomography and a geological interpretation are overlapped to the depth CDP depth migrated seismic profiles in Figs. 14 and 15. Comparison between seismic tomography and reflective images in Figs 14a and 15a shows an overall good agreement, except on Lasa1 between CMPs 700-1000 where the 3.5 km/s contour line does not overlap perfectly to the reflection from the top of the basement. This

discrepancy between the two images can be caused by presence of compacted/cemented alluvial fan deposits with overall Vp ~3.5 km/s.

2.7 Discussion

Comparison between CRS and CMP migrated stacks in Figs. 11 shows that CRS processing improved the continuity of the internal reflective package within the alluvial fans. This enhancement of continuity, although might be artificial, has been indeed very useful during interpretation to better understand the geometrical relationships between Alliz and Laas Fans and between the fan sediments and the other Units. However, CMP images are likely to provide a better representation of the real amplitudes and continuity of the horizons within the alluvial fan deposits. CMP images are also very useful in showing and locating the position of the main heterogeneities within the alluvial fan body (see for instance profile Lasa2; CMP 75-160). These heterogeneities are imaged as diffraction points, i.e. small diffraction hyperbolas not perfectly imploded by the migration algorithms, due to the very small-scale heterogeneities in the velocity field that was impossible to determine by using the semblance. Such heterogeneities are also not visible in the tomography because they are very small compared to the cell size and damping factor used.

Fig. 14b shows our geological interpretation drawn over profiles Lasa1 and Lasa2. Based on the outcropping geology [*Andreatta*, 1951], we interpret the top of the bedrock on northern and southern side below Adige River as formed by two different metamorphic units in tectonic contact: i.e. Oëtztal unit on the north side and Campo Nappe unit on the south side of the valley. [see Fig. 1: *Solva et al.,* 2005]. The nappe contact is very well imaged as a strong reflector at 1500-1900 m distance in Figure 14 at about 250 m deep. Above it, the sub-horizontal reflective series to the north of Adige River (Fig. 13) shows at least two alternating high-reflective and low-reflectivity packages that may be interpreted as fluvio-lacustrine deposits interbedded with higher energy (i.e. stream to debris flow) deposits, associated with abrupt arrival of lateral inputs from the fans. This explanation well accords with the recent history of the valley. Flooding events caused by alluvial fans have repeatedly been observed in the outcropping deposits in the Valley [i.e. *Fisher*, 1990]. Deposition of low-energy fluvial sediments and lacustrine sediments above alluvial fans are caused by

obstruction of the valley caused by the fan.

As anticipated in the previous section, the southern side of the Adige River (from CMP 275 to the end of the line on Lasa2) show instead, that the sub-horizontal reflective series is disrupted by two reflective features characterized by a broad concave shape. These shapes can be interpreted as erosional features caused by lateral migration of the Adige River, likely forced by the coeval lateral evolution of Gadria Fan from the north. CRS migrated stack of Fig. 11 clearly shows that Gadria Fan is prograding directly above these two synform features, witnessing a subsequent arrival of alluvial sediments form the south that has probably forced the river to migrate northward to its current position. Both seismic sections in Fig. 11 and 14 do not show a clear evidence of recent fluvial deposits below the present location of the Adige; at the contrary, the river seems to flow above a 50 m thick sequence of alluvial deposits with a southward (i.e. Gadria) and northward (i.e. Laas) dip and that interlock at about CMP 225-270, just to the north of Adige. In this area the CRS stack shows a clear overlap of the Gadria Fan above the Laas Fan deposits.

Seismic reflection data well depict the internal architecture of Gadria Fan allowing us to better understand the origin and the growth of this fan. Indeed, CRS but also CMP depth migrated stacks clearly show a layered structure within Gadria Fan, especially at the central part of profile Lasa1 (see Fig. 11a,b; CMPs 200 – 475). This well-devolved stratification of the fan suggests that the Gadria Fan could have evolved through mechanisms of paraglacial progradation, with a mixture of colluvial (debris-flow) and semi-alluvial (hyper-concentrated flow and bedload flows) deposits, as hypothesized by to *Brardinoni et al.,* [2012]. Presence of deposits made of mixed sediments might be related to the different characteristics of the Gadria Fan tributary basins (i.e. Gadria basin and Strimm basin) and consequently can explain the well layered seismic facies within the fan.

2.8 Conclusions

It is well known that alluvial fans development responds to climatic/anthropic changes affecting precipitation style and trend. These changes are recorded and therefore can be revealed by studying the

internal fan configuration. Often surface information, even if aided by GPR techniques, cannot provide data with the completeness required to fully comprehend alluvial fan development. The main goal of this work was to provide high-quality seismic data adequate to study with metrical resolution the internal reflective configuration of two large alluvial fans in the Adige Valley. By the analysis of our results, we can conclude that dense, wide-aperture seismic data in combination with first-arrival tomography and high-resolution CMP/CRS processing can provide high-quality, and low-cost information to aid the study of large alluvial fans in alpine environments.

Other non-secondary goals of the seismic survey were: 1) the full imaging of the valley bedrock along a crucial transect of Adige River Valley and 2) a quantitative evaluation the thickness and pattern of the sediment accumulation above the bedrock. By using dense, wide-aperture seismic arrays we were indeed able to develop reliable tomographic images across the Adige Valley in overlap with high-quality depth migrated CMP and CRS stacks. Redundant information provided by seismic reflection and seismic tomography images allowed, during interpretation, a meaningful comparison between structural and seismic-stratigraphic features visible in the depth migrated CRS and CMP stacks with their P-wave velocity retrieved from first-arrival tomography.

Geometrical relationships between the two large fans flow and fluvial deposits, are well imaged by our seismic data and are very useful to study the growth of the Gadria Fan and its recent interaction with Laas Fan and Adige River development. Moreover, the internal reflective configuration of Gadria Fan allowed us to suggest that rather than catastrophic formation, modulated by large, rapid slope failures, a paraglacial progradation, mainly mediated by debris flows, is the most probable formation mechanism for this very large fan. This last result can be ultimately used by researchers to reveal climatic changes affecting precipitation style and trend, and/or the hillslope sediment production during the Holocene.

Acknowledgments

The data for this paper are available upon request from the corresponding author. The authors are grateful AMRA s.c.a r.l. who provided the seismic source and geophone array. The authors gratefully acknowledge the Geological Survey of the Province of Bolzano (Ufficio Geologia e prove materiali) that founded the present work.

2.9 References

Ackermann, H. D., Pankratz, L. W., & Dansereau, D. (1986), *Resolution of ambiguities of seismic refraction traveltime curves*, Geophysics*, 51(2),* 223-235.

Agliardi, F., Zanchi, A., & Crosta, G. B. (2009), *Tectonic vs. gravitational morpho-structures in the central Eastern Alps (Italy): constraints on the recent evolution of the mountain range*. Tectonophysics*, 474(1), 250-270.*doi:10.1016/j.tecto.2009.02.019.

Andreatta C. (1951). *Carta Geologica d' Italia 1:100000, Foglio n°9 - M.te Cevedale*. Istituto Superiore per la Protezione e la Ricerca Ambientale.

Bergler, S., Hubral, P., Marchetti, P., Cristini, A., & Cardone, G. (2002). *3D common-reflection-surface stack and kinematic wavefield attributes*. The Leading Edge, *21*(10), 1010-1015.doi:10.1190/1.1518438

Brardinoni, F., Church, M., Simoni, A., & Macconi, P. (2012). *Lithologic and glacially conditioned controls on regional debris-flow sediment dynamics*. Geology, 40(5), 455-458.doi:10.1130/G33106.1

Bruno P.P., 2015, *High-resolution seismic imaging in complex environments: a comparison among Common Reflection Surface stack; Common Midpoint stack; and pre-stack depth migration at the Ilva - Bagnoli brownfield site, Campi Flegrei, Italy*, Geophysics, 80/6, 1–12, doi 10.1190/GEO2014-0488.1.

Bruno, P. P., Castiello, A., Villani, F., & Improta, L. (2013). *High-Resolution Densely Spaced Wide-Aperture Seismic Profiling as a Tool to Aid Seismic Hazard Assessment of Fault-Bounded Intramontane Basins: Application to Vallo di Diano, Southern Italy*, Bulletin of the Seismological Society of America, 103(3), 1969-1980.doi:10.1785/0120120071

Bruno, P. P., Improta, L., Castiello, A., Villani, F., & Montone, P. (2010). *The Vallo di Diano Fault System: new evidence for an active range-bounding fault in southern Italy using shallow, high-resolution seismic profiling,* Bulletin of the Seismological Society of America, 100*(*2), 882-890.doi:10.1785/0120090210

Cavalli, M., Trevisani, S., Comiti, F., & Marchi, L. (2013). *Geomorphometric assessment of spatial sediment connectivity in small Alpine catchments*, Geomorphology, 188, 31-41.doi:10.1016/j.geomorph.2012.05.007

Comiti, F., Marchi, L., Macconi, P., Arattano, M., Bertoldi, G., Borga, M. & Theule, J. (2014), *A new monitoring station for debris flows in the European Alps: first observations in the Gadria basin*. Natural Hazards, 73(3), 1175-1198.doi:10.1007/s11069-014-1088-5

Deidda, G. P., Battaglia, E., & Heilmann, Z. (2012). Common-reflection-surface imaging of shallow and ultrashallow reflectors. *Geophysics*, *77*(4), B177-B185.doi:10.1190/geo2011-0401.1

Dix, C. H. (1955). *Seismic velocities from surface measurements*. Geophysics, *20*(1), 68-86.doi:10.1190/1.1438126

Ékes, C., & Friele, P. (2003). *Sedimentary architecture and post-glacial evolution of Cheekye fan, southwestern British Columbia, Canada*. Geological Society, London, Special Publications, 211(1), 87-98.doi:10.1144/GSL.SP.2001.211.01.08

Ekes, C., & Hickin, E. J. (2001). *Ground penetrating radar facies of the paraglacial Cheekye Fan, southwestern British Columbia, Canada.* Sedimentary Geology, 143(3), 199-217.

Fischer, K. (1990). *Entwicklungsgeschichte der Murkegel im Vinschgau*. Der Schlern, 64(2), 93-97.

Franke, D., Hornung, J., & Hinderer, M. (2015). *A combined study of radar facies, lithofacies and three-dimensional architecture of an alpine alluvial fan (Illgraben fan, Switzerland).* Sedimentology, 62(1), 57-86. doi:10.1111/sed.12139

Garabito, G., Stoffa, P. L., Lucena, L. S., & Cruz, J. C. (2012). *Part I—CRS stack: Global optimization of the 2D CRS-attributes.* Journal of Applied Geophysics, 85, 92-101.doi:10.1016/j.jappgeo.2012.07.005

Gilbert, P. (1972). *Iterative methods for the three-dimensional reconstruction of an object from projections.* Journal of theoretical biology, 36(1), 105-117.doi:10.1016/0022-5193(72)90180-4

Harvey, A. M. 2003. *Alluvial fan.* In: Goudie, A. S. (ed.) Encyclopedia of Geomorphology. Routledge, London.

Hayashi, K., & Takahashi, T. (2001). *High resolution seismic refraction method using surface and borehole data for site characterization of rocks.* International Journal of Rock Mechanics and Mining Sciences, 38(6), 807-813.doi:10.1016/S1365-1609(01)00045-4

Hearn, T. M., & Ni, J. F. (1994). *Pn velocities beneath continental collision zones: the Turkish-Iranian Plateau.* Geophysical Journal International, 117(2), 273-283.

Hoecht, G., 2002. Traveltime approximation for 2D and 3D media and kinematic wavefield attributes. *(PhD thesis) University of Karlsruhe*.

Hornung, J., Pflanz, D., Hechler, A., Beer, A., Hinderer, M., Maisch, M., & Bieg, U. (2010). *3-D architecture, depositional patterns and climate triggered sediment fluxes of an alpine alluvial fan (Samedan, Switzerland).* Geomorphology, 115(3), 202-214. doi: 10.1016/j.geomorph.2009.09.001

Hubral, P. (1983). *Computing true amplitude reflections in a laterally inhomogeneous earth.* Geophysics, 48(8), 1051-1062. doi:10.1190/1.1441528

Jäger, R., Mann, J., Höcht, G., & Hubral, P. (2001). *Common-reflection-surface stack: Image and attributes.* Geophysics, 66(1), 97-109.doi:10.1190/1.1444927

Jarman, D., Agliardi, F., & Crosta, G. B. (2011). *Megafans and outsize fans from catastrophic slope failures in Alpine glacial troughs: the Malser Haide and the Venosta Valley cluster, Italy.* Geological Society, London, Special Publications, 351(1), 253-277.doi:10.1144/SP351.14

Mann, J., Jäger, R., Müller, T., Höcht, G., & Hubral, P. (1999). *Common-reflection-surface stack—a real data example.* Journal of Applied Geophysics, 42(3), 301-318.doi:10.1016/S0926-9851(99)00042-7

Mann, J. (2002). *Extensions and applications of the common-reflection-surface stack method* (Doctoral dissertation, Karlsruhe, Univ., Diss., 2002).

Menyoli, E., & Gajewski, D. (2002, January). *Time migrated CRS images of complex inverted basin structures.* In 2002 SEG Annual Meeting. Society of Exploration Geophysicists. doi:10.1190/1.1817104

Müller, T. (1998, June). *Common reflection surface stack versus NMO/stack and NMO/DMO stack.* In 60th EAGE Conference & Exhibition. doi:10.3997/2214-4609.201408166

Neidell, N. S., & Taner, M. T. (1971). *Semblance and other coherency measures for multichannel data*. Geophysics, 36(3), 482-497.doi:10.1190/1.1440186

Ratschbacher, L. (1986). *Kinematics of Austro-Alpine cover nappes: changing translation path due to transpression.* Tectonophysics, 125(4), 335-356.

Ratschbacher, L., Frisch, W., Neubauer, F., Schmid, S. M., & Neugebauer, J. (1989). *Extension in compressional orogenic belts: the eastern Alps.* Geology, 17(5), 404-407.

Ronen, J., & Claerbout, J. F. (1985). *Surface-consistent residual statics estimation by stack-power maximization.* Geophysics, 50(12), 2759-2767.doi:10.1190/1.1441896

Savi, S., Norton, K. P., Picotti, V., Akçar, N., Delunel, R., Brardinoni, F & Schlunegger, F. (2014). *Quantifying sediment supply at the end of the last glaciation: Dynamic reconstruction of an alpine debris-flow fan.* Geological Society of America Bulletin, 126(5-6), 773-790. doi:10.1130/B30849.1

Sölva, H., Grasemann, B., Thöni, M., Thiede, R., & Habler, G. (2005). *The Schneeberg normal fault zone: normal faulting associated with Cretaceous SE-directed extrusion in the Eastern Alps (Italy/Austria).* Tectonophysics, 401(3), 143-166.doi:10.1016/j.tecto.2005.02.005

Thoni, M. (1999). *A review of geochronological data from the Eastern Alps.* Schweizerische Mineralogische und Petrographische Mitteilungen, 79(1), 209-230.

Thöni, M., & Hoinkes, G. (1987). *The southern Ötztal basement: geochronological and petrological consequences of Eoalpine metamorphic overprinting*. Geodynamics of the Eastern Alps, 200-213.

Taner, M. T., Wagner, D. E., Baysal, E., & Lu, L. (1998). *A unified method for 2-D and 3-D refraction statics.* Geophysics, 63(1), 260-274.doi:10.1190/1.1444320

Trappe, H., Gierse, G., & Pruessmann, J. (2001). *Case studies show potential of Common reflection Surface stack: structural resolution in the time domain beyond the conventional NMO/DMO stack*: Special Topic: Seismic processing. First Break, 19(11), 625-633.

Chapter 3

Linking geomorphology and alluvial fan seismic stratigraphy for defining geomorphic process domains in Vinschgau/Val Venosta (Eastern Alps, Italy).

S.Maraio[(1)], F.J. Pazzaglia[(2)], F. Brardinoni[(1)], V. Picotti[(3)], P.P.G. Bruno[(4,*)]

[1] University of Bologna, Department of Biological, Geological and Environmental Sciences, Italy.

[2]Lehigh University, Department of Earth and Environmental Sciences, Bethlehem, PA

[3] ETH Zürich, Department of Earth Sciences, Zürich, Switzerland.

[4] The Petroleum Institute, Department of Petroleum Geosciences, Abu Dhabi, UAE.

[*] Formerly, Istituto Nazionale di Geofisica e Vulcanologia, Roma, Italy

3.1 Abstract

The debate about the formation and the growth of the fans that occupy the bottom of the formerly glaciated Vinschgau/Val Venosta is still open. The main goal of this work is to define the main geomorphic processes active within the tributary catchments of the Vinschgau/Val Venosta, in order to understand the main depositional processes responsible of the fan growth in the area. We compare the seismostratigraphic patterns recognized within the high resolution seismic reflection profiles acquired across Gadria and Lasa fan to their source basins geomorphology. A detailed interpretation of the seismic facies allowed us to identify the stratigraphy and the geometries of the fan deposits. To identify the transport processes, we used GIS analysis to extract data analyzed in the slope-area plot. The study is extended on 6 selected source basins in the valley. Results show a good agreement between the revealed dominant processes within the catchments and the depositional geometries shown by the seismic, while important elements about the formation and the growth of the Gadria fan were found; both seismic reflection data and geomorphic analysis of the source basin, witness that the fan aggradation occurred mainly by means of debris-flow processes. The internal organization of the deposits suggests that deposition was strongly influenced by paraglacial systems. Moreover, the morphology of most investigated channels appear still signed by inherit glacial topography.

3.2 Introduction

Alluvial fans are depositional landforms created by the intersection of high sediments loads and reduced stream power at a point where there is accommodation space for deposition. These conditions are controlled by bedrock, topography and climate in the contributing drainage-basin (*Gómez-Villar & García-Ruiz*, 2000; *Harvey*, 2003), and subsidence in the depositional basin. The term 'alluvial fan' is now generally used in many different environments, and it is widely recognized that these landforms are constructed of both fluvial and debris-flow sediment-transport processes (*Blair & McPherson*, 1994; *Jarman et al.,*2011; *Bierman & Montgomery*, 2014). Relevant to this study, we investigate a type of alluvial fan that occurs in alpine settings where simple tectonic offset along a range bounding fault plays little to no role in generating the typical sediment accommodation space (*Harvey*, 2002). Here we investigate alluvial fans related to the post-glacial and paraglacial sediment dynamics in alpine settings (*Church & Ryder*, 1972; *Franke et al*., 2014) where short time frames allow us to neglect tectonically-generated accommodation. Debris flow, fluvial, and perhaps landslides (*Jarman et al.,* 2011) lead to the growth of alpine alluvial fans (*Franke et al*.,2014) but their respective contributions depend on sediment availability and channel transport capacity within the catchment, characteristics that we seek to investigate in our research.

Studies concerning the alluvial fan morphology and sedimentology are numerous and have explored, with different approaches, the relationship between sedimentary facies, fan morphology, drainage-basin geology and morphology and the sedimentary processes that operate on fan surfaces (*Harvey,* 1988; *Blair & McPherson*, 1994; *Sorriso-Valvo et al.* 1998; *Blair,* 1999a, b; *Crosta & Frattini*, 2004; *Jarman et al.*, 2011; Brardinoni et al., 2012; *Savi et al.*, 2014). In particular, alluvial fan stratigraphy is an important sedimentary archive that records depositional processes (*Colombera & Bersezio*, 2011; Franke et al., 2014) and preserve information about catchment geomorphic and hydrologic change. In addition, the differentiation between debris-flow and stream-flow is of a particular importance since construction of residential buildings and transport infrastructures on alluvial fans has increased the vulnerability to mass-flow and debris-flow events, thus augmenting the overall risk (*Comiti et al.*, 2014).

The purpose of this paper is to compare the stratigraphy of a large alpine fan to its source basin geomorphology with the goal of linking sedimentological facies in the fan to the processes inferred from the geomorphology of catchment channels. We focus on 6 selected catchments within the Venosta Valley, in the Eastern Italian Alps (figure 1). Our stratigraphic model, is anchored in the Gadria fan area (figure 2) and includes high resolution seismic reflection data. There has been significant recent interest in the Vinschgau valley bottom because it hosts the biggest group of anomalously large fans within the European Alps, the origin of which is still matter of debate (*Fischer*, 1965). One model for large fan genesis (*Jarman et al.,* 2011) on the basis of morphometric analyses and interpretation of section missing in the source basins, is that they originated from giant catastrophic landslides in the immediate post-glacial period. On the other hand, *Brardinoni et al.* (2012) explains the growth of these fans as a result of paraglacial evacuation of glacial and glacio-fluvial deposits, and downstream fan progradation due to debris-flow activity, using contemporary debris-flow sediment flux and fan area and of the presence of largely eroded kame terraces in the Gadria headwaters. Four catchments (i.e. Gadria, Strimm, Lasa Valley and Zielbach) were chosen because of the seismic data availability across their relative fan; the other two basins (Planeil Valley and Plawenn) were chosen in order to test the Jarman (2011) theory about the Mals fan formation. Our work builds on earlier, similar efforts by *Savi et al.* (2014) who provides a reconstruction of the Zielbach alluvial fan system from the late Pleistocene and *Comiti et al.* (2014) who analyze the results of a monitoring network for contemporary debris-flow events in the Gadria catchment.

The first part of this paper presents a stream power law-based slope-area analysis (e.g., *Montgomery & Foufoula-Georgiou*, 1993; *Ijjasz-Vasquez & Bras*, 1995; *Brardinoni and Hassan,* 2006) to identify process-based topographic signatures for 23 channels within 6 drainage-basins in the Venosta Valley. In the second part of the paper, we are able to compare catchment geomorphology with fan stratigraphy through interpretation of the seismic facies from high resolution reflection seismic profiles, acquired across the Gadria fan (10.9 km2), one of the biggest fans in the valley. The relationship between the main depositional processes and the internal architecture of the fan has important implications for understanding alpine alluvial fan processes in general.

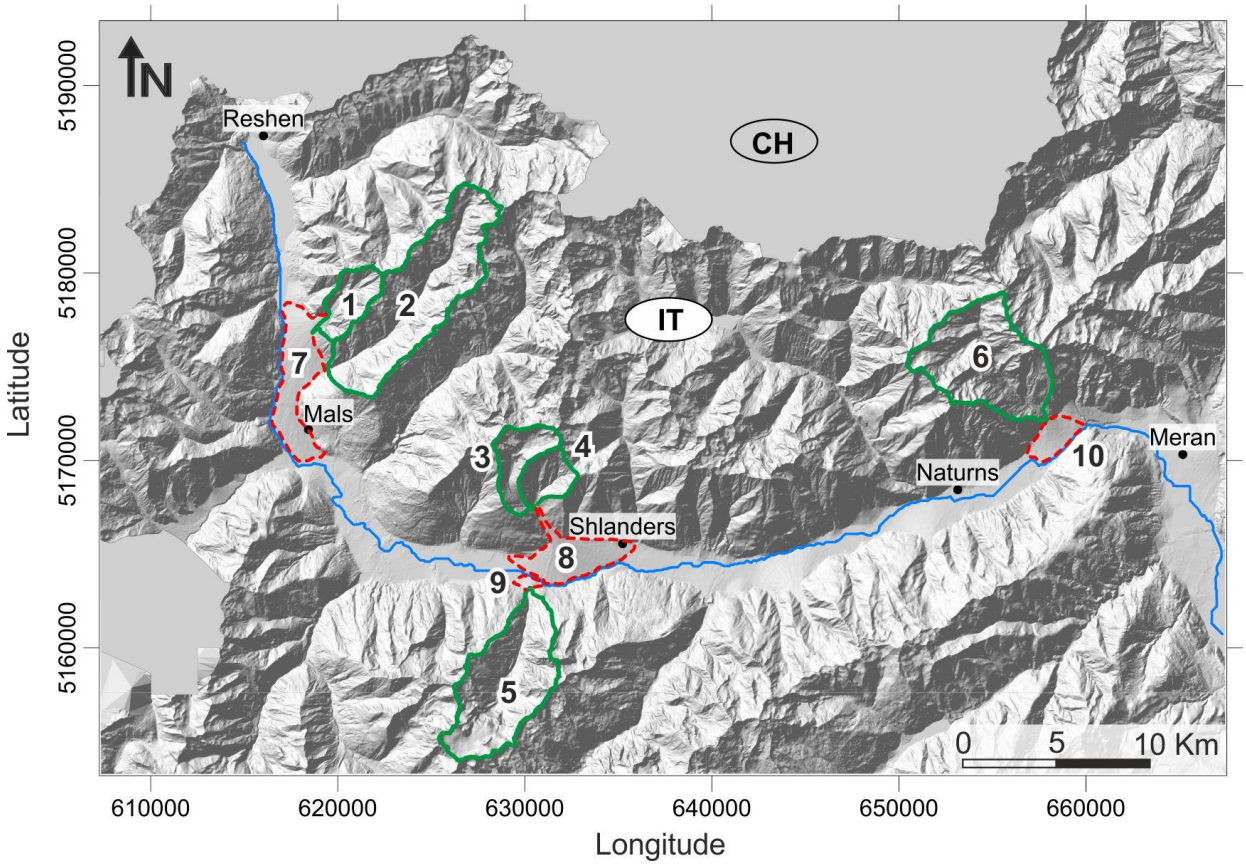

Figure 1: Map of Venosta Valley on Digital Elevation Model by Provincia Autonoma di Bolzano with location of surveyed catchments and related fans: 1) Plawenn Basin; 2) Planeil Valley; 3) Strimm basin; 4) Gadria basin; 5) Lasa Valley; 6) Zielbach basin; 7) Malser Haide fan; 8) Gadria fan; 9) Lasa fan; 10) Zielbach fan.

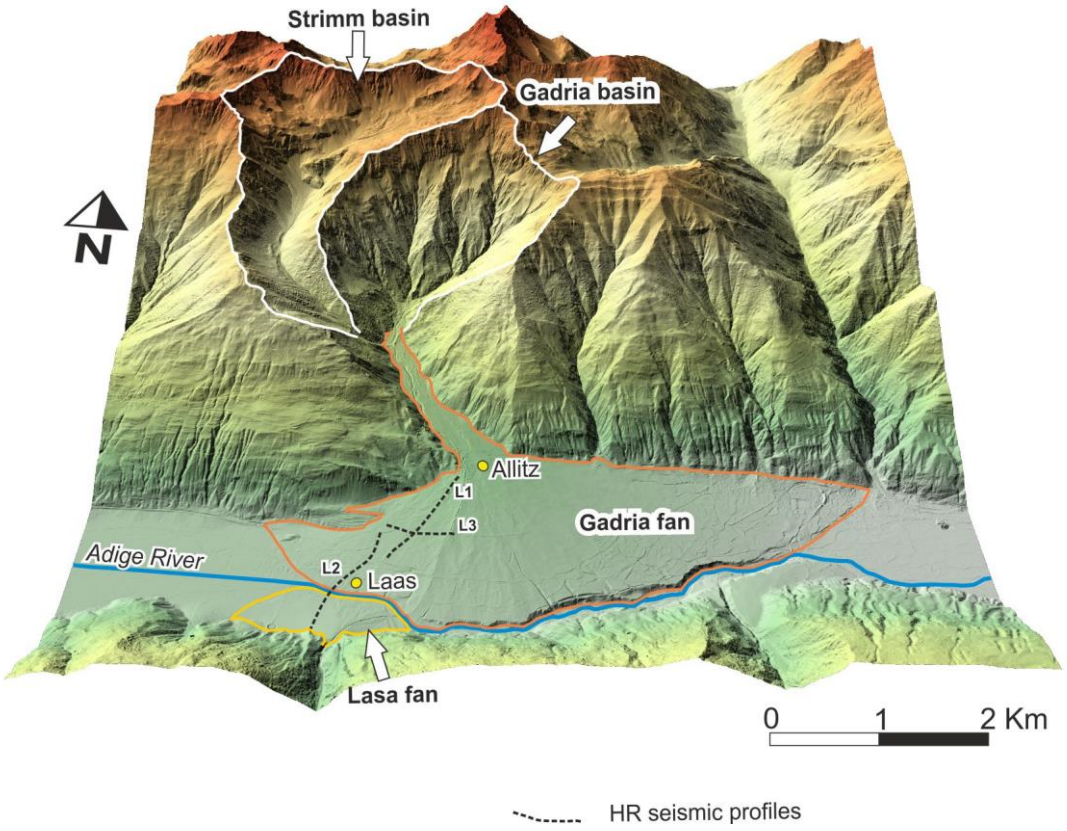

Figure 2: Digital Elevation Model of the seismic survey area by Provincia Autonoma di Bolzano, with the high resolution seismic profiles location across the Gadria and Lasa fans. Two profiles (Lasa1 and Lasa2) are transverse to the valley, while Lasa3 profile is parallel to the valley axes.

3.3 Local setting

Val Venosta (Vinschgau) is a major east-west oriented glacial trough of the east-central Italian Alps drained by the Adige River. Traversing a thick stack of Helvetic, Penninic and Austroalpine nappes, (*Ratschbacher,* 1986, 1989; *Dal Piaz et al.,* 2003; *Sölva et al.*, 2005). The Adige River flows east for 42 km, falling 400 m to Meran with its flow obstructed by a large fan complex. The headwaters of the Val Venosta ascends north into the Reschen Pass. The bedrock is composed principally of the Austroalpine metamorphic rocks of the Oetztal unit and Campo nappe comprised of metapelites and metapsammites, with subordinate orthogneiss, metabasites and calcschists (*Ratschbacher* 1986; *Thoni* 1999*; Sölva et al.*, 2005; *Agliardi et al*, 2009). The interested reader is directed towards the excellent scholarship of several authors who summarize the geologic and tectonic

evolution of these units (*Ratschbacher*, 1986; *Thöni & Hoinkes*, 1987; *Ratschbacher et al.*, 1989; *Thöni,* 1999; *Sölva et al.*, 2005). Of importance to this study, the Val Venosta exploits the east-west trending Vinschgau shear-zone, which separates the Oëtztal Unit, from the underlying Campo Nappe (*Sölva et al*., 2005). The structural patterns of these units, characterized by fractures oriented along N, E, NE and SW directions, control the spatial structure of the entire drainage network. Thick, unconsolidated Quaternary alluvial and glacial deposits fill the valley, obscuring the contact between the two units (*Comiti et al.,* 2014).

The valley has been affected by repeated glaciations in the Pleistocene that have produced glacial, while intervening paraglacial and interglacial processes, continued during the Quaternary, have influenced the distribution of surficial materials (*Hinderer,* 2001; *Brardinoni et al.,* 2012) and in some cases continue to do so. The access to sediment in this glacially sculpted landscape, tapping highly fractured metamorphic rocks, together with the steep topography, create the conditions consistent with the generation of debris flows and must contribute, in some way, to the large number of alluvial fans characterizing the Val Venosta. Indeed, the valley bottom hosts the biggest group of anomalously large fans within the European Alps (*Jarman et al.*, 2011), which often obstruct and deviate the course of the Adige River.

3.4 Methods

Slope-area analysis

A geomorphic process domain is defined as an area where a suite of geomorphic processes creates distinctive landforms and disturbance regimes defined in terms of frequency, magnitude, and duration of the associated impact (*Montgomery,* 1999). In this study, we are particularly concerned with objectively distinguishing watersheds that are dominated by hillslope processes, namely debris flows, from watersheds that are dominated by fluvial processes. Stream longitudinal profiles expressed in slope (S) drainage area (A), space represent a useful tool to delineate the process domains of the fluvial components in a landscape (*Montgomery & Foufoula-Georgiou,* 1993; *Ijjasz-Vasquez & Bras,* 1995; *Tucker & Bras,* 1998; *Stock & Dietrich,*

2003; *Brardinoni & Hassan,* 2006). Slope-area analysis assumes a steady state condition, which in rock uplift rate (U) and lowering rate (E) are balanced, and a transport-limited erosion law

$$S = (U/K)^{1/n} A^{(1-m)/n} \quad (1)$$

where *K is* a constant related to lithology, climate and erodibility, *m* represents the scaling between discharge and drainage area, and *n* is related to different erosional processes. As shown in figure *3*, in this case, erosion by hillslope or fluvial processes is characterized respectively by the positive or inverse relationship between drainage area and slope (i.e. *m < 1* or *m > 1*) (*Montgomery,* 2001).

Several authors (*Hack,* 1957; *Flint,* 1974; *Moglen & Bras,* 1995; *Hurtrez & al.*, 1999; *Snyder & al.*, 2000; *Kirby & Whipple,* 2001) have shown that the channel slope can be defined by a power law, with slope expressed as a function of drainage area:

$$S = k_s A^{-\theta} \quad (2)$$

where k_s is the steepness index and θ represents the convex index. Equation (2) is also the simple form of a straight line in a logarithmic space, where k_s is the y-intercept of the regression line and θ is the slope of regression data.

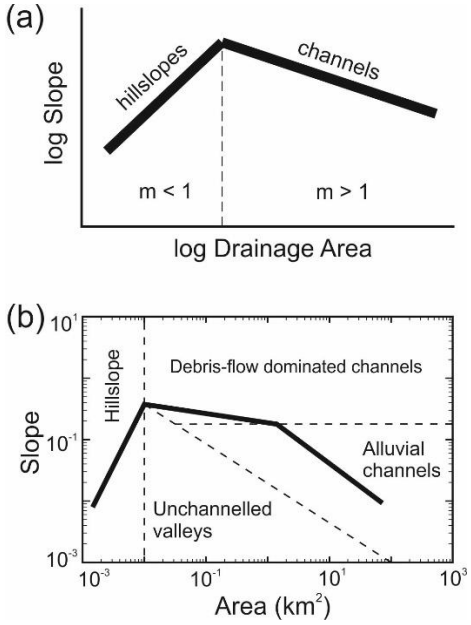

Figure 3: a) relation between area and slope described by equation (1), by Montgomery, 2001. b) schematic representation of process domains in slop area log-log plot for an unglaciated environment in steady state, by Brardinoni & Hassan, 2006.

The symmetry between equation (1) and equation (2), clearly suggests a relationship between k_s and $(U/K)^{1/n}$ and between θ and m/n. Indeed, several studies, aimed to find a correlation between k_s and tectonic uplift, (*Sklar & Dietrich,* 1998; *Hurtrez & al.* ,1999; *Whipple & Tucker,* 1999; *Snyder & al.,* 2000; *Kirby & Whipple*, 2001) indicate that k_s is dependent and θ is independent of rock uplift and it is related to other factors, like orographic precipitation variations within the basin (*Roe & al.*, 2002) and mean annual rainfall intensity and mean peak annual discharge (*Zaprowski & al.*, 2005).

We performed slope-area analysis on the longitudinal profile of 23 streams, from 6 selected catchments in Val Venosta (fig. 1 and fig. DR1). Long profiles were extracted from a 2.5 m horizontal, +/- 25 cm to +/- 45 cm vertical resolution digital elevation model from LiDAR topography by Provincia Autonoma di Bolzano. After a processing phase aimed to remove data errors and sinks in the DEM, hydrologic GIS analysis were applied using ArcView 10.1 in order to extract a valley drainage network, using a minimum common threshold drainage area of 0.01 km^2. The use of a very low minimum drainage area threshold, allowed us to extend the analysis to small headwater streams. The drainage area profiles and the elevation profile were extracted from the flow accumulation grid and DEM respectively and smoothed using a loess algorithm (elevation profile) and a running median algorithm (drainage area) in order to obtain 40 equally-spaced slope and

drainage area data. Then data were plotted in a log-log space and analyzed on the base of the regression slope (then θ) and through the comparison with the results from analogous published studies (i.e. *Montgomery et al.*, 1993; *Brardinoni & Hassan,* 2006). The selected channels represent some complex cases where the single power law for unglaciated channels is not acceptable. *Brardinoni & Hassan* (2006) verified that in formerly glaciated terrains, the slope-area relation is not totally controlled by different signature of colluvial and fluvial processes, but forced by past glacial geomorphic processes. In particular, channel profiles in glacial environments, often are affected by significant steps, not observed in unglaciated landscapes; prominent steps in glacial terrains frequently coincide with glacial macroforms, namely hanging valleys (referred to the floor of relict glacial cirques) with relative valley steps (as the transition between hanging valley and relict glacial troughs), paraglacial fans and cones. In terms of slope-area relations, this translate into multifragmented pattern, with kinks that are not always connected to a variation in process dominance; this occurrence makes the identification of the transition between different processes particularly difficult. The alternative classification of process domains in a slope-area plot has been proposed by *Brardinoni & Hassan* (2006), as result of their studies in a glaciated basins of coastal British Columbia (fig. 5); this schematic representation distinguishes colluvial and fluvial processes in relation of glacial macroforms, with positive slope-area relations corresponding with the transition between hanging valley (fluvial) and the origin of colluvial reaches, and segments characterized by negative relation, associated with colluvial channels.

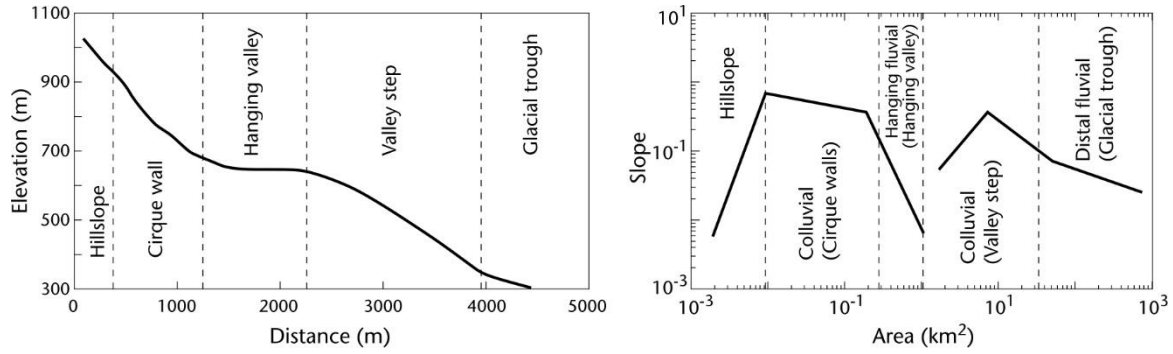

Figure 4: schematic representation of the alternative process domains classification proposed by Brardinoni & Hassan 2006 for formerly glaciated environment. See text for further explanation.

Seismic data

We acquired and processed about 4 km of high resolution reflection/refraction profiles across the Gadria fan (*Maraio et al.*, 2015). The main goals of the seismic acquisition and its interpretation are to investigate the structure and the depth of the bedrock, the morphology of the valley, the thickness of fluvial and alluvial sediment, and characterize the stratigraphic relationship between the axial fluvial facies and tributary alluvial fan facies. Two profiles are oriented n-s, transverse to the valley. They start near the Gadria fan apex, cross the Adige River, and extend to the Lasa fan apex. A third profile traverses the alluvial fan e-w, parallel to the valley and intersects the transversal profiles (figure 2). In order to define the dominant processes responsible for both Gadria and Lasa fans growth, following the classical technique in seismic stratigraphy (*Veeken,* 2013; *Shlunegger et al.*, 1997; *Vanderburgh & Roberts,* 1996; *Sangree & Widmier,* 1979) we classified the different seismic facies of the alluvial fan deposits, on the base of the seismic attributes (frequency, amplitude), geometry and continuity of reflectors and reflectors configuration (parallel, inclined, chaotic). Furthermore, several author (*Franke et al.*, 2014; *Hornung et al.*, 2010) performed a linking between lithological facies in debris flow fan environment and GPR facies, using the principles derived from seismic stratigraphy. We conducted our interpretation on the basis of these studies, in the context of the different resolution and penetration depth of our lines.

3.5 Results

Slope-area analysis

Figure 4 shows area-slope relationships data obtained from the investigated basins. As mentioned in the local setting section, the survey area has been sculpted by past glacial processes, therefore we interpreted the results from slope-area plot, using the alternative lecture key shown in figure 5.

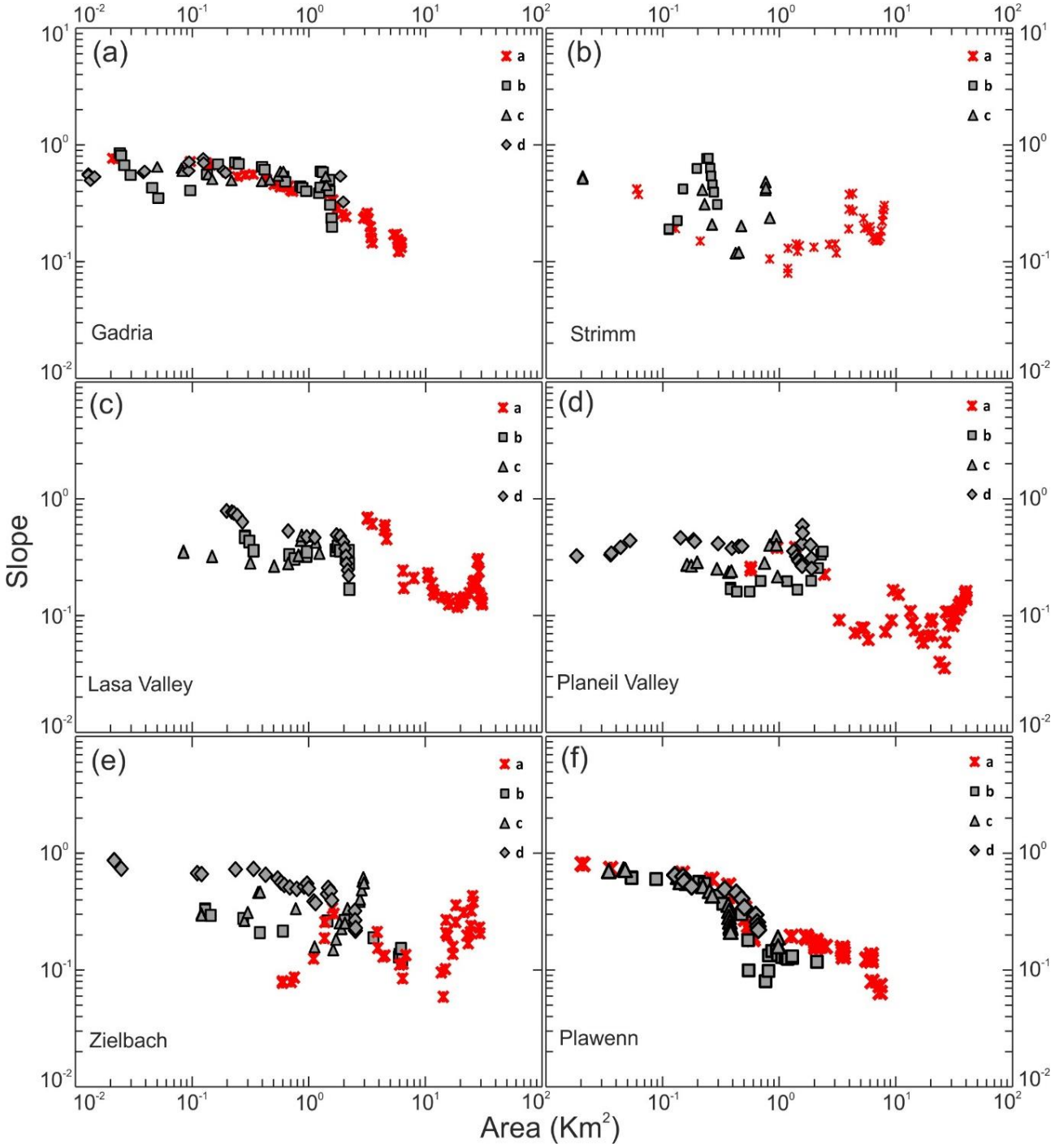

Figure 5: Slope-area relations for the six investigated basins; a) Gadria basin; b) Strimm basin; c) Lasa Valley; d) Planeil Valley; e) Zielbach basin; f) Plawenn basin. Relations series in red are related to the main channel for each catchment. It is clear that slope area relations in a formerly glaciated environment have more complex pictures.

Our analysis reveals that just the slope-area plot from Gadria catchment channels (fig. 4a) fits the *Montgomery & Foufoula-Georgiou* (1993) idealized theoretical model, within hillslope, colluvial and fluvial

domains are characterized by a clear separation. There is a good agreement between the data distribution of the investigated cirque and valley walls channels within the Gadria basin. Evidently debris flow processes dominate on the observed channels (i.e. $\theta = 0.069$) and the transition between debris flow and fluvial transport (i.e. $\theta = 0.737$) occurs at about 1 km^2 area; this value has been documented by several authors as transition point from debris flow dominated to fluvial channel (*Lague & Davy, 2003; Montgomery, 2001; Montgomery & Foufoula-Georgiou, 2003 Snyder et al., 2000)*.

Data relations on the slope area plot from the Strimm basin (fig. 4b) appear clearly multifragmented, with portions of stream channels characterized by negative concavity index, that translates into a sequence of fluvial and colluvial processes related to the presence of hanging valleys in the upper part of the catchment (fig. DR1b). Along the main channel (i.e. channel b in fig. 4b), where fluvial-alluvial transport dominates, a prominent kink occurs at about 4 km^2 area, followed by a portion of channel with $\theta = -3.978$, in correspondence of the valley step that denotes the transition between the hanging valley and the glacial trough. A strong increase in slope is also visible in the final part of the main channel (fig. 4b), caused by the valley step at the confluence of the Strimm Creek in the Gadria Creek (fig. DR1b). Dominant fluvial transport characterizes also the main channel of the Lasa Valley (i.e. channel a in fig. 4c), that present a number of kinks, principally caused by paraglacial fans and cone as well as by deposits from valley walls colluvial channels on the valley bottom. We ignored the headwater of this channel because of the glacier presence. Slope-area relations of the investigated tributary channels (i.e. b, c, d in fig. 4c) reveal colluvial processes (i.e. $0.077 < \theta < 0.161$) until about 1 km^2 area, where, the decrease in slope suggests the transition in fluvial processes (i.e. $1.42 < \theta < 5.187$). Slope-area relations from the analyzed channels within Planeil Valley (fig. 4d) exhibit a trend similar to that seen for Lasa Valley. Also within this catchment, glacial "fingerprint" seems to play a fundamental rule, producing a multifragmented data distribution, especially on the main channel (i.e. channel a in fig 4d), that generally appears dominated by fluvial-alluvial processes. One of the tributary channels from the valley walls (channel d in fig 4d) is characterized by a concavity index ($\theta = 0.118$) typically associable with colluvium dominated processes (fig. DR1d). Zielbach basin is also drained by a main channel strongly affected by several steps (fig. DR1e), probably related also to lithologic and structural features, in

addition to glacial sculpting. The presence of a number of steps along the main channel profile, is reflected on the slope-area plot as poorly defined domain boundaries from about 10 km^2 to the end of the profile. Fluvial-alluvial processes are dominant in the catchment both in the main channel and in the tributary channels b and c shown in figure DR1e, while channel d clearly show a colluvial dominance (i.e. $\theta = 0.156$) and is furthermore characterized by a very steep headwater (i.e. slope ≈ 0.9 m/m). The sixth analyzed basin is Plawenn basin, that is adjacent to Planeil valley and it can be divided in five small drainage area tributary basins. Looking at Plawenn longitudinal profiles in figure DR1f, the concave shape is undoubtedly related to debris flow processes. Indeed, the slope-area relations of the four investigated channel (fig. 4f), reflect perfectly this information. Stream channels exhibits a high slope values in the first 0.4 Km^2 area, then we observe an abrupt decrease in slope at the transition between the cirque and valley walls (debris-flow dominated $\theta = 0.177$) and the alluvial deposits that fill the catchment bottom (fluvial dominated $\theta = 1.35$).

Seismostratigraphic interpretation

High resolution seismic reflection profiles acquired across both Gadria and Lasa fan are shown in figure DR2 and DR3. The seismic profiles Lasa1 and Lasa2 show the top of metamorphic bedrock, represented by low-frequency, high-amplitude reflectors, revealing the morphology and the depth of the valley (about 300m). The high reflective package, related to the fluvial deposits of the Adige River, fill the valley, presenting different fluvial and fluvio-lacustrine depositional facies, in response to the interaction between the river and the alluvial fans. All seismic sections show an upper seismic facies, on average 100 m thick, representing the alluvial fan deposits. Vp velocities by the seismic refraction analysis and outcropping deposits support our interpretation related to the alluvial deposits. Figure 6 and 7 show the seismic migrated sections and we focused on the shallower seismic facies interpreted as alluvial fan deposits in figures DR2 and DR3.Seismic profiles in figure 6 show that Gadria fan are characterized by well-defined seismic facies and internal reflection patterns, because of the alluvial deposits thickness. In detail the proximal part of the fan is made up until about 350 m by more discontinuous, divergent, truncated and chaotic reflections characterized by variable amplitudes and frequencies (fig. 6). This seismic pattern is related to high-energy depositional environment and could be interpreted as very coarse unsorted debris flow deposits with clast and blocks,

which typically occurs at proximal position of the fan (*Veeken,* 2013; *Vanderburgh & Roberts,* 1996). Between 350 m and 800 m and between 1200 and 1600, at a depth range from ≈ 25 to the basis of the fan deposits, the seismic pattern is very similar to the previous described facies, but also is clear an increase in the continuity of reflectors and the occurrence of curve shaped reflectors at different depth. This facies resembles massive debris-flow deposits, but it also shows a higher degree of internal organization and a better lateral continuity in depositional geometries.

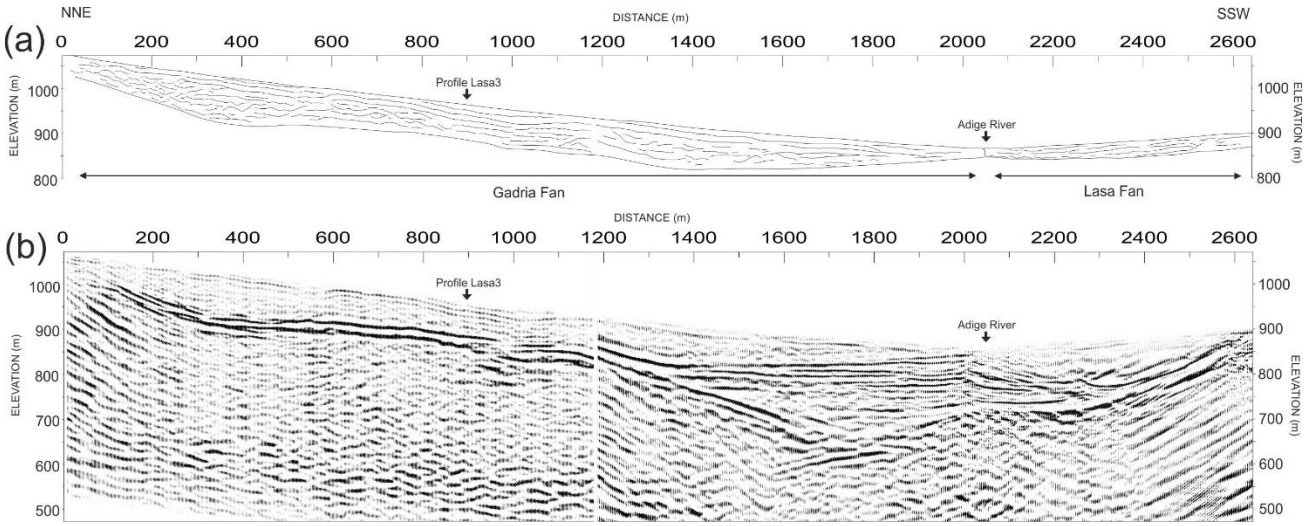

Figure 6: a) line-drawing of the seismic facies characterizing the fan deposits in profiles Lasa 1 and Lasa 2; b) seismic migrated sections for profiles Lasa1 and Lasa2, See text for further explanation. Vertical and horizontal scales are equal.

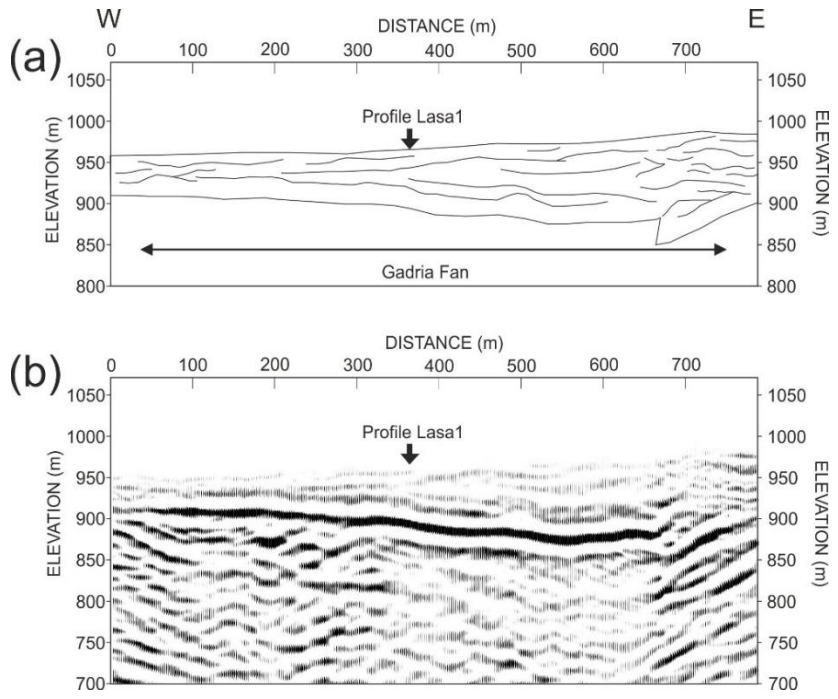

Figure 7: a) line-drawing of the seismic facies characterizing the fan deposits in profile Lasa 3; b) seismic migrated section for profile Lasa3, See text for further explanation. Vertical and horizontal scales are equal.

The curve shaped reflectors (defined "M-shaped and "W-shaped" by *Franke et al.* 2014) are consistent with debris-flow paleo-channels, active during the fan aggradation. The seismic facies of the fan medial portion is characterized by ≈ 50 meters thick and ≈ 150 meters (i.e. between 850 and 1000 meters) wide parallel and subparallel, continuous reflectors with medium amplitude and constant frequency. The lateral continuity, the stratified pattern and the higher amplitudes witness the transition to a different grain size deposits, like as matrix-rich deposits with sand and sorted cobbles and gravel, type debris-flow diamicton. Moreover, there is a perfect agreement between this seismic facies and that present on profile Lasa3 (showed in fig. 7), which intersect the profile Lasa1 at metric 900 (fig. 6). Profile Lasa3 shows, within the alluvial fan deposits, curve shaped, continuous reflectors, probably associated with debris-flow buried channels and three variable amplitudes, continuous reflectors, slightly dipping towards west, that depict a lateral accretion of Gadria alluvial fan. The same seismic facies is also visible in the distal part of alluvial fan (i.e. 1600-2000 m), showing higher continuity of the reflectors and medium to low amplitudes, parallel or subparallel to the fan topography; a sort of prograding downlaps are also detectable at the toe of the fan (*Veeken,* 2013). The

shallower part of the alluvial fan deposits, in medial and distal part, exhibits a couple of continuous and parallel reflectors interpreted as well-stratified horizontally bedded sediments. This seismic facies is interpreted as a horizon of well-sorted sands and gravel deposits, associated to bed-flow and stream-flow transport.

Internal reflectors and organization patterns are not well defined within the Lasa fan deposits (fig. 6), because of a limited thickness of the fan, however seismic internal architecture of the Lasa fan deposits appear different from that of the Gadria alluvial fan. It is characterized by a series of subparallel curve shaped reflectors, continuous for some segments, with variable amplitude (often low amplitude) and low frequency. Low amplitudes witness the low contrast of impedance within the deposits, indicating poorly-stratified sediments; the internal organization, suggest the association of this facies with reshaped deposits, probably linked with a mixture between bedload flow and mass-flow processes.

3.6 Discussion

Gadria Fan and its source basins (i.e. Gadria and Strimm basins) are one of the most studied and interesting alluvial fan system in the eastern Alps, because of the fan dimension and the geomorphic differences between the sediment alimentation basins. Slope-area analysis of all the investigated channels within the Gadria catchment (i.e. fig 4a) demonstrates that debris-flow activity is a principal responsible for the sediments transport. According to *Comiti et al.* (2014), the debris flow activity within the Gadria fan is facilitated by the highly fractured metamorphic lithology, by the steep topography (see fig. DR1 a) and by the availability of glacial sediment. On the other hand, Strimm catchment channels show a clear alternation between colluvial and fluvial domain processes, with colluvial processes that occur only in correspondence of the valley steps, present in both main and tributary channels; this essentially translates in a bedload stream dominant transport. Both sediment supplies are recognizable in the alluvial fan seismic facies. Debris flow and massive deposits, indeed, mainly occupy the proximal position of the fan and the grain size decrease is observable towards the distal part of its. Moreover, some evidence of the fan lateral accretion through

different debris-flow events are also visible on the seismic profiles, especially on profile Lasa3. The shallower part of the seismic profiles shows a well-stratified well-sorted horizon, related to deposits compatible with the Strimm dominant processes. The fan internal stratigraphy also indicatesa different sediment availability and different sediment grain size in relation to the climate changes in the area, possibly during the last deglaciation; logically, during this period, deposition of high quantity of massive deposits from Gadria catchment hindered stream flow and bedload deposits from Strimm basin, the influence of which is more marked in the shallow and in the distal part of the fan. Slope-area analysis results witness the fluvial-alluvial dominant processes in the Lasa Valley; colluvial (debris-flow) transport processes are marked generally on the valley steps, along the main channel, and on the valley walls channels, which are often linked to the main channel through paraglacial fans. The pattern on seismic profile also suggests alternated high and low energy depositional processes, namely respectively mass-flow and bedload flow. This can be explained by the higher degree of connection between the colluvial dominated tributary from the valley walls in the medial-final part of the valley (i.e. channel d in figure DR1) and the catchment outlet. In contrast with sediments from the upper part of the valley, sediments from these tributary basins are not trapped within the valley bottom, due to the absence of paraglacial fans and cones in the segment between these tributary junctions and the valley outlet. Slope-area data distribution of the channels within the Zielbach catchment clearly reveal the presence of one debris-flow dominated tributary basins (i.e. channel d in fig. 4 e and in figure DR1e), while fluvial-alluvial processes are dominant on the other investigated channels. *Savi et al.* (2014) described the Zielbach channel as divided in two different sectors on the basis of its geomorphic features: the bigger one sector (defined “main catchment”) characterized by steep topography, high cascades and steep-pool segments, in which are comprised channels a (i.e. the main channel), b and c showed in figure DR1 e and the eastern tributary debris-flow basin (defined “debris-flow catchment”), which is represented by channel d in figure DR1 e. Seismic facies (figure DR12), interpreted as Zielbach fan deposits by *Savi et al* (2014), exhibits an internal architecture characterized by low amplitude and low frequency discontinuous and divergent reflectors, associated to poorly stratified and sorted sediments, which typically occur in high energy deposition environments. Moreover, some boreholes cores (see *Savi et al.* 2014 for details) confirmed that

the Zielbach fan is mainly composed of debris-flow deposits and this suggests that the debris-flow basin identified within the Zielbach catchment (i.e. channel d in figure DR1e) is the primary responsible for the fan growth. There are no available geophysical surveys or boreholes for the Malser Haiden fan, then the link between the sediment sources and the fan deposits is no achievable. Slope -area analysis reveals that Plawenn basin is undoubtedly dominated by debris-flow processes, while Planeil Valley shows geomorphic features similar to those observed for Lasa Valley. Also within the Planeil Valley (generally fluvial dominated) there is a channel (channel d in fig. DR1 d and fig. 4 d) distinguished by dominant colluvial processes and by a good degree of connection between the hillslope and the valley outlet.

Overall, strong influence of the last glaciation conditions on the investigated landscape is revealed by our analysis. Past glaciation sculpting appear as principal cause of prominent kinks on longitudinal profiles imposing the channel morphology and also influencing the establishment of contemporary geomorphic process domains. Channels analysis reveal different timing in the channel recover from being first shaped by glacial, despite the surrounding conditions, namely lithology, tectonic, climate changes and glaciation conditions are almost equal for the entire valley. Longitudinal profiles of Gadria and Plawenn channels, contrary to what is showed in the other surveyed catchments, do not exhibit clear morphological elements related to glacial inherited topography; the same condition also appears at catchment scale in the Zielbach basin, that present clear glacial “fingerprints” along all the analyzed channels, except for channel *d*, in which there are not evident glacial signatures. This might be explained by a steeper topography characterizing these channels, that has strongly influenced the erosion and the sediment evacuation, allowing the recovering from past glaciations.

The influence of past glaciations conditions is also manifested within the surveyed fan deposits. We observed in seismic profiles a predominance of debris flow facies in the deeper portion and in the proximal part of the fans; this disposition is probably correlated to the paraglacial activity occurred in the area from the last deglaciation, in terms of both climate change and sediment availability within the catchments. For instance, in paraglacial model proposed by Ballantyne (2002) for formerly glaciated environment, he distinguish between two different paraglacial systems: the primary system, occurred immediately after the glaciers

retreat, characterized by the deposition of a large volume of glacial sediments and the subsequently secondary system, in which the sediment transport and deposition are conditioned also by re-working of older paraglacial sediments. The first phase of high sediment production and transport is also facilitated by wetter and warmer climate that increased the transport capacity of streams and rivers (Hinderer 2001), and by poor vegetation coverage. Consequently, this translates in transport and deposition of unsorted and coarse grained sediments, principally through mass-flow processes and explains the presence of this kind of material in the lower portion of investigated fans. While the second phase, marked principally by fluvial and alluvial transport processes, might be responsible for the deposition of more organized sediments, recognized in the upper and in the distal part of the fan. These two phases are dated, in the European Alps, respectively between 12 ka and 9 ka B.P. and between 5.8 ka and 2 ka BP (Soldati et al., 2004).

3.7 Conclusions

The main purpose of this research was to investigate the connection between the dominant geomorphic processes within the catchments and the internal architecture of the associated fans, using respectively the slope-area analysis and the interpretation of the sesimostratigraphic facies resulting by high resolution reflection seismic profiles. Our results confirmed that the slope-area relations for unglaciated environments are inappropriate in formerly glaciated environments, where slope-area relations have more complex features, due to past glacial geomorphic processes. In order to investigate the geomorphic processes within the catchments, we followed the alternative schematic representation of process domains in a log-log plot, proposed by *Brardinoni & Hassan* (2006) for glaciated environments. Applying this lecture key, slope-area method has been able to identify the dominant processes within the investigated channels. On the other hand, the high resolution of the seismic profiles allowed us to perform a detailed analysis of the seismic facies and the internal patterns related to the Gadria and Lasa fan deposits, witnessing the main deposits composition. Consequently, we used the high resolution seismic profile interpreted and described by *Savi at*

al. (2014) for the characterization of the Zielbach fan seismic facies and then for linking the seismic patterns with the revealed geomorphic processes within the Zielbach catchment.

Overall dominant geomorphic processes, detected within the basins through the slope-area relations, are in good agreement with the observed deposit composition of the alluvial fans, showed by the seismostratigraphic interpretation. Both longitudinal profile analysis and alluvial fan seismo-stratigraphy highlights the influence of the past glaciation on the Val Venosta landscape. Most of the investigated channels has not substantially recovered from past glaciations and their morphology is still strongly controlled by glacial inherited topography, while paraglacial activity has played an important role on the transport and deposition of alluvial fan sediments. No evidences of catastrophic landslides, as proposed by Jarman et al. (2011), are recognized in geomorphic analysis and stratified patterns within the fan deposits suggest the predominance of fluvial and colluvial (debris-flow) transport processes. Jarman et al. (2011) suggest that catastrophic mechanism hypothesis for the fan formation in Val Venosta can be confirmed if non-stratified constitution is demonstrated by depth investigations. Results from our high resolution geophysical investigations provide information about the formation of the investigated alluvial fan through paraglacial progradation, principally by means of colluvial and fluvial transport. Moreover, this research shows that the combination between geomorphic analysis and near-surface high resolution seismic, can provide a powerful tool for the study of alluvial fans, both in terms of composition and formation mechanism. The interaction between these two different methodologies in a formerly glaciated environment, is able to give also information useful for studies about climate changes in the post-glacial period.

3.8 References

Agliardi, F., Zanchi, A., & Crosta, G. B. (2009), Tectonic vs. gravitational morpho-structures in the central Eastern Alps (Italy): constraints on the recent evolution of the mountain range. Tectonophysics, 474(1), 250-270.

Ballantyne, C.K., 2002. A general model of paraglacial landscape response. The Holocene 12 (3), 371–376.

Bierman, P. R., & Montgomery, D. R. (2014). *Key Concepts in Geomorphology*. Macmillan Higher Education.

Blair, T. C., & McPherson, J. G. (1994). Alluvial fan processes and forms. In *Geomorphology of desert environments* (pp. 354-402). Springer Netherlands.

Blair, T. C. (1999a). Cause of dominance by sheetflood vs. debris-flow processes on two adjoining alluvial fans, Death Valley, California. *Sedimentology*, *46*(6), 1015-1028.

Blair, T. C. (1999b). Sedimentary processes and facies of the waterlaid Anvil Spring Canyon alluvial fan, Death Valley, California. *Sedimentology*, *46*(5), 913-940.

Brardinoni, F., & Hassan, M. A. (2006). Glacial erosion, evolution of river long profiles, and the organization of process domains in mountain drainage basins of coastal British Columbia. *Journal of Geophysical Research: Earth Surface (2003–2012)*, *111*(F1).

Brardinoni F, Church M, Simoni A, Macconi P (2012) Lithologic and glacially conditioned controls on regional debris-flow sediment dynamics. Geology 40(5):455–458

Cavalli, M., Trevisani, S., Comiti, F., & Marchi, L. (2013). Geomorphometric assessment of spatial sediment connectivity in small Alpine catchments, Geomorphology, 188, 31-41.

Church, M., & Ryder, J. M. (1972). Paraglacial sedimentation: a consideration of fluvial processes conditioned by glaciation. *Geological Society of America Bulletin*, *83*(10), 3059-3072.

Colombera, L., & Bersezio, R. (2011). Impact of the magnitude and frequency of debris-flow events on the evolution of an alpine alluvial fan during the last two centuries: responses to natural and anthropogenic controls. *Earth Surface Processes and Landforms*, *36*(12), 1632-1646.

Comiti, F., Marchi, L., Macconi, P., Arattano, M., Bertoldi, G., Borga, M. & Theule, J. (2014), A new monitoring station for debris flows in the European Alps: first observations in the Gadria basin. Natural Hazards, 73(3), 1175-1198.doi:10.1007/s11069-014-1088-5

Crosta, G. B., & Frattini, P. (2004). Controls on modern alluvial fan processes in the central Alps, northern Italy. *Earth Surface Processes and Landforms*, *29*(3), 267-293.

Dal Piaz, G. V., Bistacchi, A., & Massironi, M. (2003). Geological outline of the Alps. *Episodes*, *26*(3), 175-180.

Flint, J. J. (1974). Stream gradient as a function of order, magnitude, and discharge. *Water Resources Research*, *10*(5), 969-973.

Fischer K. (1965) Murkegel, Schwemmkegel und Kegelimse in den Alpentalern. Mitteilungen der Geographischer Gesellschaft in Munchen 56:127–159

Franke, D., Hornung, J., & Hinderer, M. (2015). A combined study of radar facies, lithofacies and three-dimensional architecture of an alpine alluvial fan (Illgraben fan, Switzerland). Sedimentology, 62(1), 57-86. doi:10.1111/sed.12139

Gómez-Villar, A., & Garcıa-Ruiz, J. M. (2000). Surface sediment characteristics and present dynamics in alluvial fans of the central Spanish Pyrenees. *Geomorphology*, *34*(3), 127-144.

Hack, J. T. (1957). *Studies of longitudinal stream profiles in Virginia and Maryland* (No. 294-B).

Harvey, A. M. (2002). The role of base-level change in the dissection of alluvial fans: case studies from southeast Spain and Nevada. Geomorphology, 45(1), 67-87.

Harvey, A. M. 2003. *Alluvial fan.* In: Goudie, A. S. (ed.) Encyclopedia of Geomorphology. Routledge, London.

Hinderer, M. (2001). Late Quaternary denudation of the Alps, valley and lake fillings and modern river loads. *Geodinamica Acta*, *14*(4), 231-263.

Hornung, J., Pflanz, D., Hechler, A., Beer, A., Hinderer, M., Maisch, M., & Bieg, U. (2010). 3-D architecture, depositional patterns and climate triggered sediment fluxes of an alpine alluvial fan (Samedan, Switzerland). Geomorphology, 115(3), 202-214.

Hurtrez, J. E., Lucazeau, F., Lavé, J., & Avouac, J. P. (1999). Investigation of the relationships between basin morphology, tectonic uplift, and denudation from the study of an active fold belt in the Siwalik Hills, central Nepal. *Journal of Geophysical Research: Solid Earth (1978–2012)*, *104*(B6), 12779-12796.

Ijjasz-Vasquez, E. J., & Bras, R. L. (1995). Scaling regimes of local slope versus contributing area in digital elevation models. *Geomorphology*, *12*(4), 299-311.

Jarman, D., Agliardi, F., & Crosta, G. B. (2011). Megafans and outsize fans from catastrophic slope failures in Alpine glacial troughs: the Malser Haide and the Venosta Valley cluster, Italy. Geological Society, London, Special Publications, 351(1).

Kirby, E., & Whipple, K. (2001). Quantifying differential rock-uplift rates via stream profile analysis. *Geology*, *29*(5), 415-418.

Lague, D., & Davy, P. (2003). Constraints on the long-term colluvial erosion law by analyzing slope-area relationships at various tectonic uplift rates in the Siwaliks Hills (Nepal). *Journal of Geophysical Research: Solid Earth (1978–2012)*, *108*(B2).

Maraio, S., Bruno P.P.G. & Picotti V. (2015). (Extend Abstract) High resolution seismic imaging in alpine environment by Common Reflection Surface method. *Near Surface Geoscience 2015 - 21st European Meeting of Environmental and Engineering Geophysics.*

Moglen, G. E., & Bras, R. L. (1995). The effect of spatial heterogeneities on geomorphic expression in a model of basin evolution. *Water Resources Research*, *31*(10), 2613-2623.

Montgomery, D. R., & Foufoula-Georgiou, E. (1993). Channel network source representation using digital elevation models. *Water Resources Research*, *29*(12), 3925-3934.

Montgomery, D. R. (1999), Process domains and the river continuum, J. Am. Water Resour. Assoc., 35, 397–410.

Montgomery, D. R. (2001). Slope distributions, threshold hillslopes, and steady-state topography. *American Journal of Science*, *301*(4-5), 432-454.

Ratschbacher, L. (1986). Kinematics of Austro-Alpine cover nappes: changing translation path due to transpression. Tectonophysics, 125(4), 335-356.

Ratschbacher, L., Frisch, W., Neubauer, F., Schmid, S. M., & Neugebauer, J. (1989). Extension in compressional orogenic belts: the eastern Alps. Geology, 17(5), 404-407.

Savi, S., Norton, K. P., Picotti, V., Akçar, N., Delunel, R., Brardinoni, F., ... & Schlunegger, F. (2014). Quantifying sediment supply at the end of the last glaciation: Dynamic reconstruction of an alpine debris-flow fan. Geological Society of America Bulletin, 126(5-6), 773-790.

Sangree, J. B., & Widmier, J. M. (1979). Interpretation of depositional facies from seismic data. *Geophysics*, *44*(2), 131-160.

Schlunegger, F., Matter, A., Burbank, D. W., Leu, W., Mange, M., & Matyas, J. (1997). Sedimentary sequences, seismofacies and evolution of depositional systems of the Oligo/Miocene Lower Freshwater Molasse Group, Switzerland. *Basin Research*, *9*(1), 1-26.

Sklar, L., & Dietrich, W. E. (1998). River longitudinal profiles and bedrock incision models: Stream power and the influence of sediment supply. *Rivers over rock: fluvial processes in bedrock channels*, 237-260.

Snyder, N., K. X. Whipple, G. Tucker, and D. Merritts (2000), Landscape response to tectonic forcing: Analysis of stream morphology and hydrology in the Mendocino triple junction region, northern California, Geol Soc. Am. Bull., 112, 1250–1263.

Soldati, M., Corsini, A., Pasuto, A., 2004. Landslides and climate change in the Italian Dolomites since the Late Glacial. Catena 55, 141–161.

Sölva, H., Grasemann, B., Thöni, M., Thiede, R., & Habler, G. (2005). The Schneeberg normal fault zone: normal faulting associated with Cretaceous SE-directed extrusion in the Eastern Alps (Italy/Austria). Tectonophysics, 401(3),

Sorriso-Valvo, M., Antronico, L., & Le Pera, E. (1998). Controls on modern fan morphology in Calabria, Southern Italy. Geomorphology, 24(2), 169-187.

Stock, J., & Dietrich, W. E. (2003). Valley incision by debris flows: Evidence of a topographic signature. *Water Resources Research*, *39*(4).

Thoni, M. (1999). A review of geochronological data from the Eastern Alps. Schweizerische Mineralogische und Petrographische Mitteilungen, 79(1), 209-230.

Thöni, M., & Hoinkes, G. (1987). The southern Ötztal basement: geochronological and petrological consequences of Eoalpine metamorphic overprinting. Geodynamics of the Eastern Alps, 200-213.

Tucker, G. E., and R. L. Bras (1998), Hillslope processes, drainage density, and landscape morphology, Water Resour. Res., 34, 2751–2764.

Vanderburgh, S., & Roberts, M. C. (1996). Depositional systems and seismic stratigraphy of a Quaternary basin: north Okanagan Valley, British Columbia. *Canadian journal of earth sciences*, *33*(6), 917-927.

Veeken, P. P. (2013). *Seismic Stratigraphy and Depositional Facies Models*. Academic Press.

Whipple, K. X., & Tucker, G. E. (1999). Dynamics of the stream-power river incision model: Implications for height limits of mountain ranges, landscape response timescales, and research needs. *Journal of Geophysical Research: Solid Earth (1978–2012)*, *104*(B8), 17661-17674.

Zaprowski, B. J., Pazzaglia, F. J., & Evenson, E. B. (2005). Climatic influences on profile concavity and river incision. *Journal of Geophysical Research: Earth Surface (2003–2012)*, *110*(F3).

3.9 Data repository

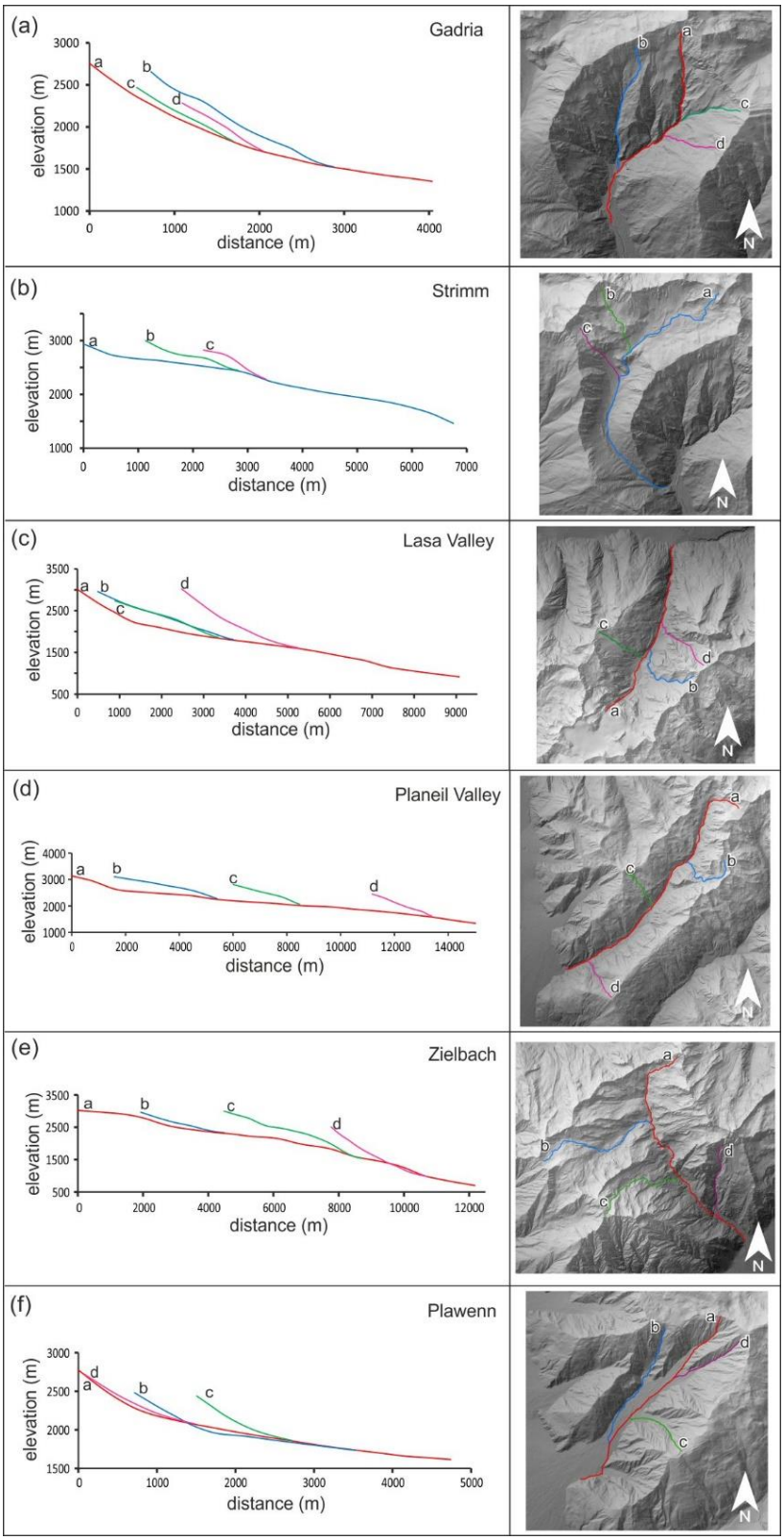

Figure DR1: on the left elevation profiles of the investigated channel; on the right map of the investigated basins with the location of the channel profiles analyzed in the work: a) Gadria basin; b) Strimm basin; c) Lasa Valley; d) Planeil Valley; e) Zielbach basin; f) Plawenn basin.

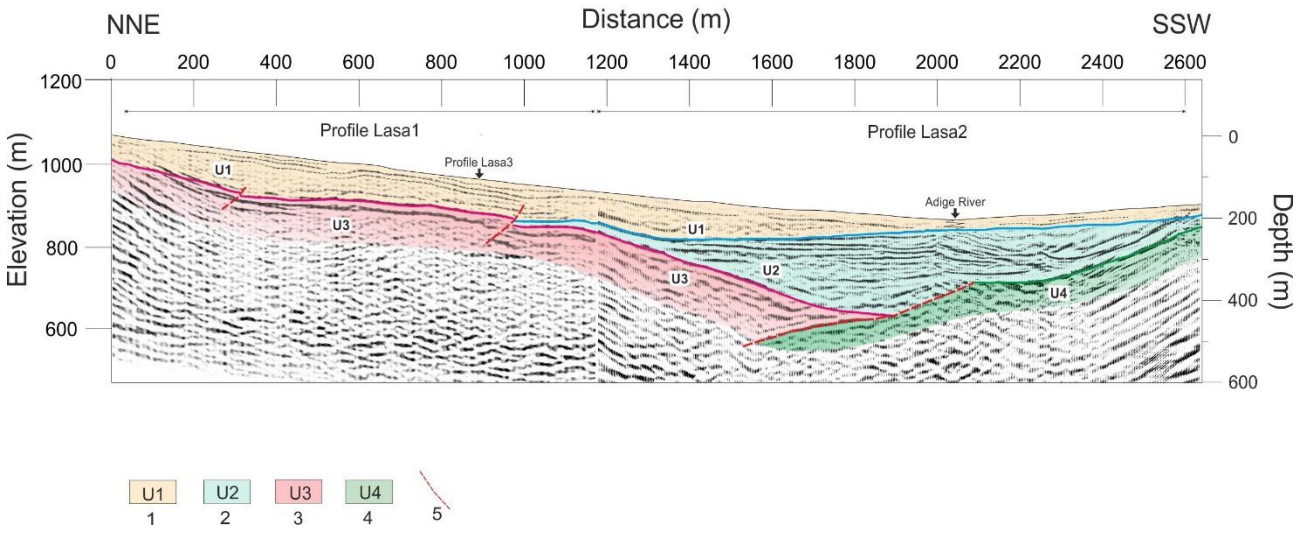

Figure DR2: Seismic and structural preliminary interpretation superimposed on migrated image: alluvial – debris-flow fan deposits (1); fluvio-lacustrine deposits (2); metamorphic bedrock (Oëtzal Unit) (3); metamorphic bedrock (Campo Nappe Unit) (4); presumed faults (5). Vertical and horizontal scales are equal.

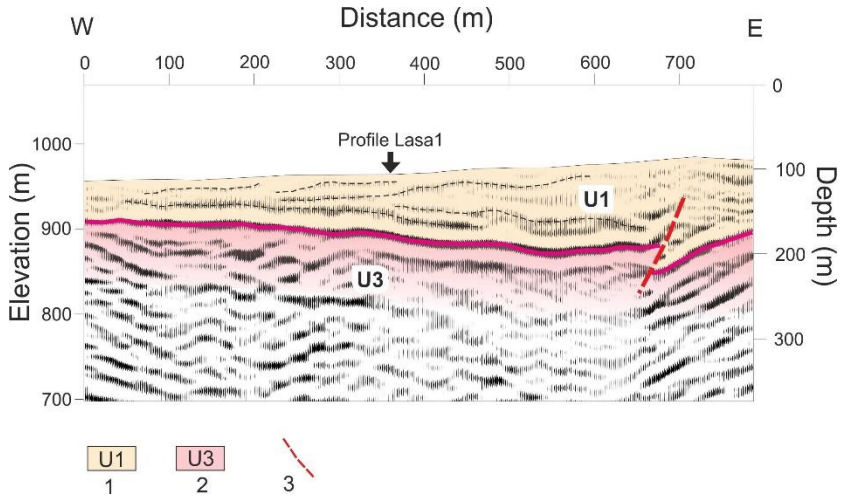

Figure DR3: Seismic and structural preliminary interpretation superimposed on migrated image: alluvial – debris-flow fan deposits (1); metamorphic bedrock (Oëtzal Unit) (2); presumed faults (3). Vertical and horizontal scales are equal.

Figure DR4: Aerial photograph of Gadria catchment.

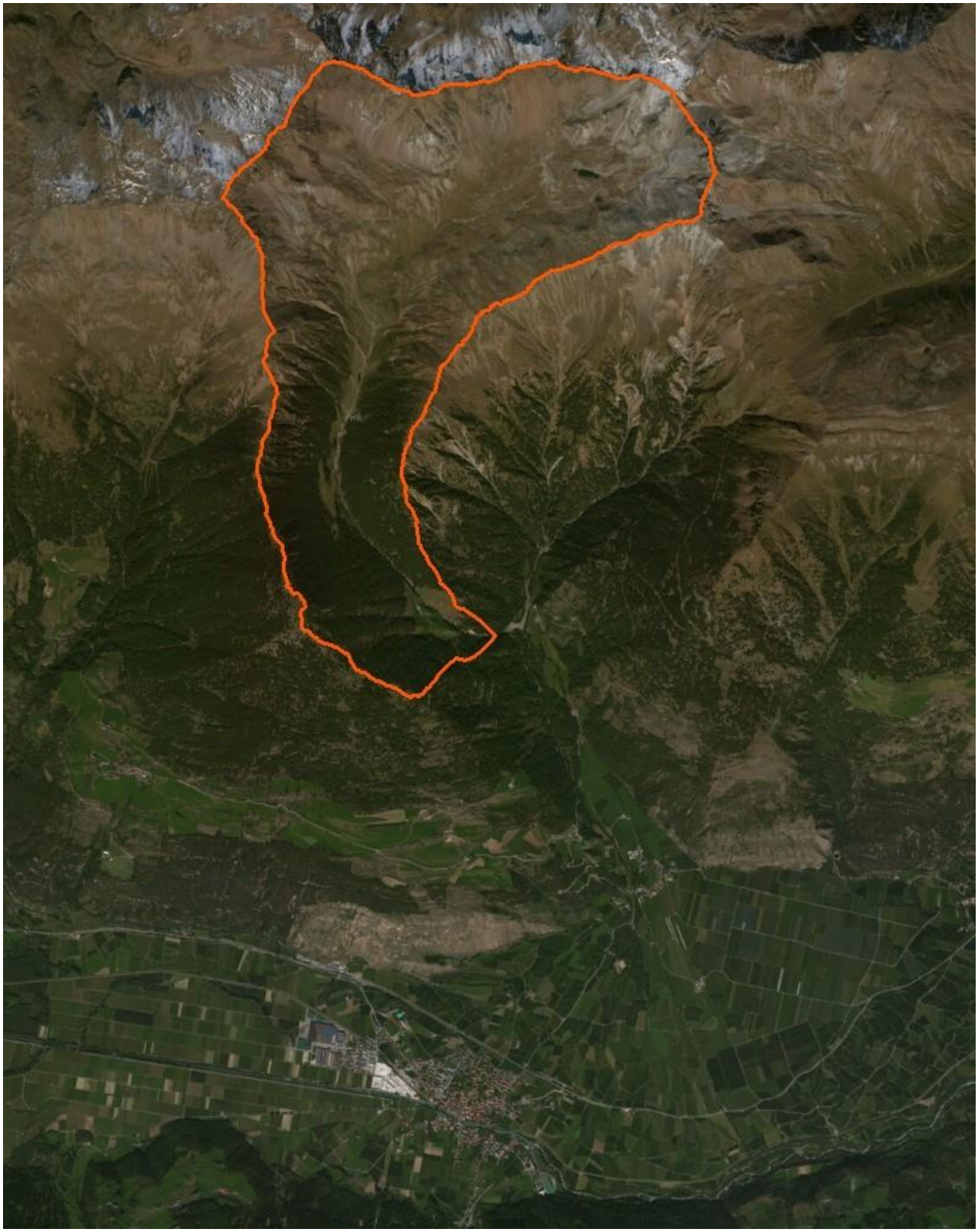

Figure DR5: Aerial photograph of Strimm catchment.

Figure DR6: Aerial photograph of northern portion of Lasa Valley.

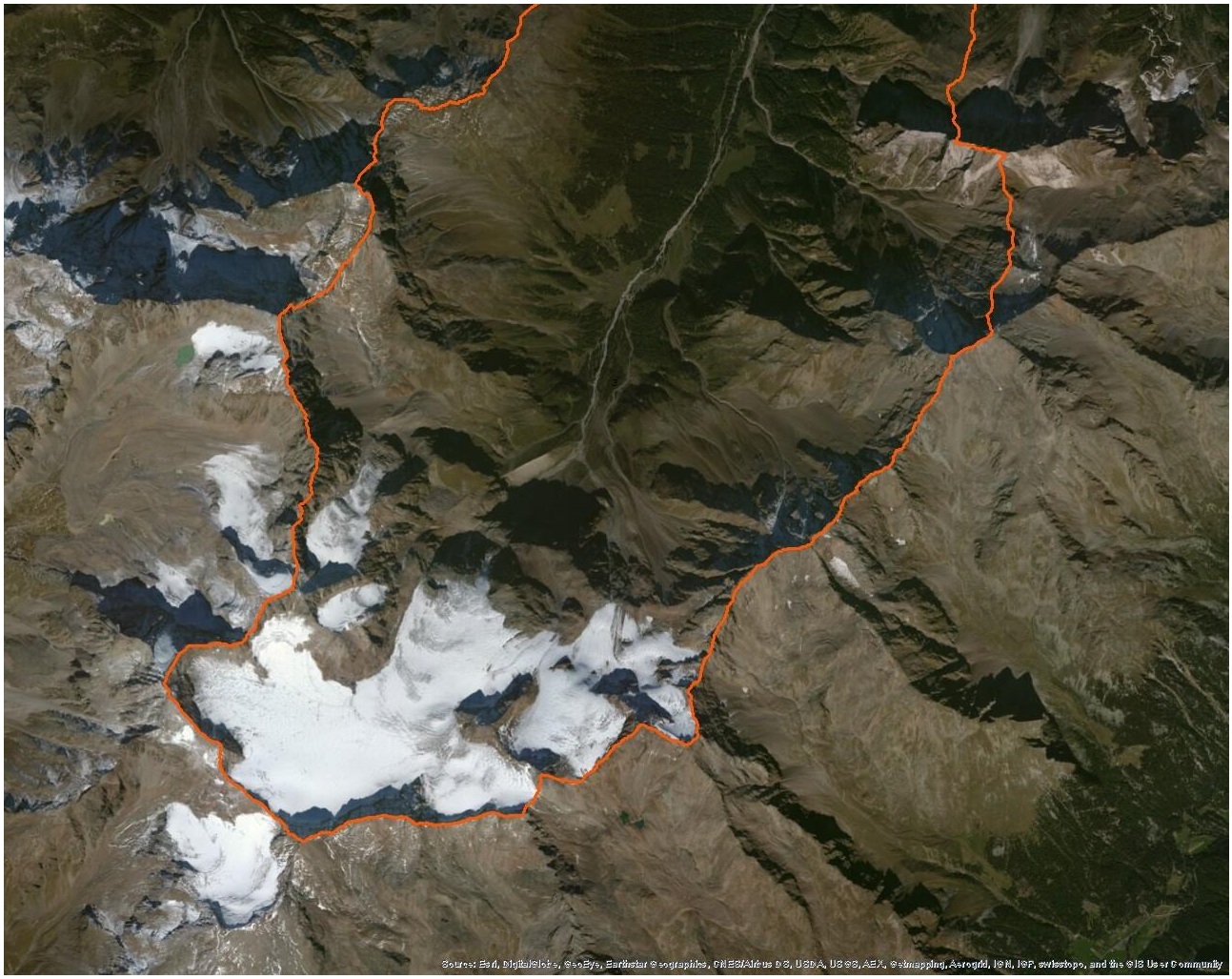

Figure DR7: Aerial photograph of southern portion of Lasa Valley.

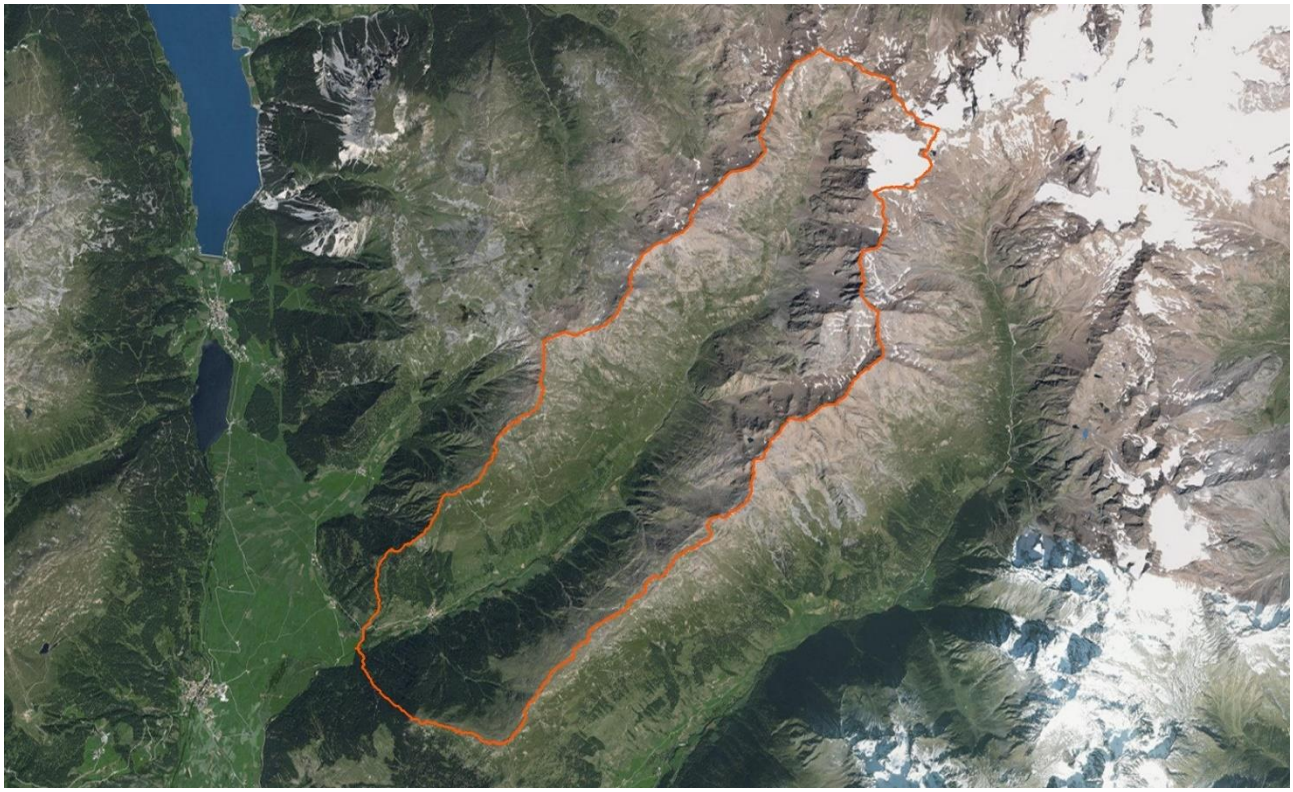

Figure DR8: Aerial photograph of Planeil Valley.

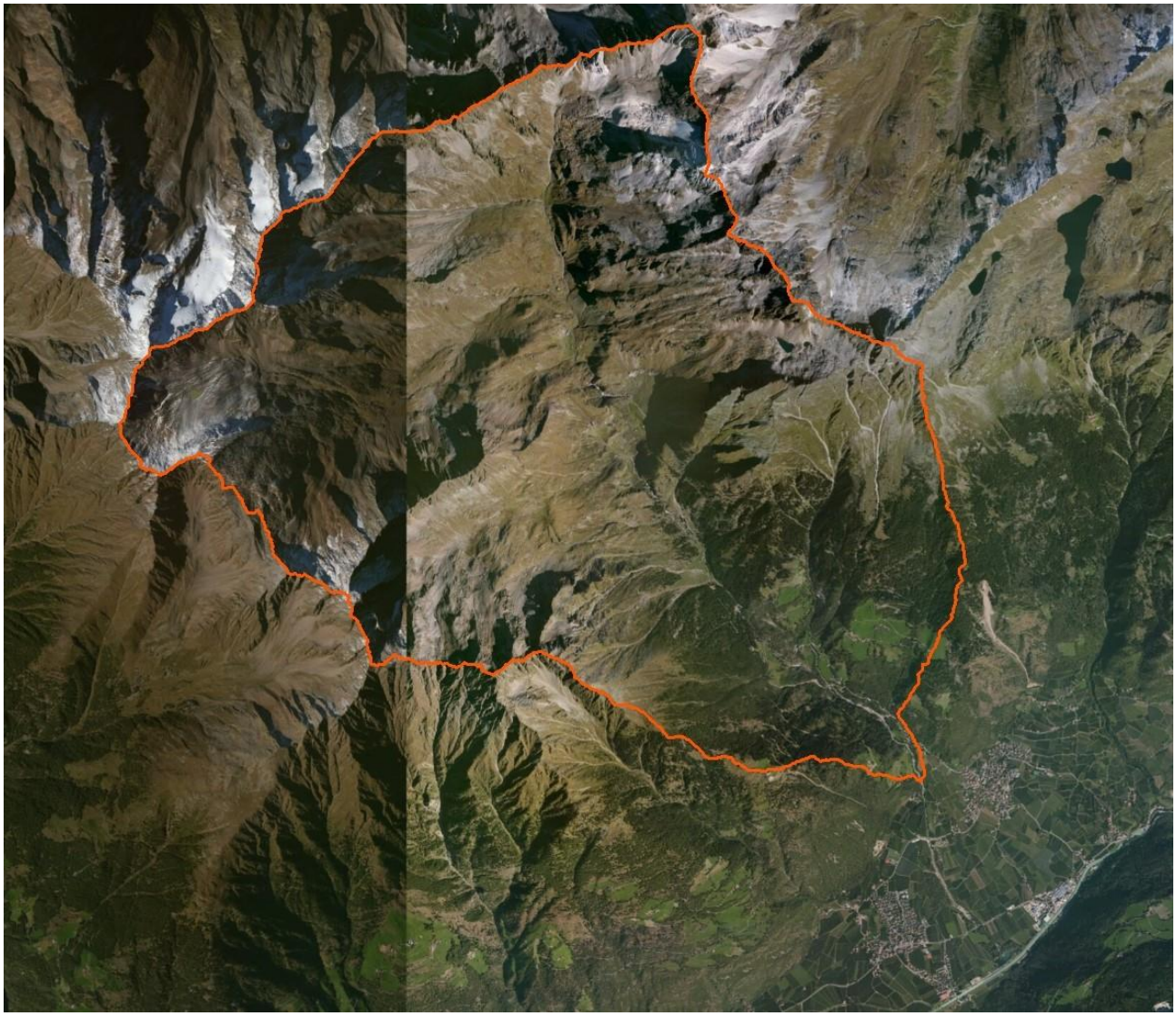

Figure DR9: Aerial photograph of Zielbach catchment.

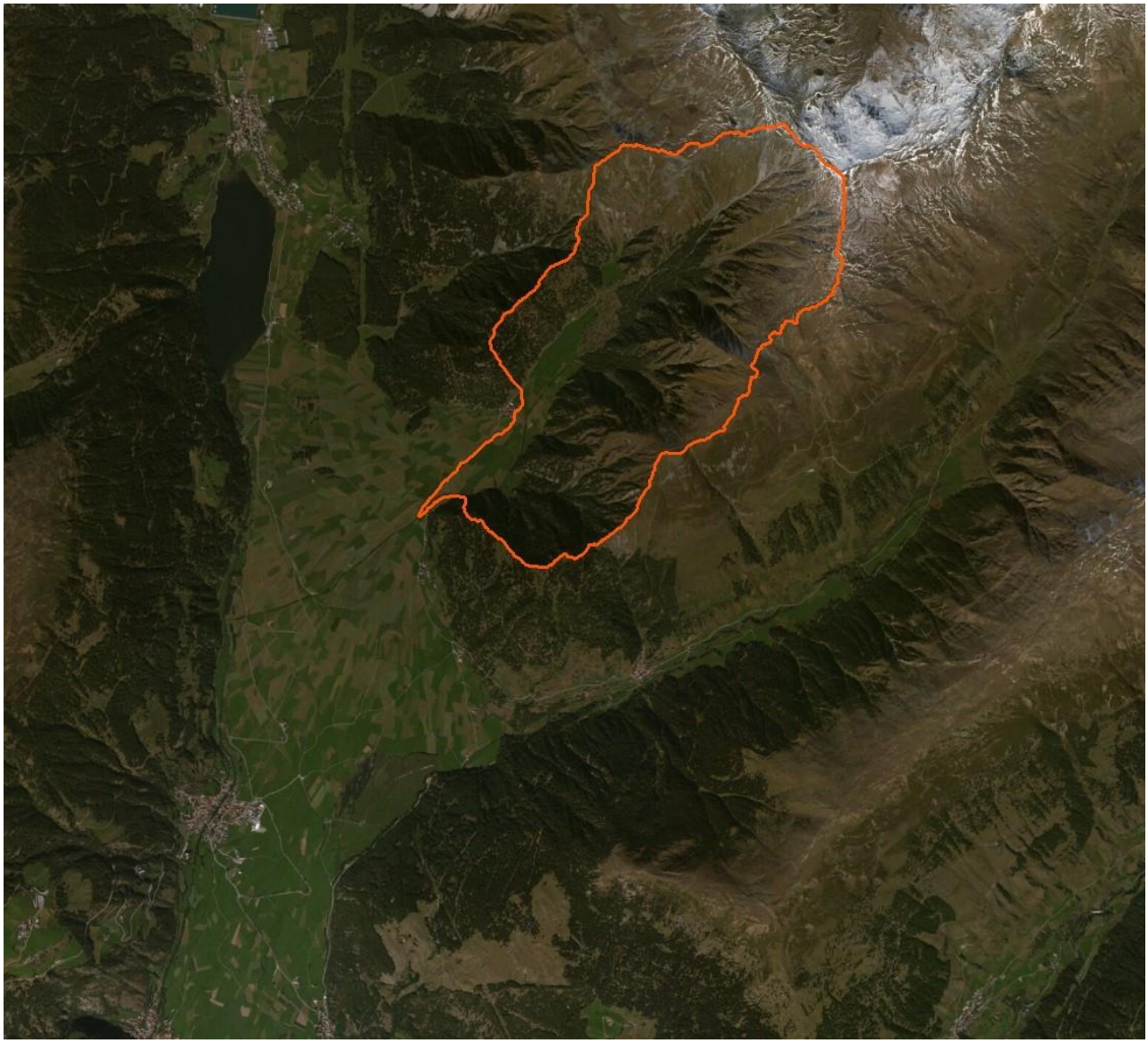

Figure DR10: Aerial photograph of Plawenn catchment.

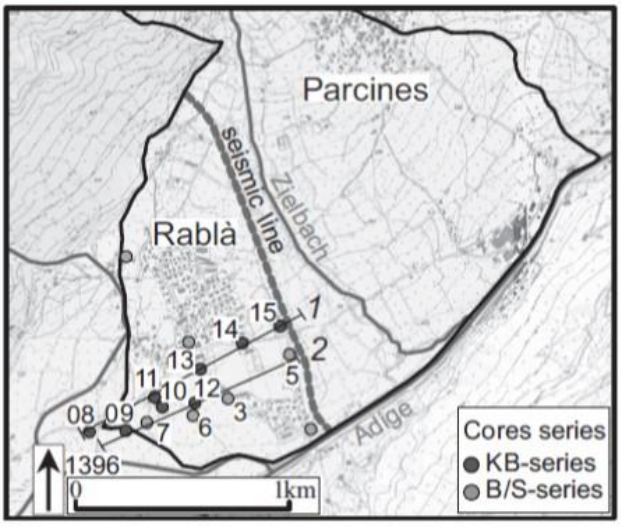

Figure DR11: Location of the seismic profile (dashed thick line) across the Zielbach fan from Savi et al. (2014).

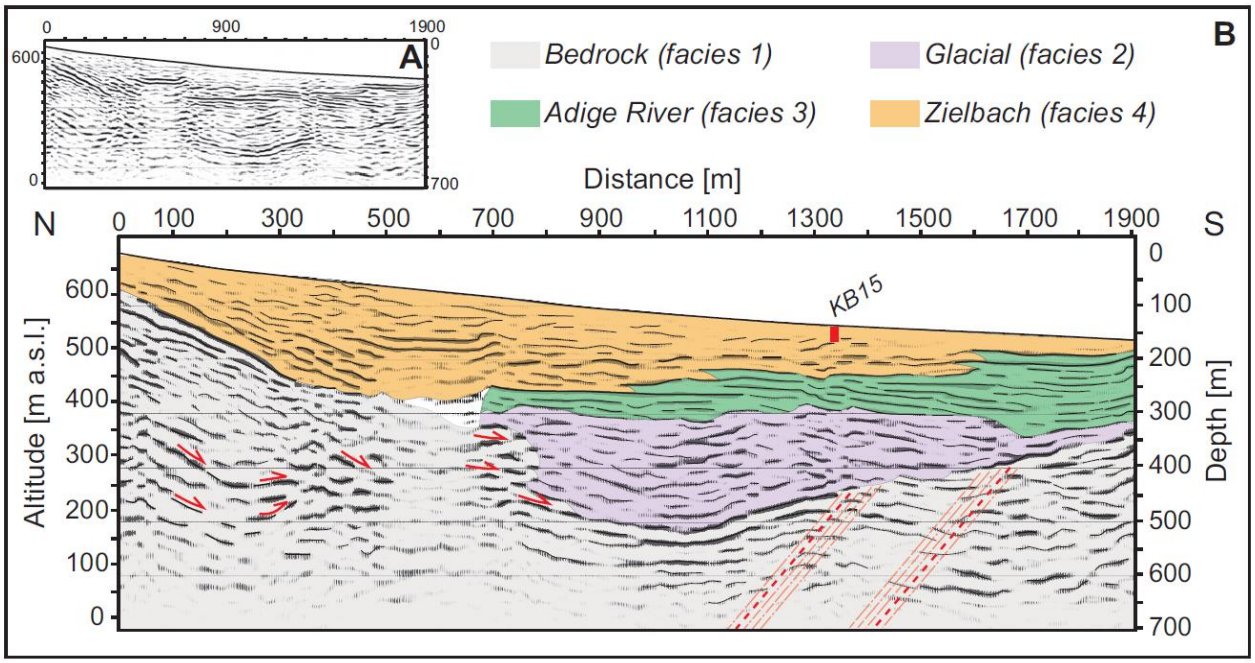

Figure DR12: (A) Seismic reflection results and (B) interpretation of the seismic profile across the Zielbach fan from Savi et al. (2014).

Chapter 4

Seismic stratigraphy of the post LGM alluvial/colluvial sedimentary dynamics of an Alpine valley (Vinschgau/Venosta, Eastern Alps, Italy)

S.Maraio[(1)], F. Brardinoni[(1)], P.P.G. Bruno[(2,*)], V. Picotti[(3)], M. Cucato[(4)],C. Morelli[(4)], F.J. Pazzaglia[(5)]

[1] University of Bologna, Department of Biological, Geological and Environmental Sciences, Italy.

[2]The Petroleum Institute, Department of Petroleum Geosciences, Abu Dhabi, UAE.

[*] Formerly, Istituto Nazionale di Geofisica e Vulcanologia, Roma, Italy

[3] ETH Zürich, Department of Earth Sciences, Zürich, Switzerland.

[4] Province of Bolzano, Office for Geology and material testing, Italy.

[5]Lehigh University, Department of Earth and Environmental Sciences, Bethlehem, PA

4.1 Abstract

Seismic and borehole data from Vinschgau/Val Venosta, a glacial trough in the Italian Eastern Alps, reveal a thick sequence of Quaternary deposits. The architecture of the valley fill deposits was defined by the detailed interpretation on about 4 km of high resolution reflection seismic profile as well as 4 borehole cores. Within the valley three main depositional systems were identified: glacial, fluvial and colluvial/alluvial. The glacial system shows a thin lower portion composed by older sediments eroded by the glacier and an upper part composed by glacial sediments from the glacier melting; fluvial system reveals different depositional characters, influenced by the quantity of fluvial and alluvial sediment supply; the colluvial/alluvial system is mainly characterized by debris-flow deposits. The colluvial/alluvial system played an important role in the valley system aggradation; in particular, the Gadria fan competed with the trunk river, creating an always higher base level and impacting the sedimentation of the Etsch/Adige River. The deposition of the fill deposits started immediately after the Venosta glacier melting (between 19 ky and 14 ky), while the major systems aggradation occurs likely between the Bølling/Allerød and the Early Holocene, (around 15 to 9 ky B.P.). Ultimately, the aggradation of the Gadria fan and consequently the increase of the base-level of the valley, were completed in the last 5.5 ky.

4.2 Introduction

The understanding of the sedimentary architecture of Quaternary intermontane basins deposits, in relation to past climate changes, represents an essential condition for estimate the contemporary climate variation (*Darnault et al., 2012*). Alluvial landscapes are considered the systems largely signed by the environmental changes, during glacial-interglacial transitions (*Marchand et al., 2013*) and consequently represent an archive that records the main depositional processes depending on climate variations. In the past decades, several studies concerning the fill deposits investigation in intermontane basins have been published, in order to retrace the main effects and the timing of climate change in the surveyed areas (Savi et al., 2014; *Lesemann et al., 2013*; *Marchand et al., 2013;)*, applying different research methodologies, such as morphological studies, outcrops analysis, geophysical surveys and drillhole data. The use of subsurface data in mountain landscapes, consisting of a combination of geophysical investigation and drillhole data, are still restricted to a small number of works (*Vanderburgh & Roberts, 1996; Hansen et al., 2009; Savi et al., 2014*). The main advantage in using a geophysical approach is to obtain final results, that reveal the stratigraphic correlations and the geometric relationships, where the outcrops information are insufficient; for instance, geophysical methods and borehole data, in contrast with outcrops analysis, permit to investigate the valley incision, the morphology of buried bedrock, and deeper fill deposits (*Franke et al., 2014; Hansen et al., 2009*). Moreover, drillhole data correlation plays an important rule, since it can provide the linking between geophysical results and local stratigraphy, or also chronostratigraphy, where dating of borehole cores is available (e.g. ^{14}C or cosmogenic nuclides).

We focus on the fill deposits of the Vinschgau/Val Venosta, one of the major glacial trough in the central-eastern Italian Alps, along a transect that explore one of the biggest alluvial fan within the valley (i.e. Gadria fan). The number of published papers in this area, aimed to understanding both the depositional systems of the Vinschgau/Val Venosta fill and the paleoclimate changes, is very limited. *Fischer (1990)*, using observations on Gadria debris-flow fan outcrops, together with ^{14}C dating from rests of subfossil trees in proximity of the fan toe, proposed a hypothesis about the fan stratigraphy, that most of the fan would have

been grown between 13 ky B.P. and 7.2 ky B.P., starting around the Bølling/Allerød interstadial (around 13 ky B.P.). On the other hand, *Savi et al. (2014)*, applied a combination of high resolution seismic profiles across the Zielbach fan, located in the same valley around 30 km east and downstream from our survey area, and radiocarbon calibrated ^{10}Be paleo-denudation rates. These authors depicted the evolution of the Zielbach-Adige system from Early Holocene to present, proposing the deglaciation of the main trunk valley at around 17 ky B.P. and the formation of most of the Zielbach fan up to ca. 12 ky B.P. Ultimately, *Bassetti & Borsato (2007)* proposed a synthesis of the knowledges about the geomorphic evolution of the lower Adige Valley from the LGM, from radiocarbon dating and seismic reflection data, indicating that from 15 ky B.P. the valley was almost ice-free.

This research mainly aims to reconstruct the sedimentary interactions of the tributary fans and the trunk stream (Etsch/Adige) in relation to the climate variations after the end of the Last Glacial Maximum (LGM), using high resolution seismic profiles calibrated by drilling investigations. This approach allows us to obtain a direct correlation between the different deposits observed at depth and the seismic geometries in order to define the depositional units that compose the valley-fill system. The first part of this paper presents a detailed interpretation of three high-resolution reflection seismic profiles, acquired in winter 2012, across the Gadria and Lasa fans that depict the stratigraphic architecture and the deep geometry of the bedrock. (*Maraio et al., 2015*). Seismic facies, described and interpreted following the basic principles in seismostratigraphic interpretation, were correlated with the stratigraphy obtained by cores drilled by the Geological Survey of the Bozen/Bolzano Autonomous Province. The reconstructed interactions between different depositional systems, together with available ^{14}C dating in the area from literature (i.e. *Fischer*, *1990*), can provide information about the dynamic of both fluvial and alluvial systems during the last 20 ky (last glacial-interglacial transition) as consequence of the main climate oscillations characterizing this period. The final step is the reconstruction of a depositional model of the valley fill and the representation of the stages in the evolution of the valley architecture between the termination of LGM and today.

4.3 Last deglaciation of the Alps background

The climate changes in the period occurring from Last Glacial Maximum (LGM) to present in the Alps have been object of many research by several authors (*Orombelli and Ravazzi, 1996; Baroni and Orombelli, 1996; Davis et al., 2003; Dapples et al., 2003; Ravazzi 2003; Joerin et al., 2006 and 2008; Kerschner and Ivi-Ochs 2008; Schmidt et al., 2008; Steffensen et al., 2008; Ivi-Ochs et al., 2006, 2008 and 2009; Favilli et al., 2009; Renssen et al., 2009; Orombelli 2011; Ilyashuk et al., 2011; Wanner et al., 2011*). The LGM reached in the Alps the maximum extent between 30 and 21 ky cal. B.P. (*Fliri et al., 1970; Cossart et al. 2010; Coutterand, 2010;*) and the last deglaciation starts around 17.5 ky cal. B.P. ago (*Darnault et al., 2012; Soldati, 2004;*). The subsequent Lateglacial period (17.5-11.4 ky cal. B.P.) is characterized by a series of climate oscillations with an overall gradual temperature increase (*Orombelli e Ravezzi, 1996; Cossart et al., 2010; Darnault et al., 2012*). Glacial climate conditions persist until about 15 ky cal. B.P., during the Oldest Dryas, (*Orombelli e Ravezzi, 1996; Cossart et al., 2010; Darnault et al., 2012*) and the transition between glacial and interglacial conditions occurs with a rapid rise in temperature and in precipitations around 14.7 ky cal. B.P., coinciding to the transition between Oldest Dryas and Bølling interstadial. *Orombelli and Ravezzi (1996)* suggest that the maximum peak of temperature (i.e. around 14.4 ky cal. B.P.) was comparable with present-day temperature. Following the generally warm Bølling/Allerød interstadial, characterized by the occurrence of a number of climatic oscillations (i.e. Older Dryas period), the beginning of the Younger Dryas cold period (dated 12.6 ky cal B.P.) is marked by an abrupt climate deterioration. During this cold period, glaciers in the Alps re-advanced as consequence of temperature and precipitations levels characteristic to the glacial stage (*Ivy-Ochs et al., 2008 and 2009; Orombelli & Ravezzi, 1996; Darnault et al., 2010*). The Younger Dryas also showed an abrupt end, in correspondence of the Pleistocene/Holocene transition, dated in the European Alps 11.7 ky cal. BP with good agreement by several authors (*Haeberli et al., 1999; Joerin et al., 2006; Steffensen et al., Ortu et al., 2008; 2008; Ivi-Ochs et al., 2008 and 2009; Favilli et al., 2009; Renssen et al., 2009; Wanner et al., 2011*). At global scale, *Wanner et al. (2011)* divided the Holocene in three main periods, on the basis of temperature and precipitations changes: Early Holocene, Holocene Climatic Optimum and Holocene Climatic Deterioration. The first period (i.e. Early Holocene) began 11.7 ky cal. BP and was

characterized by humid and cool or temperate conditions, depending on the presence of melting ice, and its end, varying between different geographic areas, is difficult to define; nevertheless, *Wanner et al. (2011)* identify the end of the first period at the transition between the Early Holocene and the Holocene Climatic Optimum. The Holocene Climatic Optimum was marked by warmer and stable conditions and its time span is correlated to the warm and drier climatic period documented by several authors between 8 ky and 4 ky BP (*Ravazzi 2003; Joerin et al., 2006; Ivi-Ochs et al., 2008 and 2009; Favilli et al., 2009; Ilyashuk et al., 2011*). The beginning of Holocene Climatic Deterioration, also defined Neoglacial, is established between 5 ky and 4 ky BP (*Orombelli and Ravazzi 1996; Baroni and Orombelli, 1996; Davis et al., 2003; Wanner et al., 2011*). Temperature and insolation decreased during this period, while generally is observed an increase in precipitations. According to *Wanner et al (2011)*, this period ends at the beginning of 20th century, due to anthropogenic greenhouse effect. Several authors (*Joerin et al., 2006 and 2008; Ivi-Ochs et al., 2008 and 2009*) documented a number of climatic oscillations during Holocene period, in particular the occurrence of cold phases with consequently glaciers re-advance in the European Alps. Particularly, *Ivy-Ochs et al. (2009)* suggest that the period between 10.5 ky and 3.3 ky BP, characterized by a generally warm and dry climate, was disturbed by several "glacier-friendly" conditions and the magnitude of the glacier advances in these phases varied in function of the glaciers size, due to the glacier response time to climatic perturbations. *Ivy-Ochs et al. (2009)* also show that the period from 3.3 ky BP signed a new climate deterioration within timberline that moved down to lower altitudes and glacier advances became more frequently, until the Little Ice Age advances from the 14th century AD to 1850 AD.

4.4 Local setting

Vinschgau/Val Venosta represents a major glacial trough of the east-central Italian Alps, drained by Etsch/Adige River and the valley originate near the Resia Pass ($\sim$500 m a.s.l.) and flow for about 74 km down to the city of Meran ($\sim$500 m a.s.l.), where intersect the north-trending Adige Valley. Vinschgau/Val Venosta extends within the Austroalpine nappe stack, between the Engandine and Periadriatic Lineament (Agliardi et

al., 2009a), then the geology of the valley is dominated by metamorphic rocks, consists principally in schists and gneisses. The upper part of the valley runs approximately north-south, down the city of Mals, where it deviates in a west-east trend, along the path of the Vinschgau Shear Zone, which separates the Oetztal Unit from the underlying Campo Nappe (e.g., Ratschbacher, 1986; Thöni, 1999) (figure 1). Fluvial and alluvial deposits fill the valley, hidering the spatial definition between the two metamorphic units that compose the valley bedrock. During the Quaternary period, Vinschgau/Val Venosta was repeatedly affected by glaciations; the valley hosted the largest Late Pleistocene glacier in Italy (i.e. Adige Glacier) that reached its maximum extend during the LGM, with a maximum surface elevation close to 2800-3000 m a.s.l. in the Engandine (Agliardi et al, 2009b). After the LGM glacier melting (i.e. started at ca. 19-18 ky BP), repeated re-advance phases in both the main valley and tributary valleys occurred during the Lateglacial and the Holocene (Bassetti e Borsato, 2005; Kelly et al., 2006; Agliardi et al., 2009a; Bargossi et al., 2010). In this paleo-climate setting, glacial, paraglacial and interglacial processes have strongly influenced the distribution of surficial material, and some of these processes result still active (Hinderer, 2001; Brardinoni et al., 2012). The availability of a quantity of postglacial sediments, together with the steep topography and the highly fractured metamorphic rocks represent favorite conditions for the generation of the large number of alluvial fans present in the valley. In fact, Vinschgau/Val Venosta bottom hosts the biggest cluster of anomalously large fans within the European Alps (Fischer, 1965), which often obstructed and deviated the course of the Etsch/Adige River.

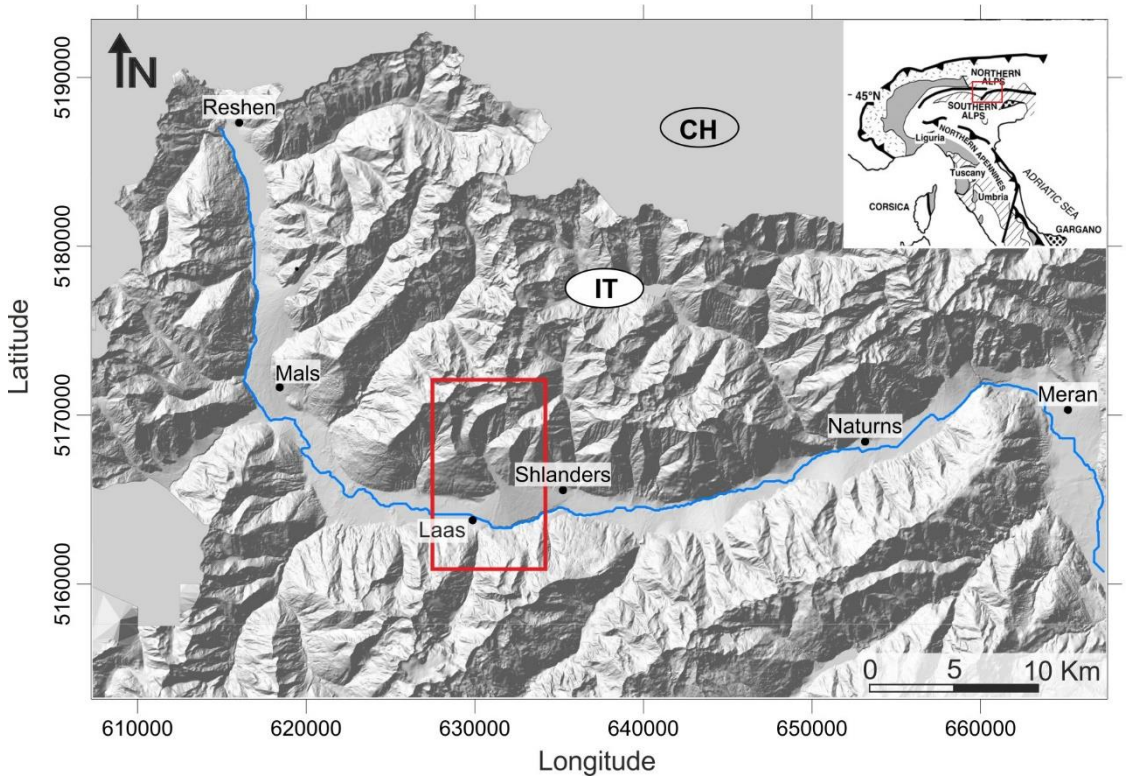

Figure 1: Digital Elevation Model of the Alto Adige province, with the location of the surveyed area (red box)

4.5 Methods and data acquisition

The data sets used in this work consist in a dataset of 4 km long high resolution seismic reflection profiles acquired across a transect of Vinschgau/Val Venosta and four drill-hole cores and cutting from Geological Survey of Autonomous Province of Bolzano (see figure 2 for location of seismic profiles and drill-holes). Using a high frequency vibratory source and a 192-channel array of 10 Hz vertical geophones with 5 m spacing and 955 m offset, three high resolution seismic reflection/refraction profiles were acquired in winter 2012, near village of Laas/Lasa (BZ). Two seismic profiles (i.e. Lasa 1 and Lasa2 in figure 2), running across the Gadria and Lasa fans, are longitudinal to the valley axes and are located to the west side of the main Gadria channel; while one seismic line (i.e. Lasa3 in figure 2) is parallel to the valley, intersecting the profile Lasa 1 in the medial portion of the Gadria fan. More details about the field acquisition geometries and the data processing are available in literature by Maraio et al., 2015. In the seismic units interpretation phase, we classify the seismic data in 4 different seismic facies using classical techniques in seismic stratigraphy (*Veeken,* 2013;

Schlunegger et al., 1997; *Vanderburgh & Roberts,* 1996; *Sangree & Widmier,* 1979) through the identification of geometry pattern, continuity, frequency, amplitude and configuration of seismic reflectors.

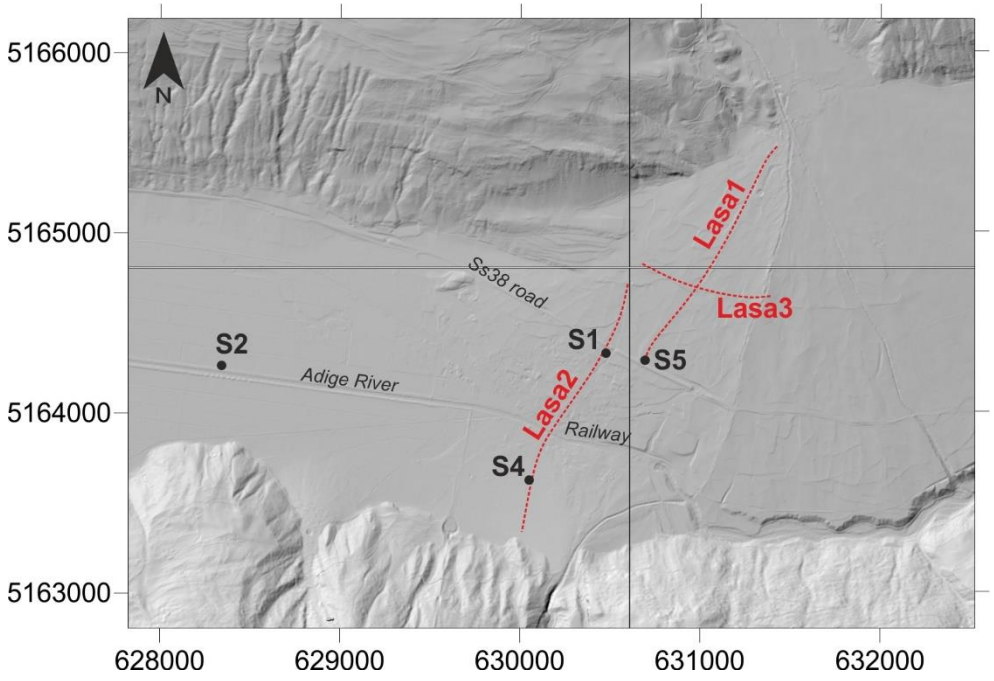

Figure 2: location of the high resolution seismic profiles (red dashed lines) and the boreholes (black dots).

In order to obtain a lithologic correlation of the seismic line, drilling targets and location were determined after the analysis of the seismic results. A total of four drilling was done in the surveyed area (figure 2): S1 borehole, located in correspondence of seismic profile Lasa2, reach a maximum depth of 80 m (fig. DR1); the goal of this drilling was to sample the whole sedimentary sequence revealed by the seismic data, in order to have a lithologic control on the seismic sections. Unfortunately, some logistic problems, occurred during the drilling operations, obligated the repositioning of the borehole to the location of the borehole S5. S5 borehole, reaching a depth of 225 m (fig. DR2), sampled the entire sedimentary sequence showed by the seismic profile Lasa2. S2 borehole (fig. DR3) is located in the Adige River alluvial plain, with the aims to sample the different facies of the Adige River fluvio-lacustrine sediments. Finally, borehole S4 (50 m in depth; fig. DR4) is located across the medial portion of the Lasa fan and its target was to sample the lithologic facies of the Lasa fan.

4.6 Seismic Unit interpretation

In this section, we describe the different seismic facies observed in the seismic profiles (figures 3 and 4). The existence of unconformities at the scale of the whole valley allow us to separate four seismic units, whose interpretation is based on the internal facies, calibrated with data from the drilling cores.

Seismic unit I

Description: Seismic unit I shows a series of semi-continuous to discontinuous reflections, characterized by moderate amplitude and low frequency; generally, these reflectors, especially in proximity of the deeper portion of the valley, dip toward the valley axes. The upper boundary of this unit is represented by a couple of high energy and low frequency continuous reflector, that testify a high acoustic impedance contrast. The definition of this unit boundary is more difficult on profile Lasa 2, below the Etsch/Adige River, for two reasons: i) the presence of a thick overlaying fill loose deposits inevitably produces an acoustic attenuation; ii) the CDP coverage in this part of the seismic line is limited because of an acquisition gap in proximity of the Etsch/Adige River and the railway (see figure 2). Unit I is found at a depth of ca. 1000 m a.s.l. at the beginning of seismic profile Lasa1 and increase in depth to at least 620 m a.s.l. in correspondence of metric 1750 on profile Lasa2; from this point, toward the southern valley margin, the unit is found at gradually shallower depths until the end of the profile, where the upper boundary of this unit is almost exposed (i.e. Campo Unit composing the southern margin of the valley). Unit I is also present on seismic profile Lasa3, where it appears particularly shallow (i.e. ~ 50-100 m) and its upper boundary shows a clear trend to dip towards east.

Interpretation: Seismic Unit I represents the bedrock basement of the valley. Defining the lithology from drilling cores is inconclusive because just one borehole (i.e. S5) has found a compact and hard lithology associable to the metamorphic bedrock, but the sampled cuttings need further accurate petrological analysis to define the composition. Nevertheless, we interpreted this unit as metamorphic bedrock considering: i) the strong acoustic impedance that characterize the upper boundary of the unit; ii) the seismic facies that testify

a poorly stratified and hardly fractured rocks compatible with micaschists and paragneiss outcropping on both valley edges (geologic map of Italy 1:100000); iii) the high seismic velocity characterizing the unit (i.e. >3.5 Km/s) documented by *Maraio et. al (2015)*.

Seismic Unit II

Description: Seismic unit II is composed by discontinuous, variable amplitude and undulated or acoustically transparent or chaotic seismic pattern, locally onlapping the unit I at the base; the topping unconformity consists of a continuous to semi-continuous reflector, with low to medium amplitude and low frequency. The geometry of the unit II appears lenticular, sub-horizontal and discordant at the base, located at the deepest part of the valley, draping and concordant at the top, where the reflectors tend parallel the flooring unconformity. Seismic unit II is recognizable in the profile Lasa2 between metric 1500 and 2050, underlying the thickest deposits at a depth range from ~ 640 to ~ 700 m a.s.l.

Interpretation: The interpretation of seismic unit II is done only on the basis of seismic facies, because drilling holes never intercepted it. Therefore, the lithologic control is not available and this interpretation is rather temptative. Sangree & Widmier (1979) and Vanderburg & Roberts (1996) associated seismic patterns consisting of semi-continuous, parallel to chaotic or reflection-free areas, with coarse-grained sediments. Vanderburg and Roberts (1996) interpreted similar seismic facies recognized in Okanagan Valley (British Columbia) as glacial deposits, distinguishing two different patterns related respectively to erosional and subsequently depositional processes as consequence of glacier melting. Considering the latter interpretation and the finding glacial deposits that fill the more depressed portion of the valley below the Zielbach fan (i.e. ~30 km east from our survey area) documented by Savi et al. (2014), we temptatively associated seismic unit II to glacial deposits. The lower part of the unit is interpreted as older glacial deposits, eroded by the glacier during the last glaciation, while the upper sub-horizontal reflectors are associated to glacial and subglacial deposits by a subsequent depositional phase, probably associable to the last stages of glacier melting.

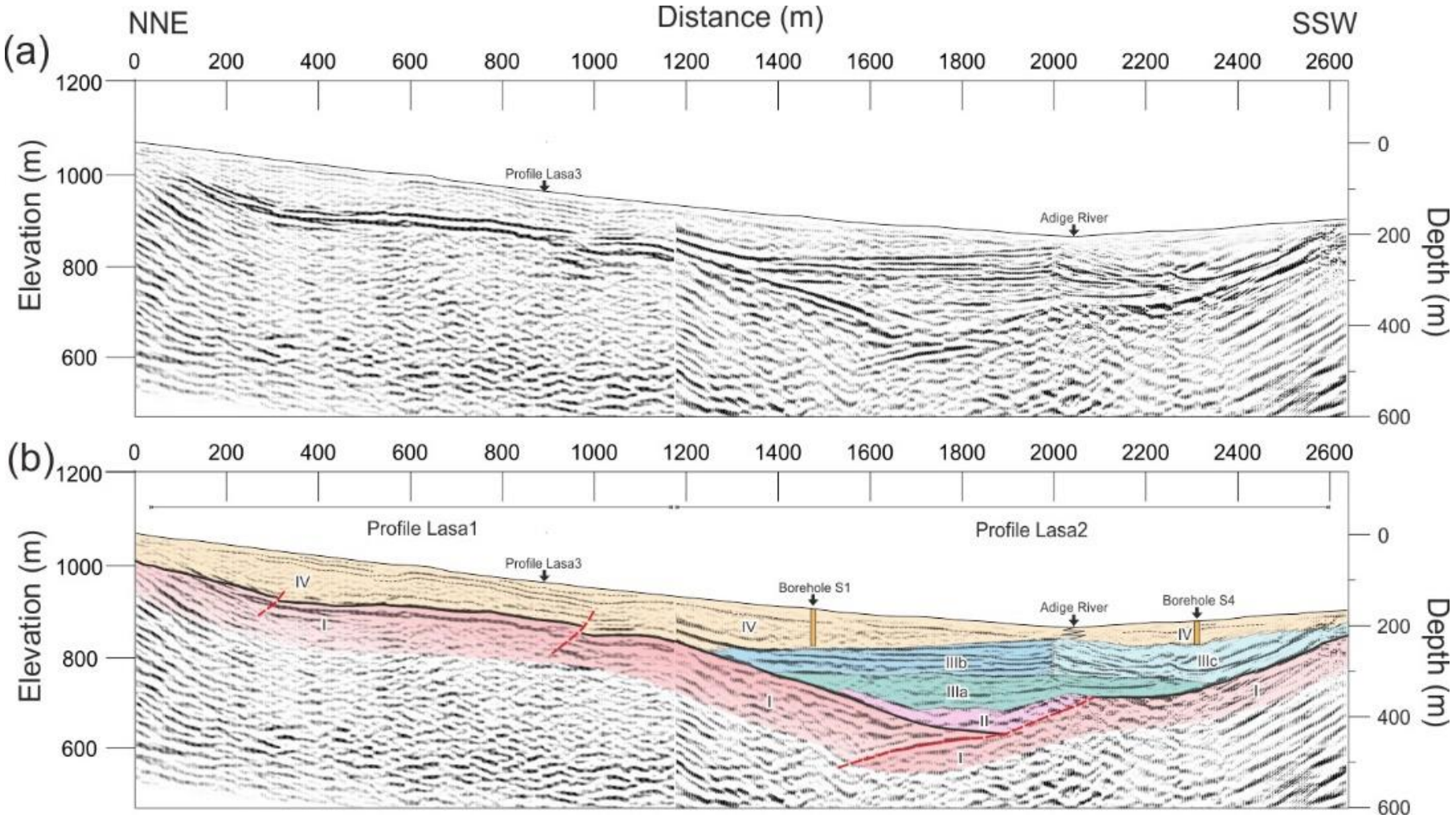

Figure 3: Seismic units interpretation superimposed on migrated seismic image of profile Lasa1 and Lasa2 with the projection of the boreholes. Vertical and horizontal scales are equal.

Seismic Unit III

We split Seismic Unit III into three subunits (i.e. IIIa, IIIb and IIIc) that are distinguished by evident difference in amplitude, continuity and curvature of the reflectors, but they are embedded between the same flooring and topping unconformities.

Seismic Unit IIIa

Description: Seismic subunit IIIa consists of a series of sub-horizontal, semi-continuous to discontinuous, variable amplitude and variable frequency reflectors that terminate in onlap on the flooring unconformity toward seismic unit II on both sides of the valley margin. Seismic unit IIIa is visible on profile Lasa2 on the deepest part of the buried valley and extends for about ~ 500 m at a range depth between ~700 and ~780 m a.s.l. Some concave shaped reflectors are detectable within the unit, especially to the north (i.e. left in the Fig. XX between 1500-1800 m), while there is a lateral transition to more continuous and sub-parallels reflectors toward the southern edge of the valley. The transition between this subunit and the overlaying subunit IIIb is marked by the presence of more continuous and higher energy reflector, whereas toward the unit IIIc by asharp change in the geometric pattern of the reflectors.

Interpretation: This subunit is interpreted as alluvial deposits, mostly composed of sand and gravel. The semi-continuous to discontinuous concave upward top and low-amplitude reflectors, visible at the northern termination of the unit, likely correspond to larger cut-and-fill channels, usually associated to an aggrading braided character of the trunk river (*Veeken, 2013*). The presence of some sub-horizontal reflectors, characterized by higher continuity, is interpreted as deposits formed in laterally continuous floodplains. This interpretation is supported by the results of drilling cores S5 (fig. DR2), that encountered this subunit. The material consists of prevailing sand and gravelly-sand locally graded, clearly associated to the Adige catchment, with few variable-thickness interbeds of silt, associated to low-energy facies. The alternation of different grain size (i.e. sands, gravelly sands, gravel), shown by the drilling S5, can denote a sequence caused

by the migration of bars within the fluvial system, representing a good confirmation of interpretation of this unit as a wide (i.e. ~ 300 m) braided bottom of the Etsch/Adige River.

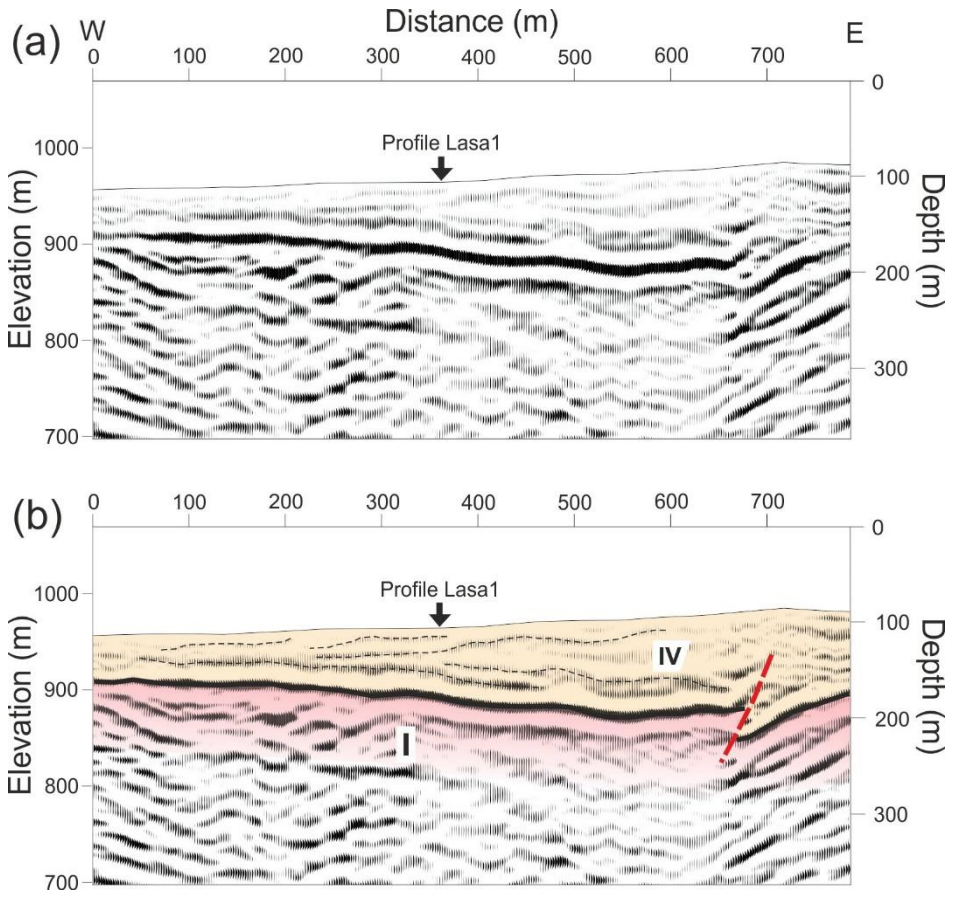

Figure 4: Seismic units interpretation superimposed on migrated seismic image of profile Lasa3. Vertical and horizontal scales are equal.

Seismic Unit IIIb

Description: Seismic subunit IIIb is identified on seismic profile Lasa2 above the subunit IIIa, from ~1400 to ~ 2000 m, at a depth range between 770 and 840 m a.s.l., and is characterized by rather continuous sub-parallel seismic reflections, with middle to high amplitude and high frequency. Reflectors, continuous for about 600 m, terminate in onlap against seismic unit I on the northern margin of the valley, while to the south, they

change abruptly in continuity, amplitude, shape and frequency in correspondence of the lateral transition between subunit IIIb and IIIc.

Interpretation: This seismic subunit is interpreted as lacustrine or low-energy alluvial facies. Several authors (Sangree and Widmier, 1979; Vanderburg and Roberts, 1996; Veeken, 2013) have shown that rhythmic, horizontal, continuous and high amplitude reflections are typical of lacustrine sedimentation. This seismic facies is not recognized in the borehole S5 that is not aligned along the seismic line, therefore a lateral change occurred, as explained in the next section. Sediments with features compatible with the seismic pattern of subunit IIIb are identified in the cores from borehole S2 (fig.DR3), located in the Etsch/Adige River alluvial plain, before the western limit of the fan (figure 2). The core materials from this latter borehole is almost completely composed of thin alternating beds of fine to medium grained sand, indicating a floodplain. Instead, few interbedded of silt and peat, within the cores, denote lacustrine and swampy stages, possibly developing in a interchannel depression.

Seismic Unit IIIc

Description: The last subunit of the seismic unit III comprises the deposits that fill the valley on the southern side of the Etsch/Adige River. The subunit IIIc is composed by semi-continuous to continuous concave shaped and generally high-amplitude reflectors. Few inclined, discontinuous and variable-amplitude reflections are also visible in this seismic facies. This subunit is recognized on seismic profile Lasa2 (i.e. between ~ 2000 and ~ 2600 m), above seismic unit I, and it is laterally adjoining the Unit IIIb. The deposits are thickest (~ 100 m) above the present-day Etsch/Adige River, while the thickness decrease to ~ 40 m farther south toward the valley edge. The upper boundary of this subunit is marked by an evident change in amplitude and frequency of the reflectors.

Interpretation: This is the last subunit interpreted as Etsch/Adige River deposits. The borehole S4, located above this subunit, reached a maximum depth of 50 m (fig. DR), but it is few meters too shallow to intercept this unit. The concave up shape of the reflectors indicates the presence of wide fluvial channels, possibly representing a meandering channel complex. The meandering character of the Etsch/Adige River reflected

in this subunit is also confirmed by sub-parallel inclined reflectors that indicate lateral migration of point bars (Veeken, 2013; Savi, 2014). The width and the strong concavity of the reflectors, suggests also a high discharge and aggradation rate of the Etsch/Adige River. The seismic pattern also testifies that the main channel of the Etsch/Adige River, in this phase, was deflected to the southern margin of the valley, and its lateral migration occurred in a limited space between ~ 2000 and ~ 2600 m on seismic profile Lasa 2.

Seismic Unit IV

Description: Seismic unit IV define the shallower portion of all seismic profiles. On profiles Lasa1 and Lasa3 this seismic unit abuts directly on seismic unit I, while, on profile Lasa 2, closes the stratigraphic sequence above the seismic units IIIb and IIIc. Seismic facies within this unit are variable: the lower portion of the unit, especially on profile Lasa1, is generally characterized by discontinuous and chaotic variable-amplitude reflections, while in the upper part the unit occurs as a more continuous medium-amplitude basinward-dipping reflectors. The lateral continuity of the seismic unit IV is observable on profile Lasa3, that shows some continuous reflectors dipping toward the western limit of the fan. The thickness of this seismic unit is almost constant (~ 90 m) on profile Lasa1, decrease to ~ 40 m toward the Etsch/Adige River location, then reached ~ 50 m across the Lasa fan. On profile Lasa3 the contact between this seismic unit and the metamorphic bedrock is at ~ 100 m in depth on the east side of the seismic sections and decrease to ~ 45 m toward the western edge of the fan.

Interpretation: Seismic unit IV is interpreted as Gadria and Lasa fans deposits, respectively on the northern and southern side of the Etsch/Adige River. The wide range of reflection patterns (parallels, continuous, discontinuous, divergent and chaotic) is often indicative of high-energy depositional environment and consequently of poorly organized deposits (Sangree & Widmier, 1979; Vanderburg and Roberts, 1996; Veeken, 2013). The presence of chaotic and stratified seismic internal geometries, depict different depositional processes, namely generally mass-flow and bedload flow. Dipping internal reflections within this seismic unit on profile Lasa3 depict a lateral progradation of the Gadria fan, highlighting the growth of the fan as a result of different depositional events through time. The interpretation of this seismic unit is supported by two boreholes, namely S1 and S4 (fig. DR1 and DR4). Borehole S1 (fig. DR1), located in the

medial-distal portion of the Gadria fan, is almost entirely composed by a monotonous succession of matrix supported diamicton, with few interbedded gravel and sand intervals; these deposits are originated by debris-flow depositional processes from Gadria/Strimm catchment (e.g. Comiti et al., 2014, alternated with variable-energy tractive processes. Borehole S4 (fig. DR4), located in the medial part of the Lasa fan, found 50 m of alternating matrix supported diamicton, sand and gravel, derived by mass-flows depositional processes (i.e. debris-flows and/or hyper-concentrated flows), alternating with tractive processes.

4.7 Depositional systems

The depositional systems approach has proven very useful for reconstructing the sedimentary architecture and major processes within intermontane basins (*Schlunegger et al.*, 1997; *Vanderburgh & Roberts,* 1996). We used seismostratigraphic data as well as boreholes data to define the depositional macro-components of the investigated Val Vinschgau/Val Venosta transect fill. Four depositional systems were identified, namely glacial, fluvial, fluvio-lacustrine and colluvial/alluvial fan.

Glacial system

The glacial system occupies the more depressed portion of the valley for a thickness of ~ 50 m, being at direct contact with the metamorphic bedrock. This system is composed predominantly by structure less compact, possibly coarse-grained and unsorted deposits (seismic unit II). The system architecture reveals the possible existence of two subunits, likely separated by glacial erosional processes that can explain the different geometries observed in the seismic. These successions could represent subglacial and/or ablation deposits, possibly reworked after the glacier retreat.

Fluvial system

The fluvial system represents the major component of the valley fill. Its stratigraphic base overlies, the glacial deposits and the bedrock, being more widespread than the first sedimentary unit, accounting about 70% of the valley fill in the acquired seismic section. The thickest interval (~ 200 m) is not centered over the bedrock valley center, but it is shifted toward the south, likely as a consequence of the competition with the large

Gadria fan to the north. This system consists of alluvial deposits, principally sands ad gravel, with provenance from the Etsch/Adige River catchment, and local presence of silt and peat interbeds, particularly in the upper portion. The variable patterns characterizing this system suggest different characters and location of the river: the lower interval, i.e. seismic unit IIIa, is interpreted as braided river deposits, mostly developed on the central/northern part of the valley. The upper interval shows a deposition pattern related to a major laterally mobile single channel (meandering river). This subunit (IIIc) is mostly developing on the southern side of the valley, whereas to the north it passes to even bedded deposits, likely corresponding to a low-energy alluvial plain environment (seismic unit IIIb).

Colluvial/alluvial fan system

The colluvial/alluvial fan system represents the shallower portion of the valley fill (seismic unit IV). During and after the fluvial deposition processes, the two main tributary valleys shed sediments, producing lateral bodies of coarse grained material, previously entrained in the tributary catchment or just produced by hillslope processes. The most effective process of sediment transport and deposition was, and still is, debris-flow, whereas fluvial processes mostly rework the finer portion, mostly transporting sediment more effectively within the trunk river. The fans are the expression of the lack of efficiency of the channels in supplying the trunk river with bedload and suspended load. The Gadria fan, to the north grew mostly by debris flow, whereas the smaller dimension of the Lasa fan to the south suggests debris flow processes have been rarer in the Lasa catchment. Colluvial/alluvial fan deposits are thickest near the hillslopes and taper toward the valley axis, prograding, in the case of the Gadria, over distances of about 2 km from the apex. This depositional system is predominantly composed by the alternation of poorly bedded and unsorted sand and gravel with abundant large boulders, typical of high density gravity flows.

4.8 Evolution of the valley

A detailed description of the valley evolution at different time period is not possible because of the unavailability of dating control: nevertheless, the stratigraphic information, revealed by this paper, permit us

to define some key steps of the post-glacial evolution of the Val Vinschgau/Val Venosta (figure 6). Previous works aimed to the reconstruction of climate change in the Eastern Alps (Agliardi et al., 2009a; Bargossi et al., 2010; Savi et al., 2014) have documented that the deglaciations occurred between 19 and 15 ky B.P. and Hinderer (2001) has shown that after 16 ky B.P. the major alpine valleys remained ice-free. Between the onset of the important deglaciation (around 19 ky) and the Bølling warm stadial (around 14 ky B.P.), the Venosta glacier retreated gradually toward the upper part of the valley, releasing sediments from the hillslopes, that filled the valley bottom (figure 6a). Soon after, while the melting was leaving ice-free the upper reaches of the main valley, sediments in most tributary catchments were still trapped due to the ice and permafrost coverage was even present. Some fans developed in this time span, because of the (re)activation of deep-seated landslide, creating a higher base-level and a large amount of crushed rock available from the hillslopes (i.e. Töllbach fan – Savi et al., 2014). The large sediment availability and the pulsating meltwater discharge allowed the rapid aggradation of fluvial deposits in the main valley, mainly in the form of braided channels (figure 6b), identified in the seismic unit IIIa. The lack of interference between the fluvial and alluvial sediments from the tributary basins revealed by seismic and borehole data at this stage suggests the low activity of the hillslopes, possibly due to the permafrost or ice cover on the lateral catchments

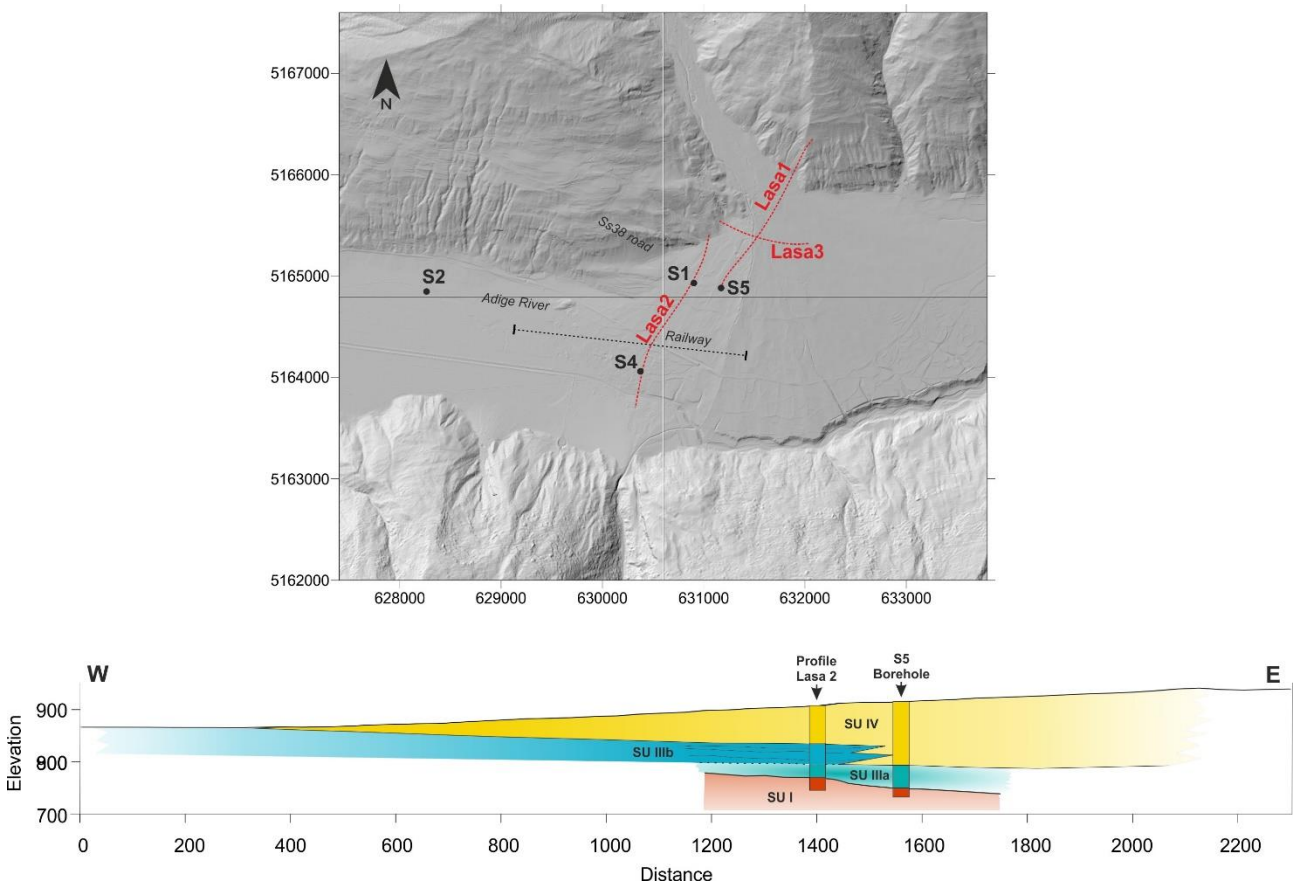

Figure 5: interaction between Gadria and Adige River deposits along the section on the map (black dashed line), revealed by the combination between the seismic and the borehole results.

Results of several researches documented that from about 15 to 12 ky the warmer and wetter climate condition, caused the melting of the last isolated small glaciers within the tributary catchments and consequently the mobilization of high quantity of sediments, representing the first of two periods of high sediment yield within the last deglaciation (paraglacial sediment pulse of Church and Ryder, 1972; see also Soldati et al., 2004; Cossart et al., 2008; Darnault et al., 2012). This first period, identified between 13 and 9 ky B.P. (Soldati et al., 2004), was marked by a very fast sediment yield, facilitated by the availability of large unconsolidated materials within the ice-free catchments, scarce vegetation coverage and high transport capacity (Hinderer, 2001). This period encompasses the short lived Younger Dryas, around 12.7 to 11.5 ky B.P., whose effects on the fan development are still not clear. The effective sediment transfers from the catchments to the main valley bottom and the consequently development of the fans are expressed on the seismic profiles by an abrupt change in seismic patterns in correspondence of the transition between the

seismic unit IIIa and the seismic units IIIb and IIIc. Indeed, the growth of the Gadria fan competed with the trunk river, creating an always higher base level and impacting the sedimentation of the the Etsch/Adige River (Fischer, 1990). This processes brought about the fast aggradation and the deposition of fluvio-lacustrine sediments as well as the passage to a meandering river system, forced toward the southern margin of the valley. The progradation of fan deposits from Gadria and the consequent river aggradation are clearly documented by the calibrated seismic section in figure 5. Furthermore, also the Lasa fan growth is related to the same time frame, as testified by the lateral migration of the Etsch/Adige River in response to the competition between the two fans (figure 6c). Fischer (1990) on the basis of radiocarbon dating from the rests of a subfossil trees, in correspondence of the Etsch/Adige River left bank, suggests that the deposition of two-thirds of the Gadria alluvial fan occurred before ~ 8 ky B.P. The rests of trees were found at about 40 m from the top surface of the fan, suggesting that the deposition of the overlying 40 m of the fan sediments occurred in the last 8 ky.

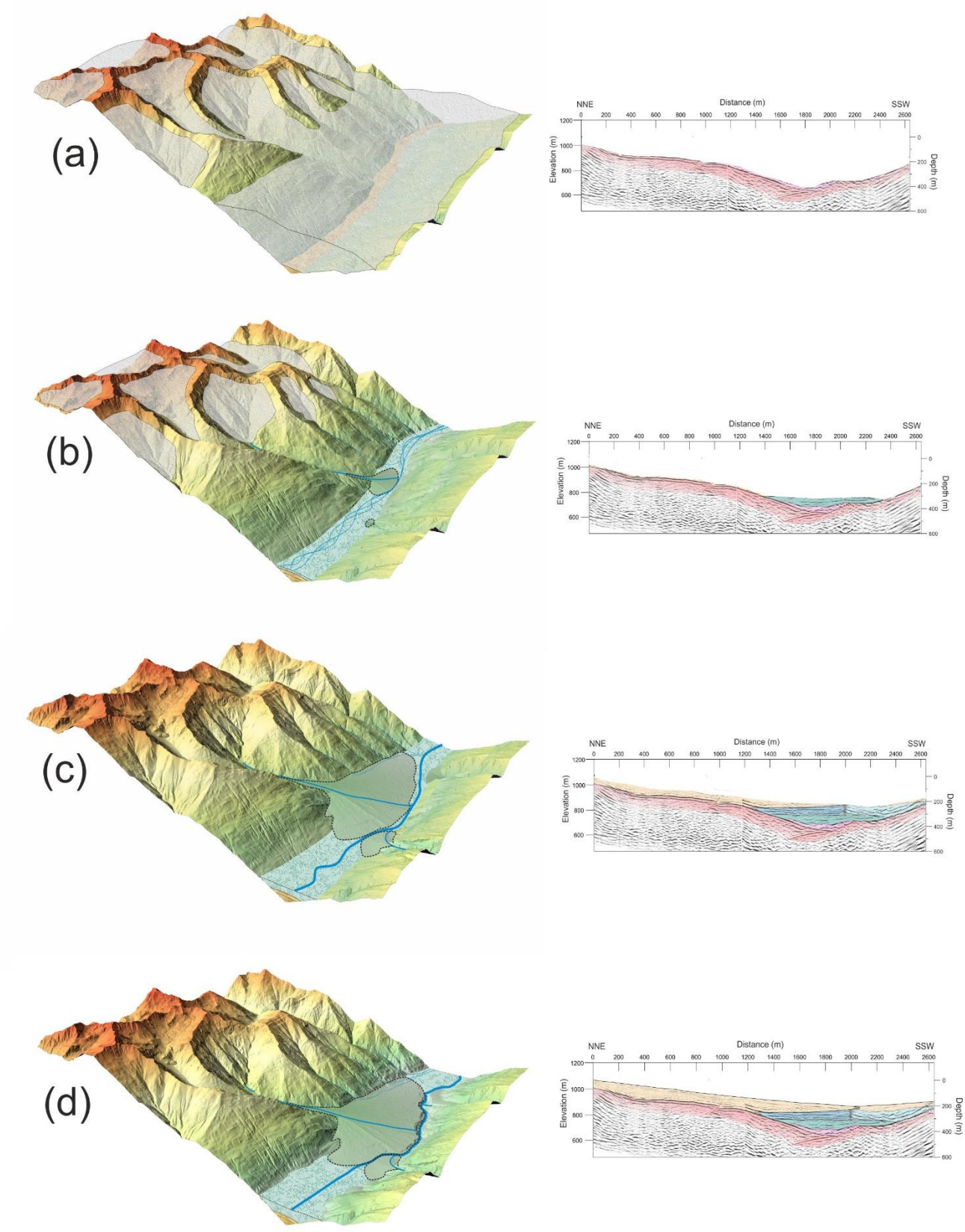

Figure 6: main steps of the valley evolution from the LGM (a) to present (d). The intermediate steps are related to ca. 14 ky B.P. (b) and 8 ky B.P. (c).

During Boreal and Atlantic period, erosion and sedimentation rates decrease abruptly, probably as response to the warm and stable climate conditions characterizing the Holocene Climatic Optimum, together with the vegetation development and general more stable precipitation patterns. Therefore, the last important aggradation of alluvial fan system probably occurs starting at ca. 5.5 ky B.P., corresponding to the beginning of the Holocene Climatic Deterioration. Moreover, the period occurring between 5.8 ky and 2 ky B.P., is related to the second period of high sediment discharge recognized by Soldati et al. (2004), within the erosion and transport interested older deposits by fluvial and alluvial processes. Finally, from 2.5 ky B.P. to present Savi et al. (2014) registered a re-activation of debris-flow processes, facilitated by the increasing impact of human activities (especially deforestation within the valley), together with a general climate deterioration in the Neoglacial.

4.9 Conclusion

This work provides a reconstruction of the post-glacial sedimentary architecture and evolution of the Vinschgau/Val Venosta, through the seismofacies interpretation of high resolution seismic reflection profiles calibrated with boreholes data. The valley fill is mainly composed by three depositional systems: glacial, fluvial and colluvial/alluvial fan. Around 50 m of deposits belonging to the glacial system are found at the lowest part of the valley fill, consisting of compact, likely coarse-grained materials, deposited during the glacial maximum and its end before about 15 ky B.P., with an internal erosional discordance pointing to older glacial deposits. The fluvial system is characterized by three patterns that substantially differ in relation to: i) sediments origin and transport capacity; ii) character of the fluvial system that show passage from braided to meandering behavior; iii) influence of the colluvial/alluvial deposits supplied from tributary basins that create local increase of the base level, inducing deflection of the river and aggradation with a general decrease of the energy of the floodplain. The colluvial/alluvial fan system, generally composed of debris-flow deposits, occupy a large part of the valley margins and prograded toward the valley axis even more then 2 km, competing with the Etsch/Adige River discharge and modifying the base-level of the valley. The major

fan system aggradation and consequently the major increase of the valley base-level occur likely between the Bølling/Allerød and the Early Holocene, (around 15 to 9 ky B.P.). In this time span, warmer and wetter climate conditions, the availability of sediment on the tributary basins slope, the scarce vegetation and the high river transport capacity, allow the deposition of about two-thirds of the fan system volume. After a decrease in erosion and sedimentation rate, in correspondence to the Holocene Climatic Optimum, the deposition of the alluvial fan system and the consequently fluvial system aggradation were completed in the last 5.5 ky as consequence of both Holocene Climatic Deterioration and human activities (Savi et al., 2014).

These main evolutionary steps, based on the interpretation of the seismostratigraphy and facies document that the main controlling factor for the development of the large colluvial/alluvial fans in the central/eastern Alps is the climate, with its large-scale fluctuations, controlling the production of sediments and its deposition through competing alluvial and colluvial processes, bringing to the development of some hundreds of meters of deposits.

4.10 References

Agliardi, F., Crosta, G., Zanchi, A. & Ravazzi, C. 2009a. Onset and timing of deep-seated gravitational slope deformations in the eastern Alps, Italy. Geomorphology, 103, 113–129.

Agliardi, F., Zanchi, A., & Crosta, G. B. (2009b). Tectonic vs. gravitational morphostructures in the central Eastern Alps (Italy): constraints on the recent evolution of the mountain range. Tectonophysics, 474(1), 250-270.

Andreatta C. (1951). Carta Geologica d' Italia 1:100000, Foglio n°9 - M.te Cevedale.

Bargossi, G. M., Bove, G., Cucato, M., Gregnanin, A., Morelli, C., Moretti, A., ... & Zanchi, A. (2010). Note Illustrative della Carta Geologica d'Italia alla scala 1: 50.000, foglio 013 "Merano". Servizio Geologico d'Italia–ISPRA, SystemCart, Roma.

Baroni, C., & Orombelli, G. (1996). The alpine "Iceman" and Holocene climatic change. Quaternary Research, 46(1), 78-83.

Bassetti, M., & Borsato, A. (2007). Evoluzione geomorfologica della Bassa Valle dell'Adige dall'Ultimo Massimo Glaciale: sintesi delle conoscenze e riferimenti ad aree limitrofe. Studi Trent. Sci. Nat., Acta Geol, 82(2005), 31-42.

Brardinoni, F., Church, M., Simoni, A., & Macconi, P. (2012). Lithologic and glacially conditioned controls on regional debris-flow sediment dynamics. Geology, 40(5), 455-458.

Cossart, E., Fort, M., Bourles, D., Carcaillet, J., Perrier, R., Siame, L., & Braucher, R. (2010). Climatic significance of glacier retreat and rockglaciers re-assessed in the light of cosmogenic dating and weathering rind thickness in Clarée valley (Briançonnais, French Alps). Catena, 80(3), 204-219.

Dapples, F., Oswald, D., Raetzo, H., Lardelli, T., & Zwahlen, P. (2003). New records of Holocene landslide activity in the Western and Eastern Swiss Alps: Implication of climate and vegetation changes. Eclogae Geologicae Helvetiae, 96(1), 1-10.

Darnault, R., Rolland, Y., Braucher, R., Bourlès, D., Revel, M., Sanchez, G., & Bouissou, S. (2012). Timing of the last deglaciation revealed by receding glaciers at the Alpine-scale: impact on mountain geomorphology. Quaternary Science Reviews, 31, 127-142.

Davis, B. A., Brewer, S., Stevenson, A. C., & Guiot, J. (2003). The temperature of Europe during the Holocene reconstructed from pollen data. Quaternary Science Reviews, 22(15), 1701-1716.

Favilli, F., Egli, M., Brandova, D., Ivy-Ochs, S., Kubik, P., Cherubini, P., ... & Haeberli, W. (2009). Combined use of relative and absolute dating techniques for detecting signals of Alpine landscape evolution during the late Pleistocene and early Holocene. Geomorphology, 112(1), 48-66.

Fischer, K. (1990). *Entwicklungsgeschichte der Murkegel im Vinschgau*. Der Schlern, 64(2), 93-97.

Fliri, F. (1970). Neue entscheidende Radiokarbondaten zur alpinen Würmvereisung aus den Sedimenten der Inntalterrasse (Nordtirol). Zeitschrift für Geomorphologie, 14, 520-521.

Franke, D., Hornung, J., & Hinderer, M. (2014). A combined study of radar facies, lithofacies and three-dimensional architecture of an alpine alluvial fan (Illgraben fan, Switzerland). Sedimentology, 62(1), 57-86. Haeberli, W., Frauenfelder, R., Hoelzle, M., & Maisch, M. (1999). On rates and acceleration trends of global glacier mass changes. Geografiska Annaler: Series A, Physical Geography, 81(4), 585-591.

Hansen, L., Beylich, A., Burki, V., Eilertsen, R. S., Fredin, O., Larsen, E., ... & Tønnesen, J. F. (2009). Stratigraphic architecture and infill history of a deglaciated bedrock valley based on georadar, seismic profiling and drilling. Sedimentology, 56(6), 1751-1773.

Hinderer, M. (2001). Late Quaternary denudation of the Alps, valley and lake fillings and modern river loads. Geodinamica Acta, 14(4), 231-263.

Ilyashuk, E. A., Koinig, K. A., Heiri, O., Ilyashuk, B. P., & Psenner, R. (2011). Holocene temperature variations at a high-altitude site in the Eastern Alps: a chironomid record from Schwarzsee ob Sölden, Austria. Quaternary Science Reviews, 30(1), 176-191.

Ivy-Ochs, S., Kerschner, H., Kubik, P. W., & Schlüchter, C. (2006). Glacier response in the European Alps to Heinrich Event 1 cooling: the Gschnitz stadial. Journal of Quaternary Science, 21(2), 115-130.

Ivy-Ochs, S., Kerschner, H., Reuther, A., Preusser, F., Heine, K., Maisch, M., ... & Schlüchter, C. (2008). Chronology of the last glacial cycle in the European Alps. Journal of Quaternary Science, 23(6-7), 559-573.

Ivy-Ochs, S., Kerschner, H., Maisch, M., Christl, M., Kubik, P. W., & Schlüchter, C. (2009). Latest Pleistocene and Holocene glacier variations in the European Alps. Quaternary Science Reviews, 28(21), 2137-2149.

Joerin, U. E., Stocker, T. F., & Schlüchter, C. (2006). Multicentury glacier fluctuations in the Swiss Alps during the Holocene. The Holocene, 16(5), 697-704.

Joerin, U. E., Nicolussi, K., Fischer, A., Stocker, T. F., & Schlüchter, C. (2008). Holocene optimum events inferred from subglacial sediments at Tschierva Glacier, Eastern Swiss Alps. Quaternary Science Reviews, 27(3), 337-350.

Kelly, M. A., Ivy-Ochs, S. U. S. A. N., Kubik, P. W., Blanckenburg, F. V., & Schlüchter, C. (2006). Chronology of deglaciation based on 10Be dates of glacial erosional features in the Grimsel Pass region, central Swiss Alps. Boreas, 35(4), 634-643.

Kerschner, H., & Ivy-Ochs, S. (2008). Palaeoclimate from glaciers: Examples from the Eastern Alps during the Alpine Lateglacial and early Holocene. Global and Planetary Change, 60(1), 58-71.

Lesemann, J. E., Brennand, T. A., Lian, O. B., & Sanborn, P. (2013). A refined understanding of the paleoenvironmental history recorded at the Okanagan Centre section, an MIS 4 stratotype, south-central British Columbia, Canada. Journal of Quaternary Science, 28(8), 729-747.

Maraio, S., Bruno P.P.G. & Picotti V. (2015). (Extend Abstract) High resolution seismic imaging in alpine environment by Common Reflection Surface method. *Near Surface Geoscience 2015 - 21st European Meeting of Environmental and Engineering Geophysics.*

Marchand, J. P., Buffin-Bélanger, T., Hétu, B., & St-Onge, G. (2013). Stratigraphy and infill history of the glacially eroded Matane River Valley, eastern Quebec, Canada. Canadian Journal of Earth Sciences, 51(2), 105-124.

Orombelli, G. (2011). Holocene mountain glacier fluctuations: a global overview. Geogr Fis Din Quat, 34(1), 17-24.

Orombelli, G., & Ravazzi, C. (1996). The Late Glacial and early Holocene: chronology and paleoclimate. Il Quaternario, 9(2), 439-444.

Ortu, E., Peyron, O., Bordon, A., de Beaulieu, J. L., Siniscalco, C., & Caramiello, R. (2008). Lateglacial and Holocene climate oscillations in the South-western Alps: an attempt at quantitative reconstruction. Quaternary International, 190(1), 71-88.

Ratschbacher, L. (1986). Kinematics of Austro-Alpine cover nappes: changing translation path due to transpression. Tectonophysics, 125(4), 335-356.

Ravazzi, C. (2003). An overview of the Quaternary continental stratigraphic units based on biological and climatic events in Italy. Il Quaternario, 16(1), 11-18.

Renssen, H., Seppä, H., Heiri, O., Roche, D. M., Goosse, H., & Fichefet, T. (2009). The spatial and temporal complexity of the Holocene thermal maximum. Nature Geoscience, 2(6), 411-414.

Sangree, J. B., & Widmier, J. M. (1979). Interpretation of depositional facies from seismic data. Geophysics, 44(2), 131-160.

Savi, S., Norton, K. P., Picotti, V., Akçar, N., Delunel, R., Brardinoni, F & Schlunegger, F. (2014). Quantifying sediment supply at the end of the last glaciation: Dynamic reconstruction of an alpine debris-flow fan. Geological Society of America Bulletin, 126(5-6), 773-790.

Schlunegger, F., Leu, W., & Matter, A. (1997). Sedimentary sequences, seismic facies, subsidence analysis, and evolution of the Burdigalian Upper Marine Molasse Group, central Switzerland. AAPG bulletin, 81(7), 1185-1207.

Soldati, M., Corsini, A., & Pasuto, A. (2004). Landslides and climate change in the Italian Dolomites since the Late glacial. Catena, 55(2), 141-161.

Steffensen, J. P., Andersen, K. K., Bigler, M., Clausen, H. B., Dahl-Jensen, D., Fischer, H., ... & White, J. W. (2008). High-resolution Greenland ice core data show abrupt climate change happens in few years. Science, 321(5889), 680-684.

Thoni, M. (1999). A review of geochronological data from the Eastern Alps. Schweizerische Mineralogische und Petrographische Mitteilungen, 79(1), 209-230.

Vanderburgh, S., & Roberts, M. C. (1996). Depositional systems and seismic stratigraphy of a Quaternary basin: north Okanagan Valley, British Columbia. Canadian journal of earth sciences, 33(6), 917-927.

Veeken, P. P. (2006). Seismic stratigraphy, basin analysis and reservoir characterisation (Vol. 37). Elsevier.

Wanner, H., Solomina, O., Grosjean, M., Ritz, S. P., & Jetel, M. (2011). Structure and origin of Holocene cold events. Quaternary Science Reviews, 30(21), 3109-3123.

4.11 Data repository

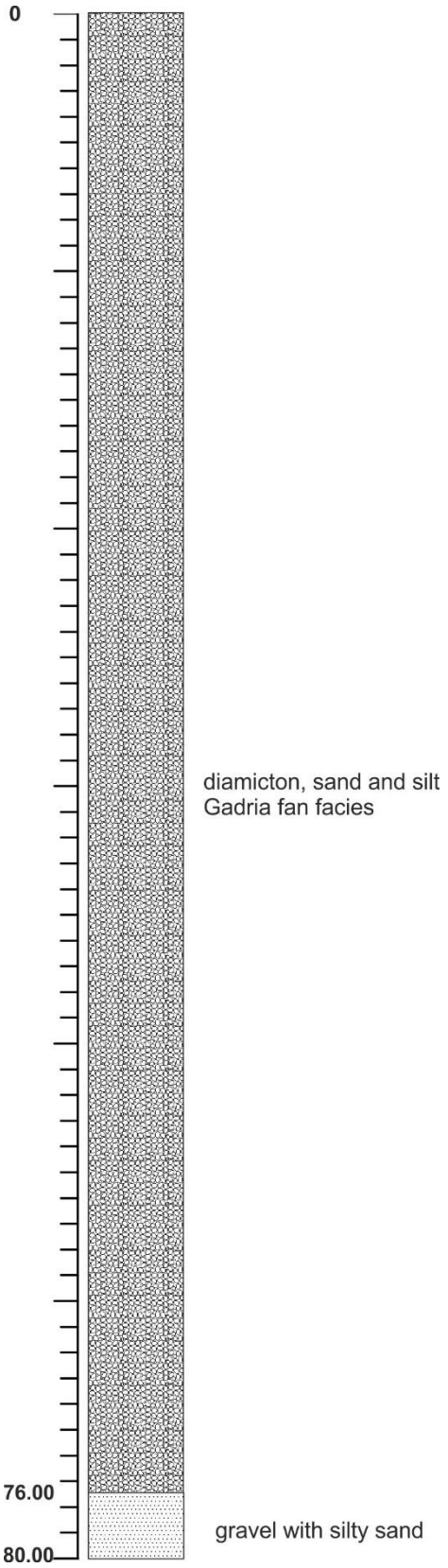

Figure DR1: Borehole S1

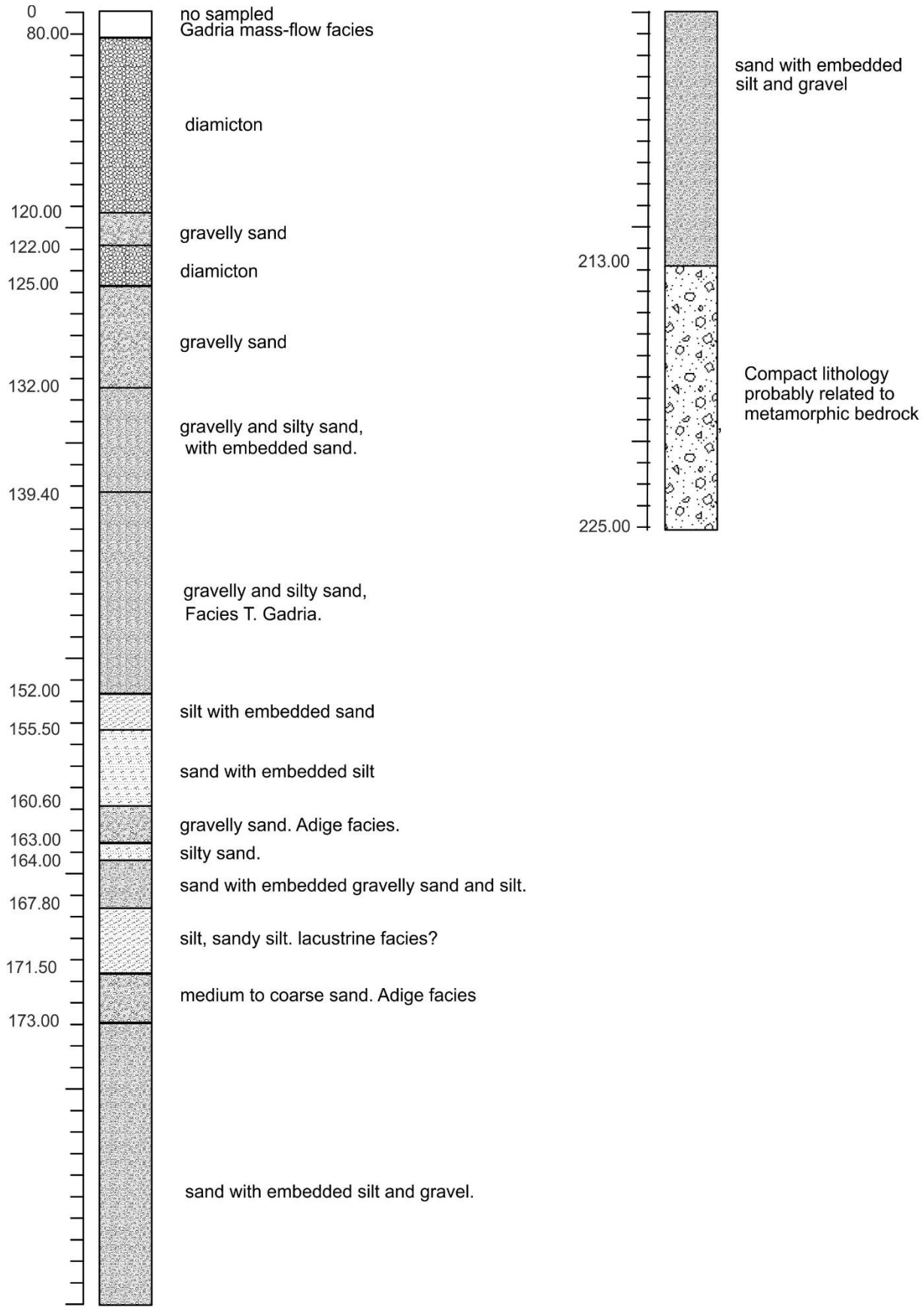

Figure DR2: Borehole S5

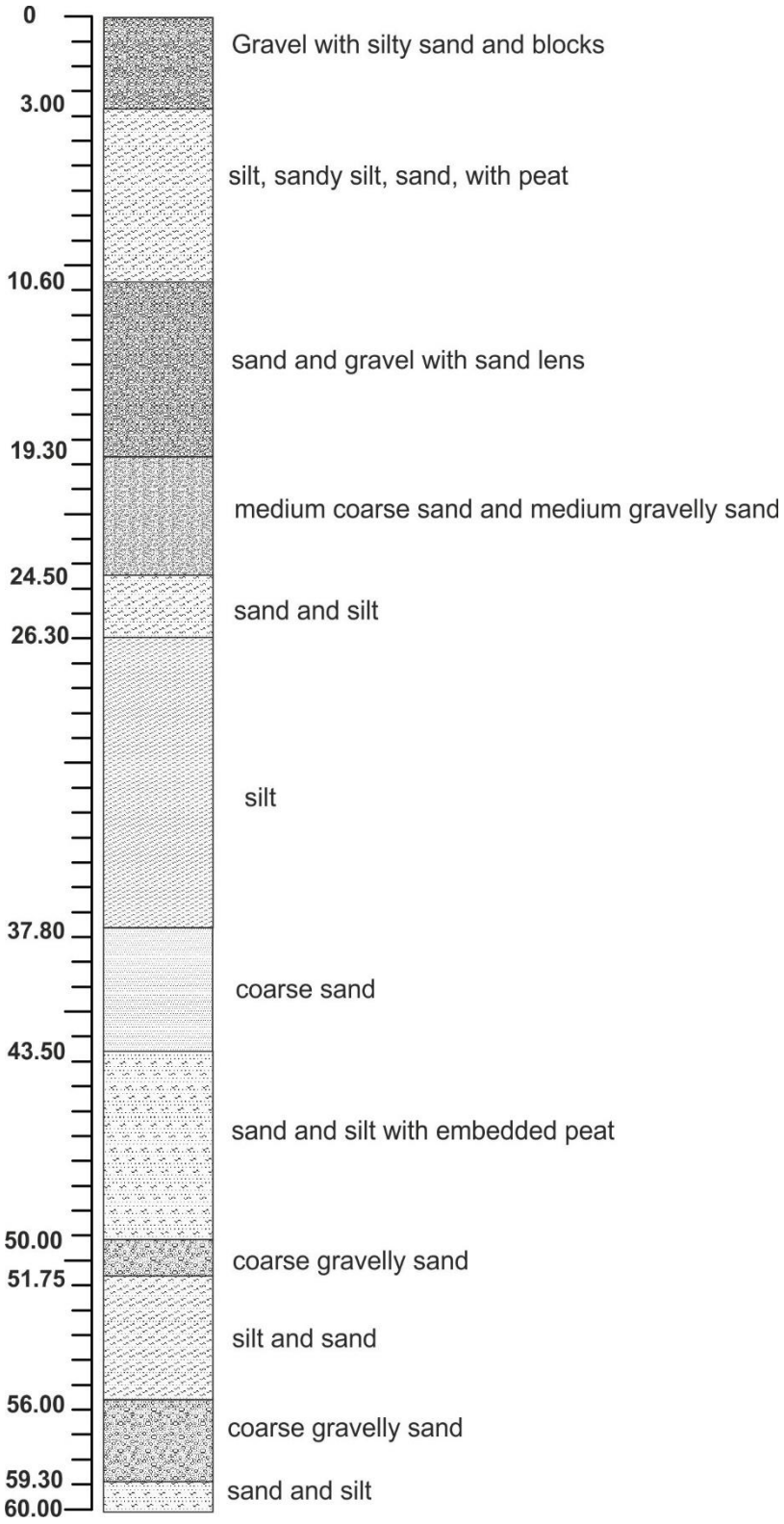

Figure DR3: Borehole S2

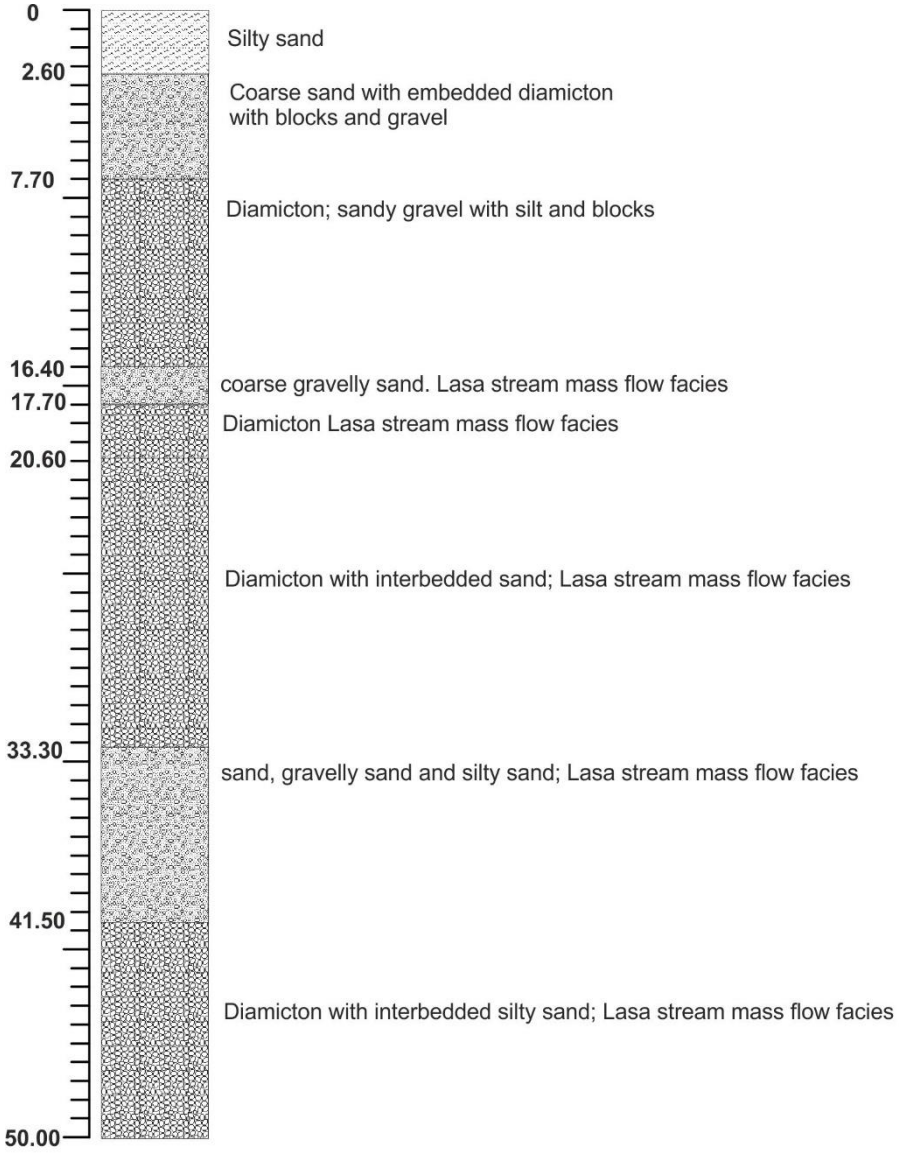

Figure DR4: Borehole S4

5 Conclusion

The research presented in the previous chapters has shown the following conclusion:

- Vinschgau/Val Venosta is characterized by a depth asymmetrical structure of the bedrock, composed by two different metamorphic units, namely Oetzal Unit and Campo Unit, respectively outcropping on the northern side and on the southern side of the valley. The spatial transition between the two units occur at a depth of about 250 m, by means of a structural contact and represent the deepest part of valley.
- The internal architecture of the Gadria fan as well as the results by the borehole investigations suggest that its formation and growth occurred by means of different aggradation phases as a result of debris-flow, hyper-concentrated flow and bedload flow transport processes. The lower part of the fan, especially in the proximal portion, is undoubtedly composed by coarse grained poorly organized deposits with abundant large boulders, typical of high-energy depositional environment (i.e. debris-flows), while the shallower part composition is associated to more fine sediments and well sorted deposition. This testifies the absence of evidence of catastrophic landslide as suggested by Jarman et al. (2011) and the predominance of fluvial and colluvial (debris-flow) transport processes as responsible of the fan growth, validating the hypothesis of Brardinoni et al. (2012) about the formation of the fan by means of the evacuation of paraglacial and glacio-fluvial sediments mainly via debris-flows. The internal organization within the fan deposits is associable to the paraglacial activity, following the paraglacial model proposed by Ballantyne (2002) for formerly glaciated environment. The two different paraglacial systems proposed in the model find confirmation respectively in the presence of unsorted and coarse grained sediments in the lower portion of investigated fans and it the deposition of more organized sediments, recognized in the upper and in the distal part of the deposits. The composition of the Gadria deposits is also influenced by the different sediments transferred by the two source basins: Gadria basin is characterized by debris-

flow processes, while Strimm catchment is dominated mainly by fluvial and bedload transport processes.

- Most of the catchments within the Vinschgau/Val Venosta are dominated mainly by fluvial and hyper-concentrated flows, due to the channels morphology strongly sculpted by glaciers erosion. The transport processes found in the source basins channels are confirmed by the composition and by the depositional facies of the related fans. The last glaciation fingerprints on the investigated landscape strongly influence the establishment of contemporary geomorphic process domains along the basins channels and most of the analyzed channels have not still recovered from being first shaped by glacial. Consequently, most of sediments remain trapped within the valley due to the presence along the main channels of prominent kinks, paraglacial fan and cone and a poor degree of sediment connectivity between the hillslopes and the basins outlet (Cavalli et al., 2013). The Gadria, the Plawenn and part of the Zielbach basins seem to be recovered from past glaciations and are dominated mainly by debris-flow processes.
- The valley fill is composed by three deposition system: the lower part of the valley is occupied by the glacial system, comprising glacial deposits pre-LGM and sediments from the last glacier retreat; the fluvial system that fill the major part of the valley, composed by fluvial and fluvio-lacustrine sediments from the Etsch/Adige River; the colluvial alluvial system, generally composed by debris-flow deposits from the tributary basins.
- The formation and the growth of the Gadria fan played an important role in the valley system aggradation. Indeed, the aggradation of the Gadria fan Indeed, competed with the trunk river, creating an always higher base level and impacting the sedimentation of the Etsch/Adige River. Therefore, the Gadria fan has repeatedly deflected the Etsch/Adige River towards the southern margin of the valley.
- The valley filling started immediately after the Venosta glacier melting (between 19 ky and 14 ky). A first phase of deposition interested only glacial and fluvial deposits due to glaciers in the tributary valleys was still present. The major systems aggradation occurs likely between the Bølling/Allerød

and the Early Holocene, (around 15 to 9 ky B.P.) because of warmer and wetter climate conditions, high availability of sediment on the tributary basins slope, scarce vegetation and the high river transport capacity. After the Holocene Climatic Optimum, characterized by low erosion and sedimentation rates, the aggradation of the Gadria fan and consequently the increase of the base-level of the valley, were completed in the last 5.5 ka as consequence of both Holocene Climatic Deterioration and human activities (Savi et al., 2014).